The University Of Sheffield.

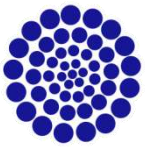

CONACYT
Consejo Nacional de Ciencia y Tecnología

CHARACTERISATION OF A NOVEL MODEL OF BONE CRUSH REPAIR AND *IN VIVO* ANALYSIS OF SKELETAL REGENERATION IN ZEBRAFISH

Thesis submitted for the degree of Doctor of Philosophy

by

Luis Medina Sánchez

The Bateson Center

Department of Biomedical Science

University of Sheffield

September 2016

Acknowledgments

Firstly, I would like to express my gratitude to Dr. Henry Roehl for letting me pursue my goal of doing a Ph.D. abroad in his laboratory. Thank you very much.

To my advisors, I appreciate their guidance to improve my project.

To all the people who I met during the four years in BMS department; I have had the privilege to collaborate with very talented scientists.

I feel grateful to have now amazing friends from all over the world, thank you guys for those amazing times outside the lab.

Also, I want to thank my sponsor CONACyT for giving me the opportunity to make my post-grad research at Sheffield University. During these years, I met talented compatriots who are making a difference to develop the Mexican science.

Lastly, I would like to thank my fiancé Bere and the rest of my family for their love and support during my absence from home.

.

Abstract

In mammals, repair of bone fractures is believed to be achieved by local activation and differentiation of osteogenic progenitor cells. However, lineage-tracing studies after fin amputation have demonstrated that bone regenerates from mature osteoblasts in the zebrafish fin through a process of partial dedifferentiation, migration and proliferation. Thus, this raises the question whether osteoblast dedifferentiation is specific to appendage regeneration, or a process found more generally to repair bone in this animal. These studies used tail amputation which is a more severe form of damage than a bone fracture. Nevertheless, Sousa and colleagues (2012) proposed a novel crush assay for adult bones in zebrafish fin rays which showed promising results and was also developed for this project.

The first objective of the thesis was to go beyond to find differences in zebrafish compared to what is already known in the mammalian fracture model during the different healing stages (inflammation, repair, remodeling). Interestingly, my analysis showed no remarkable differences at the cellular or molecular level in comparison to mammalian fracture repair. Notably, reactive oxygen species (ROS) production, which are one of the first signals to be induced after damage, depend on the lesion type in adult zebrafish. IL1β cytokine is induced early after bone damage and neutrophils are recruited at the fracture site after few hours as well. Both seem to induce directly or indirectly osteoclast recruitment. Osteoclasts participate early but also remained active after several days.

Moreover, to determine whether osteoblasts dedifferentiation is restricted to appendage regeneration, efforts were done to stablish the Cre-Lox system in adult zebrafish. As a first step, a set of six double transgenic lines were created to enable tracking of bone cells *in vivo*. Afterwards, different tamoxifen-induced Cre-recombination strategies were implemented but no successful results were obtained. Further research is needed to get positive results.

The knowledge generated in this research can contribute to set the basis for the development of further studies of bone repair in zebrafish that can complement the ones performed in classical models.

Table of Contents

CHAPTER 3.

Characterisation of the Different Fracture Healing Stages in Zebrafish.

CHAPTER 5

Construction of zebrafish transgenic lines with bone-associated promoters to induce controlled site-specific recombination.

CHAPTER 6

Usage of different strategies to induce Cre-recombination in adult double transgenic lines.

CHAPTER 7

CHAPTER 8

CHAPTER I

General Introduction

1.1 Appendage Regeneration

The goal of regenerative medicine is to restore cells, tissues and structures that have been lost or damaged after disease, injury or aging. Human beings have a limited capacity to restore and replace tissue or organs. This field has taken advantage of the knowledge obtained from diverse animal groups that at multiple levels can regenerate lost cells, tissues, organs or even an entire body (Bely and Nyberg., 2010; Brockes and Kumar., 2005) (Figure 1.1)

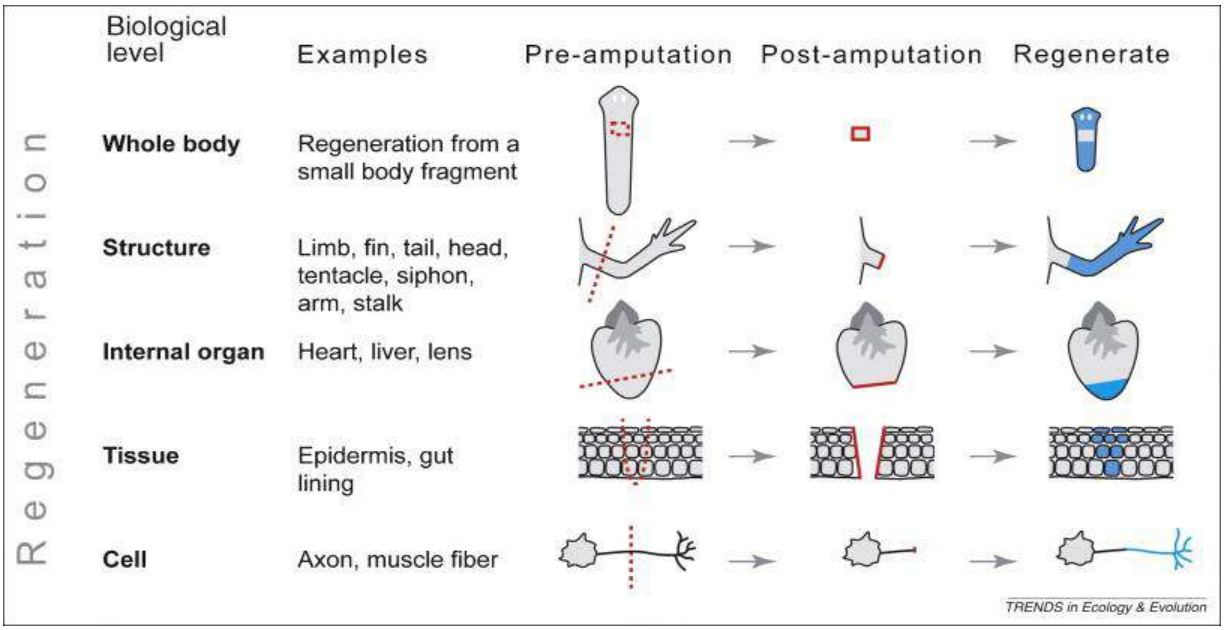

Figure 1.1 Different degrees of regeneration in the animal kingdom. Adapted from (Bely & Nyberg, 2010).

To illustrate this, animals such as cnidarians and flatworms have the capacity to regenerate the whole body from a small body fragment; also, species like *Drosophila*, *Xenopus* and *Zebrafish*, have an extensive ability to regenerate a missing portion of body lost to trauma (imaginal disc; limb; and heart and fin, respectively) (Martin and Parkhurts, 2004; Brockes and Kumar., 2005; Reddien and Sanchez Alvarado, 2004; Tanaka and Reddien., 2011).

Moreover, urodele amphibians (salamanders, axolotls and newts) are outstanding animals employed since many years ago to study vertebrate regeneration; they can regenerate several body parts such as : its limbs, tail, upper and lower jaws and ocular tissues, (Ghosh *et al.*, 1994; Oberpriller *et al.*, 1974; O'Steen *et al.*, 1962).

In these animals, limb regeneration is one of the most studied regenerative models due to two key features: the body part accessibility and its remarkable restoration efficiency. Dedifferentiation is believed to be the main mechanism involved in this process. After amputation, the wound closes and a layer of cells, called wound epidermis, covers it. Then, cells surrounding the wound will migrate towards it and form a mass of cells called the blastema. This group of cells is thought to be undifferentiated and highly proliferative. Cell proliferation will start and these cells re-differentiate into the tissue or tissues that will reconstruct the absent structure (Kawakami 2010; Poss *et al.*, 2003)

Tanaka and colleagues showed that regeneration of the limb is lineage-restricted. By using transgenic axolotls expressing a GFP transgene, they labeled different cell types independently and performed amputations to detect the fate of those cells during the regeneration process. Results showed that for example, labeled cartilage cells did contribute to the regrown bone but not to other tissues like muscle or epidermis (Tanaka and Reddien 2011) (Figure 1.2)

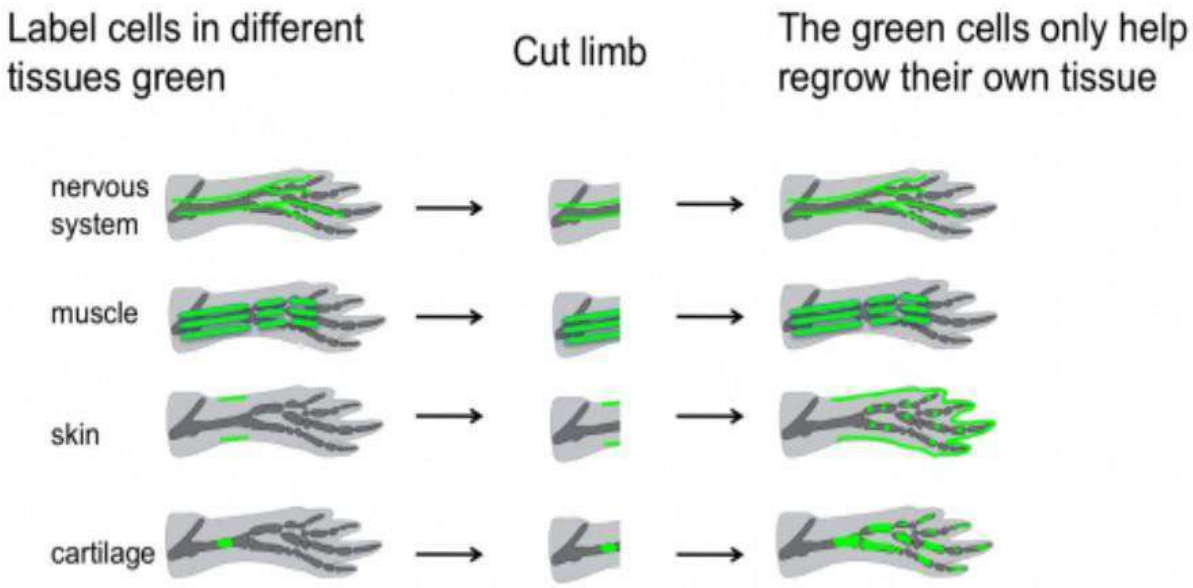

Figure 1.2. Axolotl limb amputation experiments demonstrated that cells are lineage-restricted. Each tested labeled cell type (bone, muscle, nerves etc.) showed that it helps to regrow their own tissue after limb amputation, but not a different one. (Tanaka and Reddien, 2011).

Moreover, like urodeles, the zebrafish has become another attractive model to study regeneration due to its enhanced capacity to regenerate many tissues: tail fin, spinal cord, ocular tissues and heart (Becker *et al.*, 1997; Johnson and Weston, 1995; Poss *et al.,* 2002; Vihtelic and Hyde, 2000). This model is going to be described in detail in the next section.

1.2 Zebrafish as an Experimental Model to Study Regeneration

The zebrafish has emerged as a powerful vertebrate regenerative model. Advances in genetics, rapid generation time, the ability to obtain vast quantities of externally fertilised eggs, and also the ability to transiently modify gene function during development, are valuable features (Lieschke and Currie., 2007; Tal TL. *et al.*, 2006). The zebrafish is considered one of the most spectacular regenerative animals in the natural world because of its natural capacity to regenerate its heart muscle, retina, optic nerve, liver, spinal cord and the tail fin. In most of the cases, this occurs due to the formation of a highly proliferative tissue at the injury site (blastema structure) which contains undifferentiated cells needed to complete the regeneration process (Poss, 2010;

Nakatani *et al.*, 2007; Akimenko *et al.*, 2003). It is notable that many human conditions such as injury, disease or aging, could have the potential to benefit from the knowledge that will be generated by zebrafish research in the coming years (Tal TL. *et al.*, 2006).

The zebrafish caudal fin has been used for some time in the regeneration field for research of vertebrate appendage regeneration by several groups. This regenerative phenomenon is known as "epimorphic regeneration" which is going to be explained later in this chapter. The popularity of the caudal fin as a model is due to its structural simplicity, rapid and robust regeneration (Kawakami, 2010; Akimenko *et al.*, 2003).

The caudal fin structure is composed of a series of fin rays called (lepidotrichia) which are joined by soft tissue interrays that do not contain skeletal elements. The fin rays are a series of bony segments and its function consists of protecting different components (mesenchymal cells, blood vessels, nerves, melanocytes and fibroblasts). Also, it gives support and allows locomotion in water (Tu and Johnson, 2011; Tal TL . *et al.*, 2006; Akimenko *et al.,* 2003) (Figure 1.3)

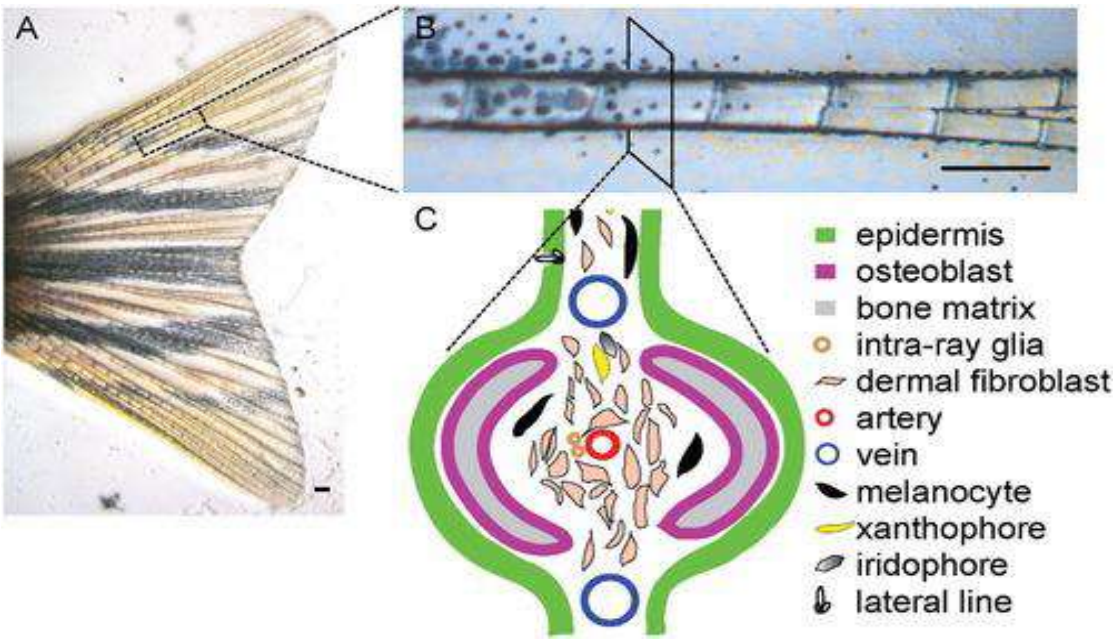

Figure 1.3. **Adult zebrafish caudal fin architecture.** (A) Adult caudal fin picture. This structure contains several fin rays connected by soft tissue interrays that lack skeletal elements. B) Single zebrafish fin ray zoom in. Each is formed by a series of bony segments comprised of a pair of concave hemirays. C) Cross section diagram showing different cell types found within a bony ray. (Tu *et al.*, 2011)

1.2.1 Epimorphic Regeneration in Zebrafish Caudal Fin.

Just after the tail fin is amputated, a series of regenerative stages are initiated in order to restore the complete structure (Figure 1.4). First, the wound is closed by actins strings, and then a wound epidermis will be formed along the injury. In a second step, cells next to the amputation plane migrate towards it, dedifferentiate and then form a mass cell structure known as the blastema. Those blastema-like cells proliferate, and they will be the responsible for generating tissue outgrowth that will restore the lost part (Tu and Johnson, 2011; Kawakami, 2010; Nechiporuk and Keating, 2002).

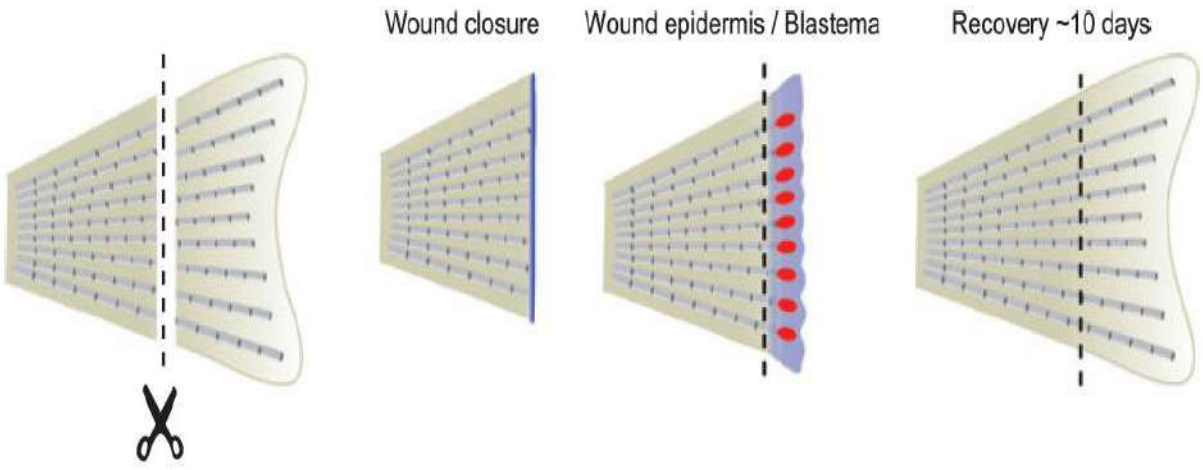

Figure 1.4. Zebrafish caudal fin regeneration process. Approximately 10 days are needed to complete the adult zebrafish tail fin regeneration after wound. Epithelial tissue is formed along the amputation plane and following this, cell migration and proliferation take place to create the blastema structure. This is the source of new material to restore the lost part. Blue area: Wound epidermis. In red: blastema zone. (Kawakami, 2010).

It is currently known that different signaling pathways take part in zebrafish regeneration. For example, the Wnt pathway is a highly evolutionary conserved mechanism in animals that has different roles in regeneration. This pathway was first implicated in zebrafish fin regeneration due to Lef1 expression after wound, which is a Wnt target (Poss *et al.*, 2000). The Canonical Wnt signaling that involves B-catenin is required for wound healing, blastema formation and regenerative outgrowth (Poss *et al.*, 2000, Stoick Cooper *et al.*, 2007). Interestingly, it has been

observed that different Wnt factors perform different functions during the regeneration process. For example, Wnt5 which is part of the Noncanoncial Wnt signaling (no B-catenin involved), its over expression gave rise to an absence of tail outgrowth (Stoick Cooper *et al.*, 2007). Therefore, this suggest that Noncanoncial Wnt signaling negatively regulates regeneration after fin amputation.

FGF signaling is also important for wound healing, blastema formation and regenerative outgrowth like Wnt signaling pathway. For example, experiments done with mutants that lack some *fgf* factors sucha as *fgf20*, and the suppression of *fgf* receptors (*fgfr1*), showed absence of fin outgrowth after amputation (Whitehead *et al.*, 2005; Poss *et al.*, 2000).

Hedghehog (Hh) and bone morphogenetic protein (BMP) are other signaling pathways that have a role in zebrafish regeneration. The data suggest that Hh signaling seems to be upstream of BMP (Quint *et al.*, 2002) and both are involved in different tasks during regeneration such as: bone-cell proliferation, ray patterning and formation.

In addition, more signaling pathways have been identified that have a participation in fin regeneration such as: Retinoic Acid (RA) which has emerged as an important regulator of regenerative cell proliferation. RA signaling specifically controls the formation, proliferation and survival of the blastema (Blum *et al.*, 2012). Insulin-like growth factor (IGF) is important for the correct regenerative growth of the fin due to its effect on the wound epidermis patterning. IFG signaling sees to mediate mesenchymal-epithelial interactions during regeneration (Chablais *et al.*, 2010). Calcineurin phosphatase pathway, was recently identified as an inhibitor of regenerative growth; its interference enhanced this process. Also, data suggests Calcineurin might act via inhibition of RA signaling but further experiments are needed to confirm it. (Kujawski, *et al.*, 2014). Notch, is important to maintain blastemal progenitor cells in a proliferative state and when attenuated allows differentiation to proceed. It is still unknown whether Notch acts in osteoblast progenitors (Grotek *et al.*, 2013; Munch *et al.*, 2013). Mechanistic target of rapamycin complex 1 (Mtor), is activated in different cell types during regeneration such as: epidermis, osteoblasts and in the proliferative proximal regions of the blastemal. It has been found that Wnt/β-catenin and IGF signaling induce its activation and regeneration is arrested when it is blocked (Hirose *et al.*, 2014). ROS signaling pathway triggers

cell proliferation in the blastema to orchestrate fin outgrowth. (Gauron *et al*., 2013; Han P. *et al*., 2014) (Figure 1.5).

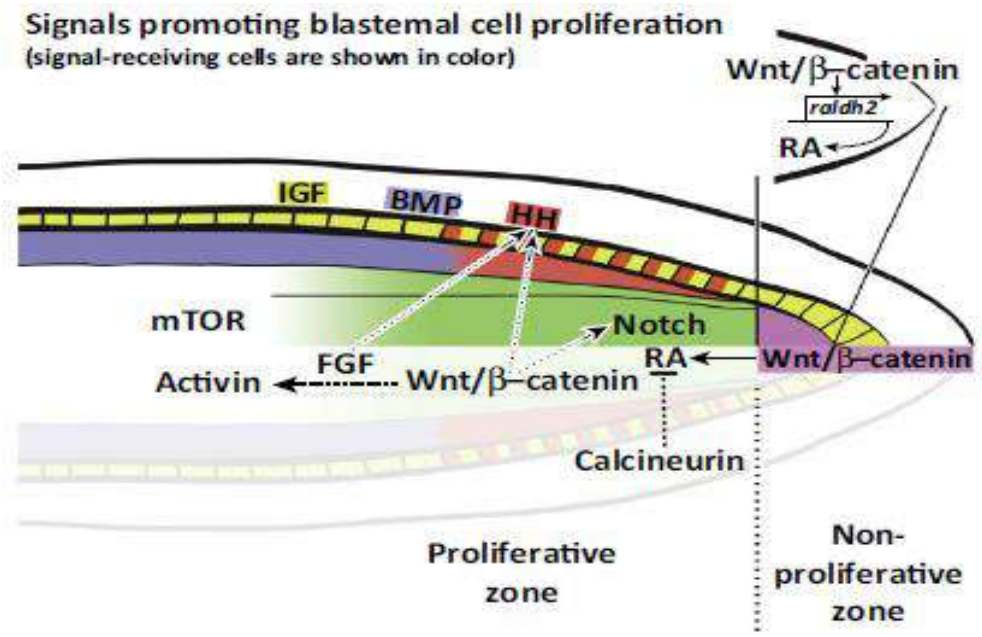

Figure 1.5 Different signaling pathways are involved in blastemal regulation. Many major signaling pathways that regulate development have also been found to be essential for fin regeneration. Wnt, IGF, FGF, Notch Hh, BMP, mTOR signaling pathways have an effect regarding blastemal cell proliferation. FGF was the first pathway known to regulate this process. 6Colored areas show regions where pathways are active (Wehner and Weidinger 2015).

Regeneration is a mechanism where different cell types interact with each other; it is essential to identify the exact sources of the different cell types that are restored after injury. Only recently have genetic fate-mapping approaches been applied to address those questions. Cre-recombinase-based technology is now a common technology used with zebrafish to answer fundamental questions in the regeneration field (Akerberg *et al*., 2014; Knopf *et al* 2010; Hans *et al*., 2009).

It is important to remark that one of the principal goals to achieve in the regeneration field is to determine the cellular source of regenerated skeletal elements. That means, to identify different

cell types which can produce regenerated bone elements. (Tanaka and Reddien, 2011; Poss, 2010).

1.2.2 Use of Zebrafish to Study Bone Regeneration and Development

Most of the significant findings in bone research have been done in the classical models such as mice, chicken, or cell cultures but in the last 15 years, the zebrafish has become a popular animal model to study skeletogenesis (Spoorendonk *et al.*, 2008). Zebrafish can be used as a powerful tool to complement the studies done with the other models in the past and to understand different unresolved issues regarding bone regeneration and development.

1.2.3 Differences between zebrafish and mammalian bone cells

In the following lines, I am going to mention some similarities and differences regarding bone cells between zebrafish and mammals.

Firstly, it is important to mention that key regulators of bone formation are highly conserved between zebrafish and mammals (Flores *et al.*, 2004; Yan *et al.*, 2005; Li *et al.*, 2009). Both have in common the same cellular components such as osteoblasts and osteoclasts cells which regulate bone formation and degradation. At the subcellular level, the situation is the same, different factors such as Sox9 (chondrocyte differentiation) or Runx2 (osteoblasts differentiation) known to be involved in bone development and regeneration in mammals are also conserved in zebrafish (Apschner *et al.*, 2011).

Regarding disease, several orthologous genes implicated in mammalian skeletal disease are expressed in zebrafish (Rivadeneira *et al.*, 2009). Interestingly, it has been shown that zebrafish mutants can display similar phenotypes associated to human bone diseases (Laizé *et al.*, 2014).

However, differences exist which make researchers skeptical to use zebrafish for bone associated studies in the past. For example, fish show an absence of haematopoietic bone marrow tissue like in mammals; hematopoiesis is maintained in the kidney instead (Witten and Huysseune,

2009). Also, due to its natural aquatic environment, zebrafish do not depend on their skeleton to maintain plasma calcium homeostasis. Compared to mammals, additional skeletal tissue subtypes are recognized in fish, which makes sometimes difficult to compare studies with mammals.

Research using zebrafish is giving us an insight to understand skeletogenesis and is helping considerably to understand mammalian bone physiologies during development, maintenance, regeneration and disease (Hammond and Moro, 2012; Spoorendonk *et al.*, 2009; Marí-Beffa *et al.*, 2007).

To understand how bone regenerates in zebrafish which have an outstanding regeneration capacity, different lab groups using different cell tracking experiments demonstrated that bone regenerates from mature osteoblasts (bone- forming cells) in the zebrafish fin by acquiring progenitor cell properties, in a process known as dedifferentiation (Knopf *et al.*, 2011; Singh *et al.*, 2012; Sousa *et al.*, 2011; Stewart and Stankunas, 2012; Tu and Johnson, 2011). It has been found by using Cre/LoxP-marking technology after tail amputation, that those cells display partial dedifferentiation, a process which was corroborated by the down-regulation of osteoblast markers, followed by a proliferative stage. Interestingly, osteoblasts only contributed to generate new bone, a result that suggests that osteoblasts possess a cell fate restriction (Knopf *et al.*, 2011). Lineage restriction is a general event find in other cell types, such as: in epidermis and fibroblasts (Tu and Johnson, 2011).

Retinoic acid (RA) has been found to control the osteoblast differentiation state at different time points. Osteoblasts need to protect themselves from retinoic acid signaling via cyp26 expression to be able to dedifferentiate, while later retinoic acid promotes osteoblast proliferation (Blum and Begemann 2012; 2015) (Figure 1.6).

These findings are different from what it is known in mammals, where repair of bone fractures is believed to be achieved by local activation and differentiation of osteogenic progenitor cells (Maes *et al.*, 2010; Park *et al.*, 2012)

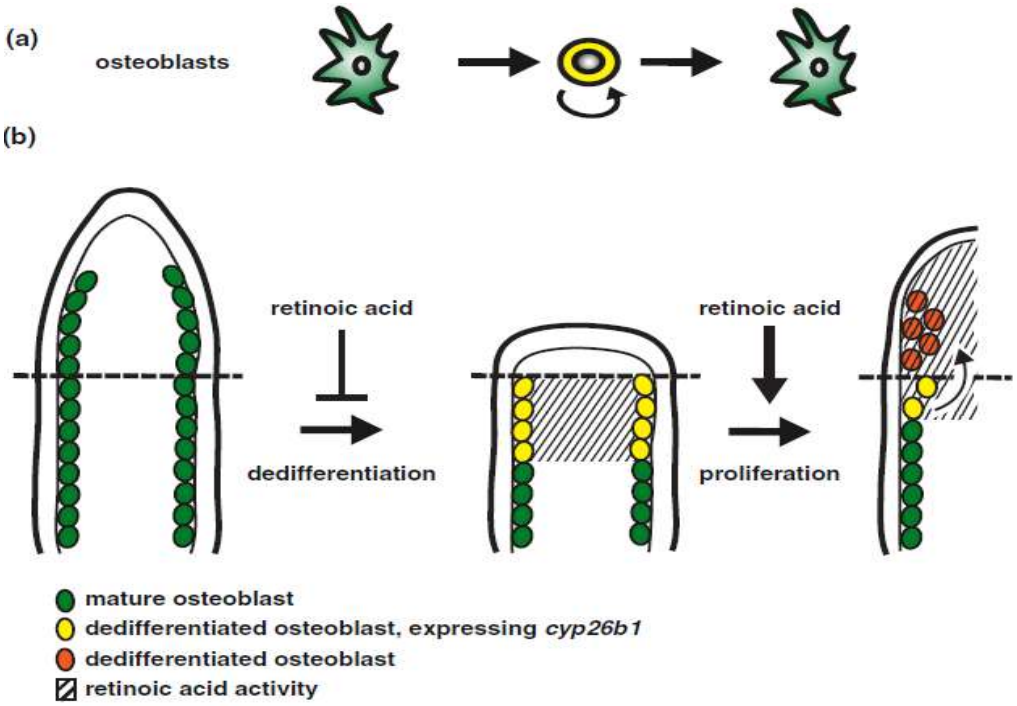

Figure 1.6 Osteoblasts dedifferentiate during zebrafish regeneration. A) After damage, osteoblasts will undergo a dedifferentiation process (progenitor cell like phenotype), important to create new cellular material. B) Retinoic Acid produced by fibroblasts is an important regulator of osteoblast regeneration due to its inhibitory effect. The RA-degrading enzyme cyp26b1 is upregulated by osteoblasts to protect themselves of RA influence. This enzyme expression is ceased afterwards by dedifferentiated osteoblast in the blastema region, allowing RA to promote their proliferation. Modified from (Shering *et al.*, 2016)

Interestingly, Singh and colleagues (2011) showed that a reserve population of cells which have not been identified yet, can regenerate osteoblasts when these are experimentally depleted. This study gave rise to the possibility that stem cells could be involved in bone formation when osteoblasts are not present. Further experiments are needed to explain this finding. Authors eliminated all the osteoblast cells by using the Nitroreductase-mediated cell/tissue ablation technology. The reaction of nitroreductase (NRT) in contact with a metronidazole (Mtz) compound generates a harmful drug, leading to cell death in a bone tracking transgenic line. After fin amputation, fish with no osteoblast population regenerated new rays as compared with the control group where this population was intact. Afterwards, cell tracking experiments with the use of a triple transgenic fish, with tamoxifen-dependent Cre-Lox technology, Tg (osx:CreER; β-actin2:Lox-DsRed-Stop-Lox-EGFP; osx:NTR), the authors showed that new

bone cells formed in the regenerated fin and that do not proceeded from dedifferentiated osteoblasts (Figure 1.7).

This finding answered an important question that emerged regarding fin regeneration, whether the absence of a cell lineage such as osteoblasts during the fin regeneration reestablished the same cell lineage or not.

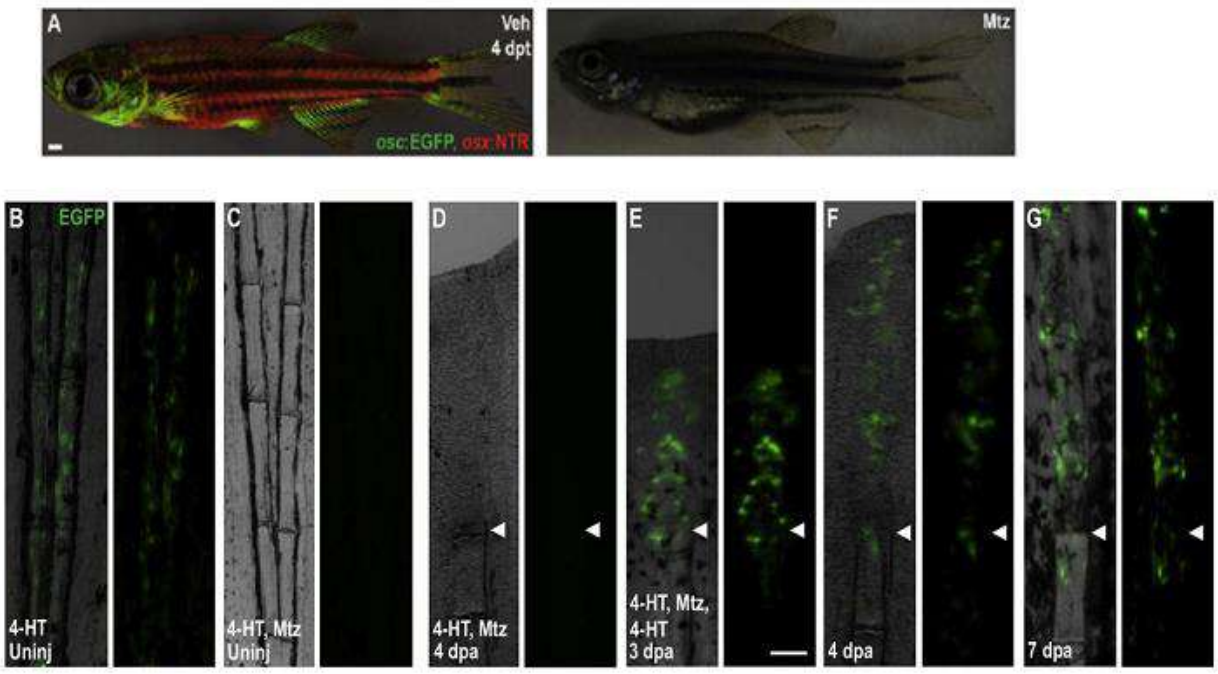

Figure 1.7 Zebrafish can regenerate new bone without the presence of osteoblasts. A) Left, transgenic line expressing osterix and osteocalcin bone markers. Right) After Mtz administration, gene expression was depleted**.** (B-C) Controls, no fin amputation performed. (D-G) after fin amputation and osteoblast ablation, GFP+ bone-positive cells (white arrowheads) were detected in the regenerating fin after continuing days post amputation (dpa) (Singh *et al*, 2012).

1.3 A New Zebrafish Bone Crush Injury Model

The amputation model has been used by several groups for years to study fin regeneration. Specifically, this phenomenon is called epimorphic regeneration, which consists of the formation of a blastema structure, described in the previous section. The main disadvantage of using this model is that even though humans can regenerate some tissues (bone) or organs they do not undergo epimorphic regeneration.

Thus, in order to understand how skeletal cells regenerate and to try to outline a model that could be more comparable to human bone fracture repair, Sousa and colleagues (2012) proposed a novel crush assay for adult bones in zebrafish fin rays. The main feature is that this model does not involve removal of tissue and is less disruptive than the classical amputation model. The assay involves the crush of single bone rays using forceps.

To start characterizing the novel bone crush model, the authors showed in the first instance, that both assays (bone crush vs partial amputation of the fin) presented different tissue architecture when fins were analysed and compared in the same fin (Figure 1.8, A). The damage produced by the crush assay was noticeable when comparing it with the amputation plane which was not distinguishable after 10 days (Fig. 1.8, C). Interestingly, a structure similar to a callus was formed after the crush in the damaged rays (Fig 1.8. E), reminiscent of the process that occurs during mammalian bone repair after a bone fracture (Schindeler *et al.*, 2008), as a control, the callus-like structure was absent from amputated fins. (Fig 1.8, C left side).

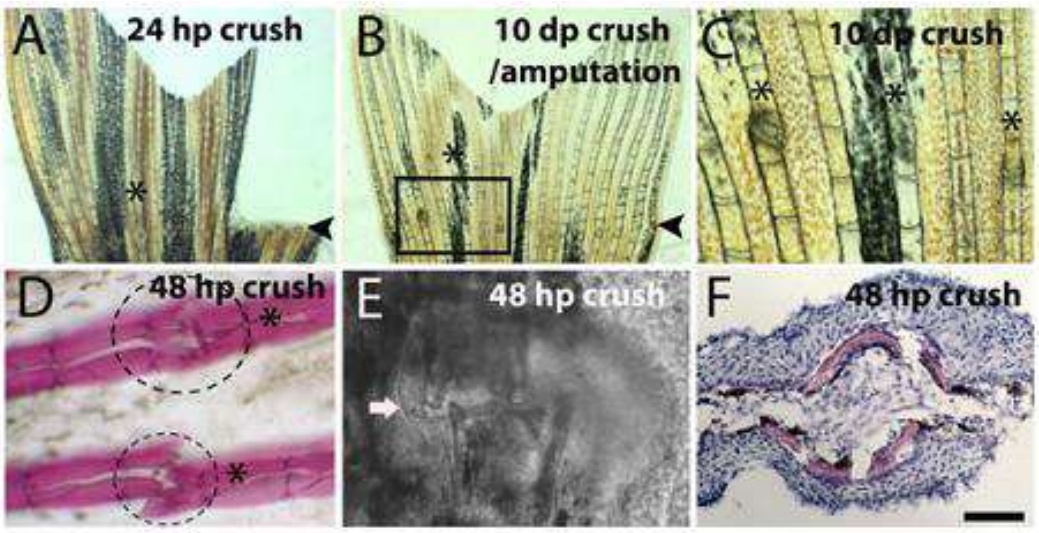

Figure 1.8 The bone crush showed differences in tissue architecture respect to amputation model. (A–C) Bright field images showing the result of both assays (bone crush vs amputation) applied in the same caudal (A) 24 hpc and (B) 10 dpc. (C) Magnification of the inset in picture B. (D) Bone stained with Alizarin Red at 48 hpc; dashed lines indicate the region of callus formation. (E) Bright field confocal image of 48 hpc injury site. The arrow highlights the callus structure. (F) Hematoxilin/Eosin staining in a transversal section of a 48 hpc ray to show tissue thickness. Arrowheads indicate the amputation plane and asterisks indicate crush injury area in A and B, and crush injury sites in C and D. (hpa = hours post-amputation; hpc = hours post- crush injury). Source (Sousa *et al.*, 2012)

Authors continued to characterize the model and showed that expression of wound healing markers was delayed in the bone crush injury model compared with amputation. One of the first events that occur after the amputation injury is the formation of a wound epithelium that surrounds and cover the damage site. By using immunofluorescence, it was shown that the p63 protein, a structural epidermis marker (Stewart *et al.*, 2009) was detected after 24 hours post-crush (hpc) surrounding the injury (Figure 1.9, A). Interestingly, the epidermis layer was thicker in the callus- like-structure compared with non-damaged rays. Other several epidermis markers were tested during the regeneration process to compare both models; for example, the *pea3* gene (ETS-domain transcription factor) is one of the several targets of FGF which is one of the factors secreted by the wound epidermis (Stoick-Cooper *et al.*, 2007) (Fig 1.9 B-E). The *lef1* gene *(lymphocyte enhancer binding factor 1)* was also tested. This is a member of the Wnt signaling pathway used to define the correct specification of the basal layer of the wound epidermis (Poss *et al.*, 2000). Both genes were detected by *in situ* hybridization assay at 24 hours post- crush but surprisingly, the expression levels were lower when those of the post-amputation epidermis. At

48 hpc, the *pea3* gene was also detected with lower levels when compared with the amputated rays, however for the *lef1* gene, expression level was similar to the control (Figure 1.9 F-I). The results suggested that perhaps activation of FGF/Wnt pathways were delayed following the bone crush repair.

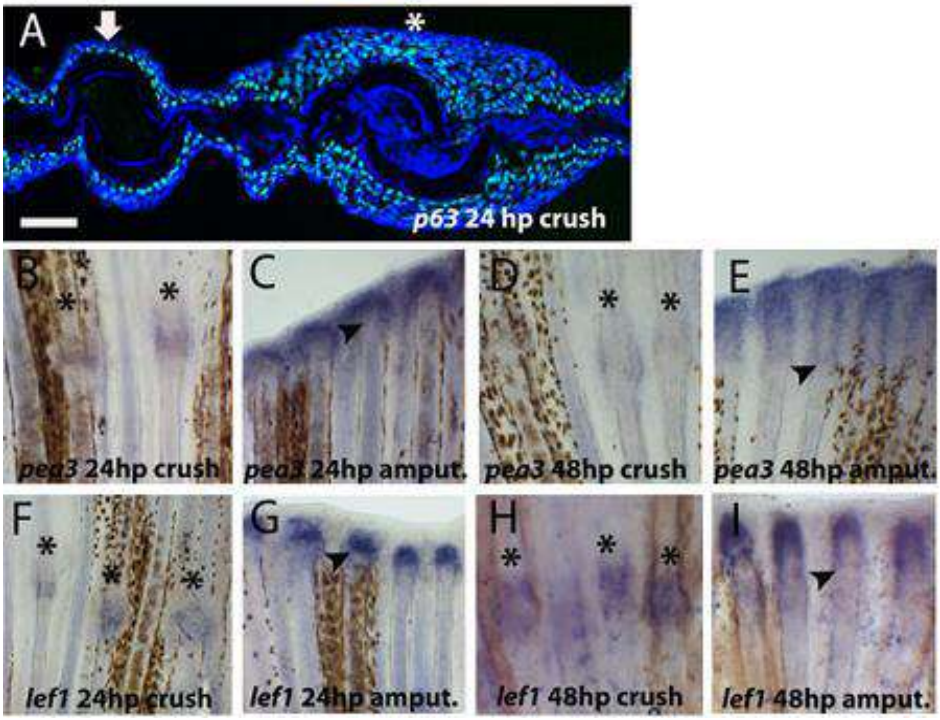

Figure 1.9. The tested wound healing markers showed a delayed expression in the bone crush model compared with amputation. A) Caudal fin transversal section. p63 Immunohistochemistry (green dots)**.** Blue represents DAPI-positive nuclei. The arrow indicates an intact bony ray and the asterisk is the site of crush injury. (B–I) pea3 and lef1 whole-mount *in situs* at 24 and 48 hours post injury (crush/amputation). Arrowheads indicate the amputation plane and asterisks indicate the crush injury sites. (hpa= hours post-amputation; hpc = hours post-crush injury). Source (Sousa *et al*., 2012)

To investigate the expression of different skeletogenesis markers, *osterix (osx), collagen I (colI)* and *osteonectin (osn*) *in situ* hybridisations were performed at 24 and 48 hpc (Figure 1.10).

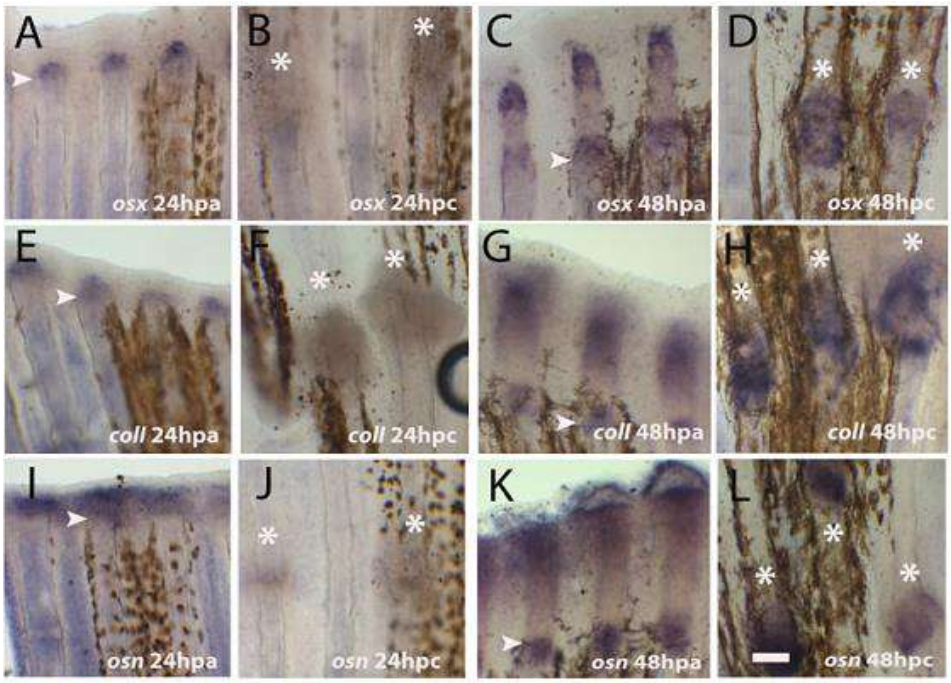

Figure 1.10. The tested skeletogenesis markers showed a delayed expression in the bone crush model compared with amputation. (A–L) *osterix*, *collagen I* and *osteonectin* whole-mount *in situ*s, performed at different times in both tested models. Arrowheads indicate the amputation plane and asterisks indicate the crush injury sites. (hpa = hours post-amputation; hpc = hours post-crush injury). Source (Sousa *et al.*, 2012)

These data showed that the three genes were expressed until 48hpc but not during the first hours after injury, in comparison to the control. These results followed the same trend as the wound healing markers, in that expression of genes involved in skeletogenesis was also delayed.

The findings suggested that both models share the same molecular programs but it seems that in the crush model the expression of important genes is delayed.

The novel bone crush model of bone repair in zebrafish showed encouraging results in relation to comparison with mammalian bone fracture models. It is of interest to continue with its characterisation, supported using novel tools (i.e. the Cre-Lox system for cell tracking experiments) that have emerged for zebrafish research.

In the Aims and Objectives section, several questions that emerged from this study are outlined.

1.4 Fracture Healing Process

Most of the knowledge that we have of fracture healing is based on mammalian classical animal studies, (rats and mice) which offered distinct advantages over large animals (dogs, goats etc.); animal housing is easier and less expensive, large number of animals can be kept in a limited space and breeding cycles are shorter. Also, the use of genetically-manipulated animals allows us to study distinct molecular and cellular mechanisms of the bone healing process (Histing *et al.*, 2011)

Interestingly, even though each model differs on healing capacity and speed, the general mechanisms of repair seem to be similar to humans. Determining a fracture model in a small animal such as zebrafish could have some advantages as mentioned in the previous section.

1.4.1 Phases of Fracture Healing

Fracture healing is a process that can be divided into three partially overlapping phases: inflammation, repair, and remodeling (Einhorn and Gerstenfield, 2015). This sequence of events has been observed in many animal species, and it is best illustrated in rodents (mice and rats) (Histing *et al.*, 2011). Moreover, the healing process varies among animals in the speed and thus the repair time. I am going to provide an overview of this repair process.

1.4.1.1 Inflammatory Phase

Blood vessel rupture and damaged cells and tissues promote the initiation of the inflammatory cascade and fracture healing process (Kolar *et al.*, 2010). Consequently, a hematoma is formed which is characterised by hypoxia and low pH. This structure houses inflammatory cells together with pro-inflammatory and anti-inflammatory cytokines (Kolar *et al.*, 2010), and acts as a temporary scaffold for the invasion of additional inflammatory cells. The first cells to arrive to the damaged site are the neutrophils cells, attracted by death cells and debris (Chung *et al.*, 2006). These cells release several cytokines (such as IL6, C-C motif chemokine 2 [CCL2]) which attract macrophages to the site (Bastian *et al.*, 2011; Glynne *et al.*, 1994; Xing *et al.*, 2010) Two different

macrophage populations affect this process, the resident population (osteomacs) present on healthy unfractured bone seem to be important for intramembranous bone formation (the process of bone development from fibrous membranes, involved in the formation of flat bones: such as the skull and mandible) during fracture healing. By contrast, inflammatory macrophages that are recruited to the site of injury, promote endochondral ossification, the process of bone development from hyaline cartilage. (Xing *et al.*, 2010).

Moreover, many pro-inflammatory cytokines (IL-1β, IL-6, TNF, receptor activator of nuclear factor kB ligand [RANKL], macrophage colony-stimulating factor [MCS-F] and members of the transforming growth factor (TGF)-β superfamily (bone morphogenetic protein [BMP]-2/6) are released early in the inflammatory phase (Al-Aql *et al.*, 2008; Gerstenfeld *et al.*, 2003). Revascularization is essential for fracture healing, angiogenic factors (angiopoetin-1, vascular endothelial growth factors) are also released due to the hypoxic conditions in the injury site. (Al-Aql *et al.*, 2008).

All these early events are thought to initiate the repair cascade by stimulating anigiogenesis, attracting and promoting differentiation of mesenchymal stem cells (MSCs) and enhancing extracellular matrix synthesis (Xing *et al.*, 2010; Gerstenfeld *et al.*, 2003).

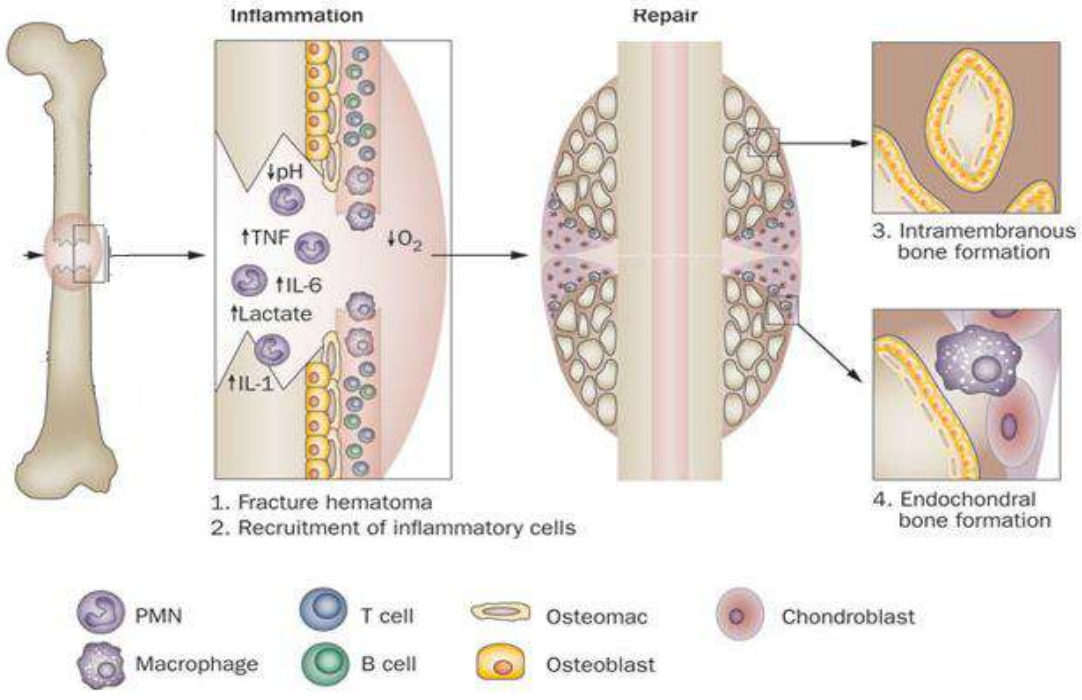

Figure 1.12. Inflammation and repair stages during fracture healing process. The first event is the appearance of a fracture hematoma after damage; formed due to blood clotting. Also, it is characterised by the presence of hypoxia, low pH conditions and the release of pro-inflammatory and anti-inflammatory cytokines.
1 -Immune cells are rapidly recruited to the site of injury. 2 – The first cell to invade the callus are neutrophils, followed by other immune cells such as macrophages and lymphocites. 3- Osteomacs influence osteoblast by attracting them to zones of intramembranous bone formation. 4- Whereas inflammatory macrophages mainly contribute to endochondral bone formation (4). Abbreviations: PMN= polymorphnuclear neutrophils. Modified from (Claes *et al.*, 2012).

1.4.1.2 Repair Phase

1.4.1.2.1 Soft Callus Formation

This process is very active and begins after the inflammatory response. Commited osteoprogenitor and undifferentiated mesenchymal cells proliferate and produce a semi-rigid cartilaginous template adjacent to the fracture site (Barnes *et al.*, 1999). This tissue will later undergo mineralization, resorption and is superseded by the production of the bony callus.
Coordinated expression of different growth factors, such as TGF-β2, TGF-β3, PDGF, FGF-1, and insulin-like growth factor (IGF), stimulate the proliferation/differentiation of the emerging fibroblastic and chondrocytic cells (Gerstenfeld *et al.*, 2003; Cho *et al.*, 2002; Einhorn, 1998) while chondrogenesis is promoted by various members of the BMP family of cytokines, such as BMP-2, -4, -5, and -6 (Al-Aql *et al.*, 2008).

Chondrocyte cells synthesize an extracellular matrix composed predominantly of type II collagen (Col2) and proteoglycans. As these cells mature, they undergo hypertrophy and begin to prodce type X collagen (Al-Aql *et al.*, 2008). Prior to the synthesis of hard callus, the deposited cartilage scaffold undergoes calcification, gradual removal of soft callus, neovascularisation, and the deposition of woven bone through the expression of several cytokines and pro-angiogenic factors that include: VEGF, BMPs, FGF-1 and TGF-β (Marsell *et al.*, 2009; Gerstenfeld *et al.*, 2003; Cho *et al.*, 2002). Other factors are also important for the resoprtion process such as: macrophage colony stimulating factor (M-CSF), receptor activator of nuclear factor NF-LB ligand (RANKL), osteoprotegerin (OPG) and TNF-α (Gerstenfeld *et al.*, 2003; Barnes *et al.*, 1999).

1.4.1.2.2 Hard callus formation

In the hard callus stage, the soft callus becomes extensively vascularised and is replaced by woven bone. This occurs by a combination of endochondral bone formation and some areas of intramembranous bone formation. This stage of bone repair is characterised by high levels of osteoblast activity and represents the most active period of osteogenesis, leading to the formation of mineralized bone matrix. The progression of the hard callus stage involves the replacement of the calcified cartilage with woven bone which provides mechanical rigidity to the healing bone (Gerstenfeld *et al.*, 2003) b). MMP13 produced by cells in the osteoblastic lineage is important for this last event which invades the cartilage matrix (Nakamura *et al.*, 2004). MMP9 is another important degradative enzyme for cartilage resorption (Colnot, 2005), synthesized by osteoclast cells (bone-degrading cells), which follow the early osteoblast in- growth phase.

1.4.1.3 Remodeling Phase

In this process the generated rigid hard callus which is composed of woven bone, requires to be remodeled back to the original bone configuration. A second phase of resorption takes place to replace the unorganized woven bone of the hard callus with a more organised lamellar bone structure (Marsell *et al.*, 2011; Gerstenfeld *et al.*, 2003). This phase is regulated by different

biochemical factors such as IL-1β, TNF-α, BMP-2, which show a reasonably high expression level during this stage of bone healing (Marsell and Einhorn, 2009; Al-Aql *et al.*, 2008; Mountziaris and Mikos, 2008). This process involves the balanced coordination of lamellar bone synthesis by osteoblasts, followed by hard callus resorption by osteoclasts (Marsell and Einhorn, 2009; Schindeler *et al.*, 2008). As I mentioned previously in more detail, osteoclasts (bone-degrading cells) developed from hematopoietic progenitors in mammals are the principal factors. These cells remodel the external bone surface and decrease the callus size restoring the original anatomy. This process takes a variable amount of time depending on the animal model.

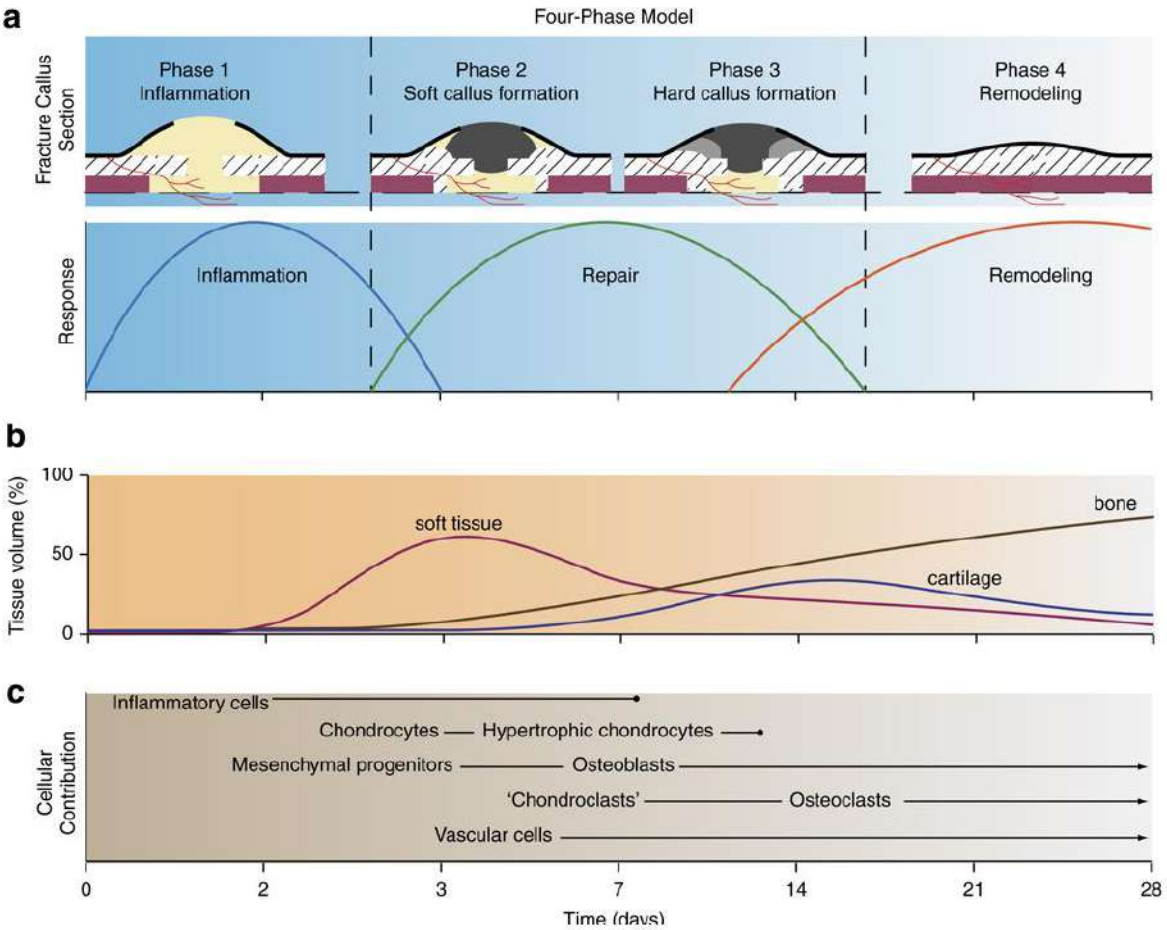

Figure 1.13. Schematic of fracture healing process in rats. The most studied animal model related to the topic. A, Three different overlapping stages occur during the fracture healing process: inflammation, repair (soft and hard calls formation) and remodeling. Inflammation is the first event to happen which triggers the next responses. Intramembranous bone and endochondral formations are part of the repair phase, the objective is to promote callus formation, essential to enhance new bone formation. Blood vessels invade the cartilaginous callus,

osteoclast-like cells resorb the calcified cartilage and osteoblasts build new bone. In the last part of the process, the callus decreases its diameter due to the participation of osteoclasts (bone remodeling cells).
C) It has been shown that a set of different cell types are involved in the fracture healing process. Modified from (Povinka and Dunstan., 2012).

1.5 Aims and Objectives

Mammals have only a limited capacity to regenerate some structures such as: skin, muscle, bone, blood or liver. They fail to regenerate other important structures or tissues such as the heart, retina, spinal cord or limbs. The potential of the regenerative capacity in animals varies across the animal kingdom.

Interestingly, the zebrafish has an outstanding regenerative capacity which makes it an important animal model for the research of its outstanding regenerative properties. Therefore, many human conditions such as injury, disease or aging have the potential to benefit from the usage of therapies based in regeneration knowledge. In addition, the zebrafish has also become a popular animal model to study skeletogenesis. Importantly, key regulators of bone formation are highly conserved between fish and mammals. Therefore, zebrafish can be used as a powerful tool to complement the skeletogenesis studies performed in classical models.

In recent years, regeneration after partial amputation of the tail fin in zebrafish has been studied by several researchers. However, it is not possible to compare this model with a bone fracture repair in humans. Therefore, in order to understand how skeletal cells regenerate which could be more comparable with a human bone fracture repair or other non-regenerating systems, Sousa and colleagues (2012) proposed a novel crush assay for adult bones in zebrafish fin rays that does not involve removal of tissue and is less disruptive than the classical model. Interesting results were found; thus, further research is needed.

Firstly, in this thesis we planned to go beyond continuing with the characterization of the novel zebrafish fracture model to find differences at the cellular and molecular level compared to what is already known in the mammalian fracture model during the different healing stages (inflammation, repair, remodeling). We focused our attention on inflammation stage which is the earliest event and essential to trigger the bone healing process.

Second, with the use of powerful zebrafish genetic tools such as the Cre-Lox technology, we wanted to determine which cell types contribute to the new tissue formation. This knowledge could provide molecular targets for the development of pharmaceuticals for enhanced skeletal regeneration, for example.

In this last section, unfortunately, negative results were obtained regarding the detection of founders and in other cases, the induction of spatio-temporal recombination in adult transgenic lines for the project objectives. These topics are explained and analysed in detail in the following chapters.

Question 1.

To what extent is the zebrafish fracture healing process like the mammalian model? Can we find differences at the cellular or subcellular level?

Aims:

Characterisation of the different fracture healing stages (inflammation, repair, remodeling) in zebrafish.

Inflammation:

- ROS production analysis.
- (IL1-β) cytokine production analysis.
- Role of neutrophil cells by using the *Tg (mpx:GFP)* transgenic line

Repair stage:

- Osteoblast cells (bone-forming cells) participation, (*osteocalcin* expression analysis)

Remodeling stage

- Osteoclast cells (bone degrading cells) participation, (*cathepsin K* and TRAP expression analysis).
- Generation of *tg (ctsk: Kaede)* and *tg (ctsk: creER2)* lines to enable tracking of osteoclast cells *in vivo*.

Question 2.

Different cell types could have a role during the bone fracture repair in zebrafish. In this process, which cells are recruited to promote repair? Do the same bone cells also ossify the break point?

- Generation of Cre driver transgenic lines, *tg (osc:creER-ins)* and *tg (twist2:creER2)* to enable tracking of bone cells *in vivo*.

CHAPTER 2

Materials and Methods

2.1 Zebrafish maintenance

Adult zebrafish (wild type and transgenic lines) were kept at 27 – 28°C with a 14 hours light and 10 hours dark cycle. Fish were supervised by the aquarium staff from BMS Department. (University of Sheffield). All tests with zebrafish manipulation were composed ahead as a Study Plan (ISP); this document was submitted to the aquarium manager in turn for its approval. Following this, experiments were carried out under supervision.

2.2 Fish manipulation and tail fin amputations / bone fracture injuries.

Adult zebrafish (6-12 months old) were anesthetized in 0.1 % benzocaine (Aminobenzoic acid ethyl ester, Ethyl 4-aminobenzoate**,** Sigma-Aldrich). To perform fin ray fractures in the tail, fish were set horizontally onto a Petri Dish. With the utilization of forceps, a single fracture was produced in a fin ray, in a zone proximal to the bifurcation of the dorsal fin rays (Figure 2.1). For most of the trials, the 2nd and 4th rays from both lobes (counting them from outer to inner) were damaged and the neighbors were left untouched as controls (occasionally the 3 th and 5 th rays were used instead if fins were heavily pigmented) . Occasionally, only one fin ray (central) was fractured in each lobe, whereas the rest were left untouched. After performing the injury, animals remained for some minutes in fish water to recover at 28.5 °C.

Tail fin amputations were done with a micro scalpel. A piece of tape was used as a surface while performing the removal. Fish stayed in fish water to recover at 28.5 °C as well.

For whole- mount *in situs*, the fracture injuries were performed as described above at different time points, animals were culled by a Schedule 1 procedure (anesthesia sobredosis) and then fixed (4% PFA).

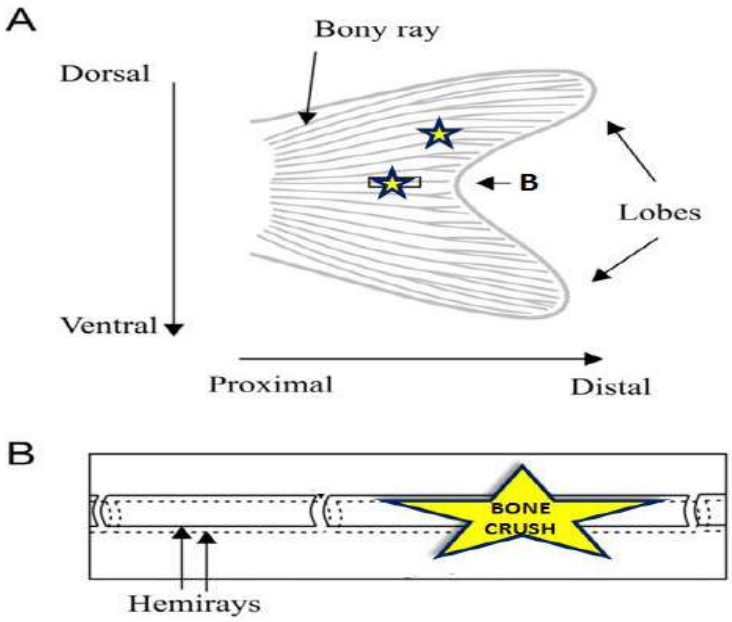

Figure 2.1 Adult zebrafish caudal fin scheme. (A) The caudal fin is composed by two lobes which contain bony fin rays. With the use of forceps, a single fracture was produced in a fin ray (stars). For live experiments, the 2nd and 4th rays from both lobes (counting them from outer to inner) were damaged and the neighbors were left untouched as controls. In some experiments, only one fin ray (central) was fractured in each lobe, whereas the rest were left untouched. (B) Detail of the crush of single bony ray.

2.3 Identification of tartrate resistant acid phosphatase (Trap) enzyme in zebrafish tail fins.

To detect Trap activity (Acid Phosphatase) in zebrafish tail fins, the Sigma-Aldrich Diagnostics Acid Phosphatase kit was utilized. Trap5b (tartrate resistant acid phosphatase) is commonly used in bone research as an enzyme that detects osteoclasts in mammals and other different animal models. Several compounds are used to form a final red precipitate *in situ* that can be visualized by microscopy.

Steps:

The fixing solution was made by adding (24 % Citrate Solution, + 65 % acetone, + 8 % (37 % of formaldehyde); tail fins were kept in this solution for 40 mins at room temperature (RT).

Several washes with PBST (3 x 5 mins) were done afterwards to eliminate the solution. Subsequently, different solutions were mixed to make Trap staining:

- Fast Garnet GBC and Sodium nitrate solutions were mixed, shacked and left for 2 min before use.
- (91 % deionised water (37°C), 2 % diazotonized Fast Garnet GBC solution, 1% Naphtol AS-BI Phosphate solution, 4% Acetate and 2% Tartrate solution) were mixed and added to the previous solutions.

Tail fins were kept with the staining during 3 hours in dark, rinsed with PBST (3x 5 mins), post-fixed in 4% PFA for 30 mins and stored in 75% glycerol. The samples were visualized by light microscopy.

2.4 DNA digestion

This procedure is used in the molecular biology field to manipulate or analyze DNA by using restriction enzymes.

DNA Digestion Steps:

- 1 microliter (ul) of DNA.
- 2 ul of buffer (depending on the enzyme).
- 2 ul of BSA (bovine serum albumin).
- 1 ul of restriction enzyme.
- Water to make a final volume of 20 ul.

The DNA digestion mix was put into an eppendorf tube and incubated into a metal rack at 37 °C for 2 hours.

2.5 DNA electrophoresis, DNA gel extraction.

DNA electrophoresis is also a procedure used in the molecular biology field to separate DNA by length through an agarose matrix.

Electrophoresis steps:

- Agar gel made at 1% concentration dissolved in a suitable buffer such as 1X TBE (Tris, Borate, EDTA) and Ethidium Bromide (EtBr).
- Addition of with 16 ul of the DNA digestion enzyme mix + 4 ul of loading dye (NEB company) + 3 -5 µl of 1 KB DNA ladder (NEB) to load the gel wells.
- The DNA bands were analysed under ultra violet (UV) light for detection.

2.6 DNA dephoshorylation.

In molecular biology, DNA dephosphorylation is needed to avoid plasmid self-ligation, for example. To overcome this, phosphate sides needed to be removed from DNA. Shrimp Alkaline Phosphatase (rSAP) enzyme from NEB, was used for this reaction as the following:

- 3 ul of rSAP reaction buffer
- 1 ul of rSAP enzyme
- 10 ul DNA
- 6 ul mQ H_20

2.7 Bacterial transformation

In molecular biology, bacterial transformation means the introduction of foreign DNA into the bacterial genome for a specific goal.

The protocol for bacteria transformation commonly used in Roehl`s lab is described as follow:

- Maintenance on ice of competent *E. Coli* cells during 10 minutes.
- Addition of 1-2 ul of the plasmid of interest into 25 ul of *E. Coli* cells.
- Maintenance of the mix on ice during 30 minutes.
- Heat shock step in hot bath at 42º C during 30 seconds.
- Maintenance on ice during 5 more minutes.
- Addition of 450 ul of Super Optimal Broth (SOC) medium at RT and placed in the shacker during 1 hour.
- Distribution of the mix in different agar plates containing a specific antibiotic (Ampycilin etc)
- Incubation at 37 °C overnight for growth.

2.8 Plasmid preparation (Miniprep, Midiprep)

Plasmid preparation is a method used for DNA extraction and purification. Plasmid miniprep and midipreps were used to get purified samples at high concentrations.

Miniprep preparation steps:

- Growth of the bacteria colony of interest inside a Falcon tube containing 2 ml of Lysogeny broth (LB) with the desired antibiotic. Conditions: 37º C overnight.
- After 24 hrs. cell recovery by centrifugation (3 minutes at 80,000 rpm.)
- Cell resuspension by addition of 200 ul of Resuspension Buffer (50mM Tris-Cl, pH 8.0, 10mM EDTA, 100ug/mL RNase A).
- Addition of 200 ul at RT. of Lysis Buffer (200mM NaOH, 1% SDS w/v).
- Addition of 200 ul of Neutralization buffer (3.0 M potassium acetate, pH 5.5)
- Centrifugation of the mix during 5 minutes at 250,000 rpm.
- Addition of chill isopropanol for DNA precipitation and kept at -20 C for 30 minutes.
- Pellet washes with 700 ul of PE buffer.
- Addition of 700 ul (TE buffer) and storage at -20º C.

Midiprep preparation steps:

- Growth of the bacteria colony of interest inside a Falcon tube containing 2 ml of Lysogeny broth (LB) with the desired antibiotic. Conditions: 37º C overnight during 6 hours.
- Use of the standard Qiagen Midiprep kit for plasmid amplification and purification.

2.9 Whole- mount *in situ* hybridization.

The purpose of this technique is to visualize the location of expressed RNAs in the entire structure (the fin tail in this project). In this process, synthetically produced RNA probes are first complementarily bound, or "hybridized," to the transcripts of target genes. This protocol was adapted from (Thisse *et al.*, 2008).

2.10 Probe synthesis.

Production of the template for probe synthesis was carried out by first amplifying a region of a stock plasmid containing the gene, or using primers, designed using primer3, from IDT (Table 1) to amplify zebrafish cDNA. Templates were then transcribed using their respective RNA polymerase. The PCR program was run for 35 cycles, each consisting of 45 seconds at 94°C; 30 seconds at 58°C; 120 seconds at 72°C.

Table 2.1 List of primers used for anti-sense probe synthesis.

Probe	Primers	RNA pol.	Source
IL-1β	drIL-1β: 5' ATGGCATGCGGGCAATATGA 3' drIL-1β:5' CTAGATGCGCACTTTATCCT 3'	T7	Probe provided by Renshaw's lab (BMS, Uni. Sheffield)
cathepsin K	ctskF: 5'CCTTAGTCCTCAGAACCTGGTG 3' ctskR: 5' ATCCAGTACTTCTTGCCTCTCG 3'	T7	Plasmid from Roehl's lab
osteocalcin	oscF: 5' CTGACACAGAAAGCGAACATG 3' oscR: 5' TGTGTGTGTGTAGAAGGGAATG 3'	T7	Plasmid provided by Cancela's lab (Uni of Algarve, Portugal)

For templates from cDNA an initial PCR reaction using specific primers was setup, the steps were the following:

- 2.5 μL 10X PCR Buffer
- 1 μL of a 1:3 NTP mix 0.5 μL TAQ DNA Polymerase
- 1 μL of 2.5 μM F1 and R1 primers
- 1 μL cDNA 18 μL MilliQ H2O

Templates from plasmid used the PCR reaction below only. After the first – nested –PCR the amplification product was carried over:

- 20 ng plasmid / 1 μL nested PCR amplification in 85 μL H2O
- 10 μL 10X PCR Buffer
- 1 μL NTP mix 2 μL TAQ DNA polymerase
- 1 μL of primer F2 and R2-T3/7 at 25 μM

The PCR products were purified using centrifugal filter units (Millipore: UFC505024) according to manufacturer's instruction. Finally, DNA was quantified using a spectrophotometer.

Transcription:

- 1 μg DNA template in 21 μL H2O
- 3 μL Transcription buffer 10X (NEB)
- 3 μL Digoxigenin-RNA labelling mix (Roche) 1.5 μL RNase Inhibitor, murine (NEB: M0314)
- T3/T7 RNA polymerase

Last steps of probe synthesis:

- Incubation of reaction mix for 2 h at 37°C.
- Addition of 2 uL RNase-free DNase I (NEB, M0303).
- Addition of 18 μL depc H20.
- Incubation for 30 min. at 37º C.
- Filtration of transcription mix through (Sigma-Aldrich, S5059) columns.
- Addition of 14 μL RNA later (Sigma, R0901).
- Validation by analysis on a 1% agarose gel.

2.11 *In situ* hybridization (ISH) protocol.

- Tail fin fixation and storage - 4% PFA in PBS overnight at 4°C.
- PBST washes (X2) for 2 minutes.
- Methanol series (30%, 60%, 100%).
- Rehydration process- by reverse methanol series and PBST washes.
- Sample digestions with 10 μg/mL Proteinase K at RT during 45 minutes.
- Refixation in 4% PFA for 20 min.
- PBST washes (4 X 5 min).

- Prehybridization step –

- Incubation of samples in the hybridization solution (+) for 2 hours at 70°C.
- Solution replacement with fresh Hyb (+) containing 1 to 4 μl of the RNA probe.
- Incubation of samples overnight at 70º C for hybridization.

- Washing series - 2xSCCT/Hyb (+) – Different dilution percentages (25%, 50 % and 75%).
- Washing of samples (x2) in PBST, at RT.
- Blocking, tail fins kept in blocking buffer (sheep serum, BSA) for 3 hours at RT.
- Anti-DIG antibody addition (1:10000; Roche, USA) with fresh blocking buffer and left overnight at 4º C.
- Washing of samples (x6) in PBST.
- Staining Buffer incubation for 1-3 hours.
- Addition of PBST 1mM EDTA for 15 min.
- Methanol series and maintenance of samples in 100% MeTOH for 2 hours at RT.
- Washing of samples in in PBST (x2) for 5 min.
- Bleaching step - (hydrogen peroxide) for 10 min at 37°C.
- Tail fin washes in PBST (x3) for 5 min.
- Glycerol series (50 and 70%) for storage.

2.12 Reactive oxygen species (ROS) detection.

The compound 2', 7'- dichlorofluorescin diacetate (H_2DCFDA, ThermoFisher Scientific) was used to monitor the accumulation of reactive oxygen species in adult zebrafish fin. Fluorescent DCF was formed thorough ROS oxidation. This method is useful to provide an overview of general ROS production.

ROS detection procedure:

- Incubation of adult zebrafish with H_2DCFDA (30μM) during 15 minutes.
- Anesthetization with (0.1 % benzocaine).
- Injury - amputation or bone fracture procedure.
- Imaging – anesthetized fish (horizontal position).

- Microscopy details: Zeiss fluorescence microscope, using excitation sources and filters appropriate for fluorescein detection. ROS indicator specifications: Ex/Em: ~492–495/517–527 nm.

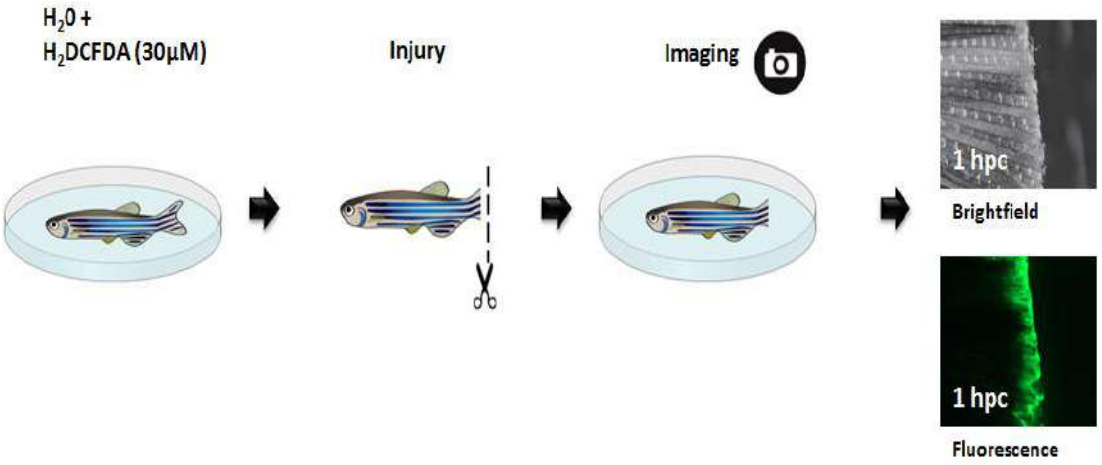

Figure 2.2 ROS detection in adult zebrafish. Wt adult zebrafish were incubate with H_2DCFDA (30µM) during 15 minutes and anesthetized (0.1 % benzocaine) for amputation or bone fracture. Immediately, fish were kept anesthetized for imaging. Fluorescence was monitored using a Zeiss fluorescence microscope, using excitation sources and filters appropriate for fluorescein detection**.**

2.13 Zebrafish imaging

- *In situ* analysis- ProgRes R camera and its image capture software were used.
- Fluoresce analysis - Zeiss fluorescence microscope.

2.14 Microinjection and screening for stable transgenic lines.

DNA constructs generated for this thesis (described in detail in the next Chapters) were injected into AB wild-type zebrafish at the one-cell.

Procedure:

- Mix of: construct of interest + tol2 transposase mRNA (25 ng/µl final concentration of both).
- Microinjections: a) micro injector (World Precision Instrument, USA), b) dissecting microscope (Leica Microsystem GmbH, Wetzler, Germany) and c) glass capillary needles (Kwik-Fil Borosiliocate Glass Capillaries, World Precision Instruments Inc, USA)
- Embryos incubation in with E3 medium (5 mM NaCl, 0.17mM KCl, 0.33mM CaCl2, 0.33mM MgSO4 plus 0.000001 Methylane Blue)- 28°C for 3 days.
- Fluorescence microscope analysis - positive fish larvae expressing GFP in the eyes (genome integration marker) were collected into Petri dishes (50 positive embryos approximately) containing E3 medium.
- Fish maintenance to adulthood – 5 dpf. embryos sent to the Sheffield University aquarium facility until sexually mature.
- F2 obtainment by out crossing of generations with wild type AB stains and selection of positive fish (GFP expression in the eyes).

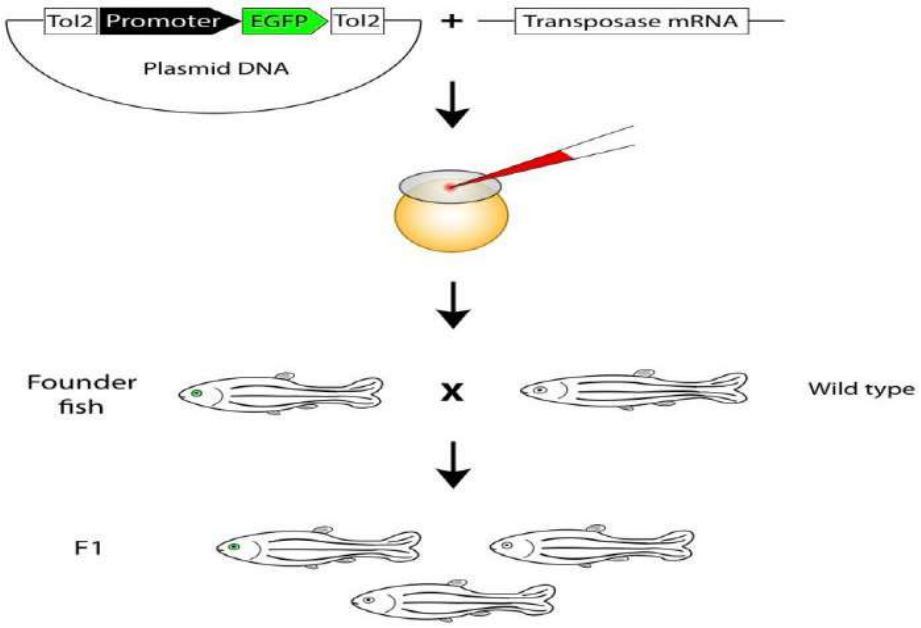

Figure 2.3. Transgenic zebrafish lines generation. Firstly, the DNA construct is designed to have a transgene marker (*alpha crystalline* promoter) for easy detection of positive fish. For injections, a mix of the construct of interest + tol2 transposase mRNA is incorporated into the cell of the fertilized egg. Afterwards, founder fish and its progeny will be detected by expression of EGFP in the eyes. (Mater Methods. 2012; 2:109).

.

2.15 Generation of Cre/lox double transgenic zebrafish lines.

Table 2.2, shows the set of the different stable Cre driver transgenic lines generated for this thesis (each described in detail in the next chapters) and their controls (Cre driver lines previously generated by lab members). All the lines were crossed with two different Cre-dependent reporter lines, Tg(*EF1a: loxPGFPloxP-DsRed*) or Tg(*ubiquitin:loxPGFPloxP-mCherry*) and raised to adulthood to test Cre recombination in the target tissue by tamoxifen administration.

Table 2.2 Double transgenic lines generated for Cre-Lox based experiments

Cre driver transgenic line	Reporter transgenic line	Cre/lox double transgenic line	Target tissue
Tg (osc:creERT2-ins)	*Tg (EF1a: loxPGFPloxP-DsRed)*	*Tg (osc:creERT2-ins; EF1a-DsRed)*	Osteoblasts
Tg (osc:creERT2-ins)	*Tg (ubiquitin: loxPGFPloxP-mCherry)*	*Tg (osc:creERT2-ins; ubi-mCherry)*	Osteoblasts
Tg (osc:ERT2creERT2-ins)	*Tg (EF1a: loxPGFPloxP-DsRed)*	*Tg (osc: ERT2creERT2-ins; EF1a-DsRed)*	Osteoblasts
Tg (osc:ERT2creERT2-ins)	*Tg (ubiquitin: loxPGFPloxP-mCherry)*	*Tg (osc: ERT2creERT2-ins; ubi- mCherry)*	Osteoblasts
Tg (twist2:creERT2)	*Tg (EF1a: loxPGFPloxP-DsRed)*	*Tg (twist2:creERT2; EF1a-DsRed*	Mesenchymal cells
Tg (twist2:creERT2)	*Tg (ubiquitin: loxPGFPloxP-mCherry)*	*Tg (twist2:creERT2-ins; ubi-mCherry)*	Mesenchymal cells
Controls			
Tg(fli1a:ERT2CreERT2)	*Tg (EF1a: loxPGFPloxP-DsRed)*	*Tg (fli1a:creERT2; EF1a-DsRed*	Blood/Endothelium
Tg(fli1a:ERT2CreERT2)	*Tg (ubiquitin: loxPGFPloxP-mCherry)*	*Tg (fli1a:creERT2-ins; ubi-mCherry)*	Blood/Endothelium
Tg(nestin:ERT2CreERT2)	*Tg (EF1a: loxPGFPloxP-DsRed)*	*Tg (nestin:creERT2; EF1a-DsRed*	Neurons
Tg(nestin:ERT2CreERT2)	*Tg (ubiquitin: loxPGFPloxP-mCherry)*	*Tg (nestin:creERT2-ins; ubi-mCherry)*	Neurons

2.16 Pharmacological treatments for Cre^{ERt2} induction and live imaging.

To exemplify Cre recombination after Tamoxifen administration in fish, the following scheme illustrates the process during larvae stage.

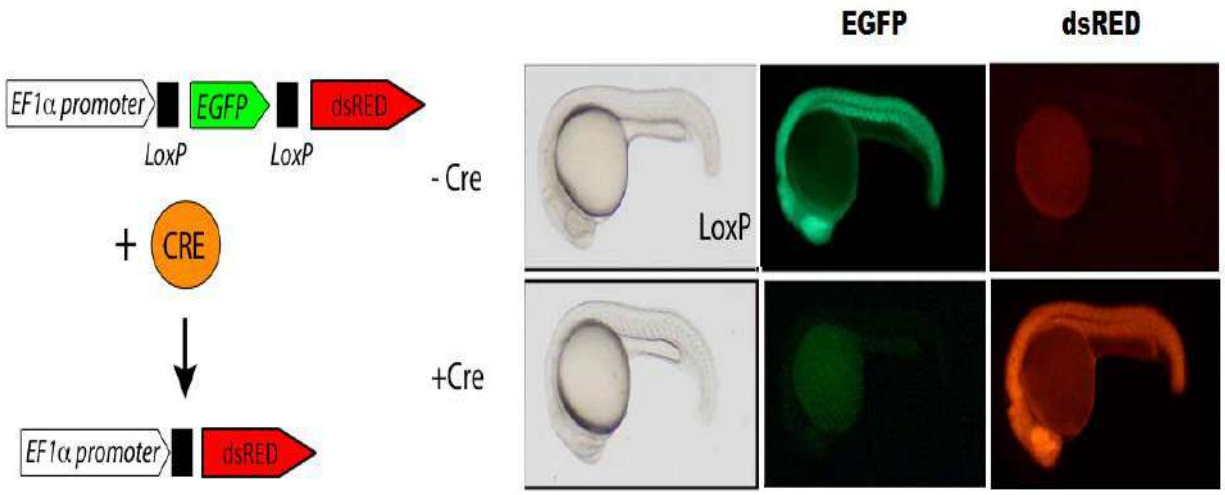

Figure 2.4 Cre-induced recombination in zebrafish. To induce CreERT2 recombination, Tamoxifen (TAM) or 4-OHT administration in the water is needed. Without drug addition, EGFP is expressed in the whole body due to the EF1 promoter effect in this scenario. After drug administration, dsRED expression is detected due to the elimination of the EGFP cassette. Adapted from (Hans *et al.*, 2009).

Tamoxifen administration to induce Cre recombination in adult fish:

- Dissolution of Tamoxifen (Sigma) or 4-Hydroxytamoxifen (4-OHT) (Sigma) in DMSO or 100% ethanol respectively for 2 hours at 70 ºC. 10Mm final concentration aliquots.
- Warm up at 70°C for drug administration.
- Fish acclimatization inside an incubator (28 °C during 4 - 5 days).
- Soaking of fish in water with specific drug concentration depending on treatment. Controls - Vehicle DMSO or ethanol were added in the water with the same experimental concentrations.

Drug treatments

- Incubation overnight of fish in dark with a specific drug concentration (light-sensitive chemicals).

- Recovery period, change to fresh water without chemicals.
- Injury procedure (fracture or amputations).
- Imaging- Analysis at different time points post- injury to detect tissue recombination. The recombined tissue should express the DsRed fluorescent protein. Fish were imaged using the ZEN pro software. (Figure 2.5)

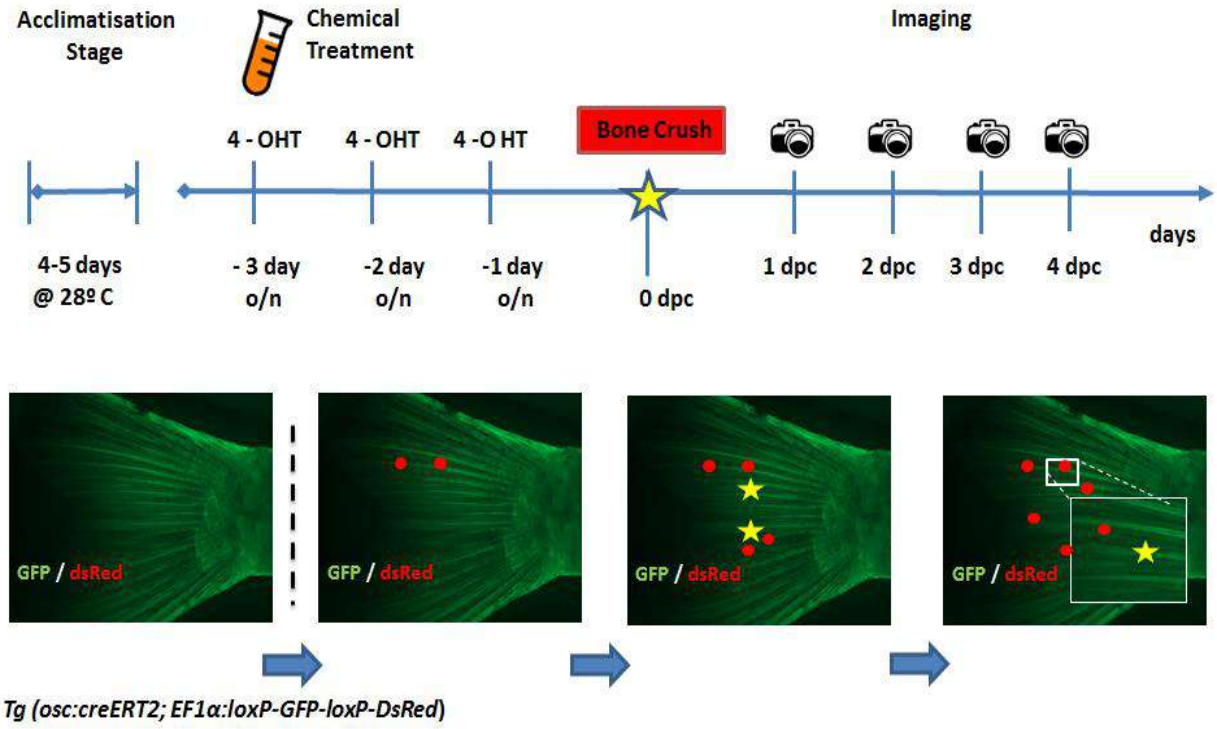

Figure 2.5 Experimental strategy scheme for Cre^{ERt2} induction and exemplification. The *Tg (osc:creERT2; EF1a:loxP-GFP-loxP-DsRed)* transgenic line is showed to represent the expected results. Tamoxifen or 4-OHT were administrated to induce tissue-specific recombination of few cells in the tail fin, positive samples could start to express dsRed fluorescent protein. Subsequently, fish will be injured (stars) and photographed at different time points, to detect and track cells of interest.

2.16.1 Jopling`s strategy to induce Cre^{ERt2} recombination in adult tail fins.

This protocol is similar to the described above with drug concentration and number of treatments as the main differences. The treatment was shared by members from Jopling´s lab (Uni. of Montpellier. France).

- Incubation overnight of fish with **4-OHT at a 3uM final concentration** in dark.
- Injury procedure (fracture or amputations).
- Imaging- Analysis at different time points post- injury to detect tissue recombination. The recombined tissue should express the DsRed fluorescent protein. Fish were imaged using the ZEN pro software. (Figure 2.6)

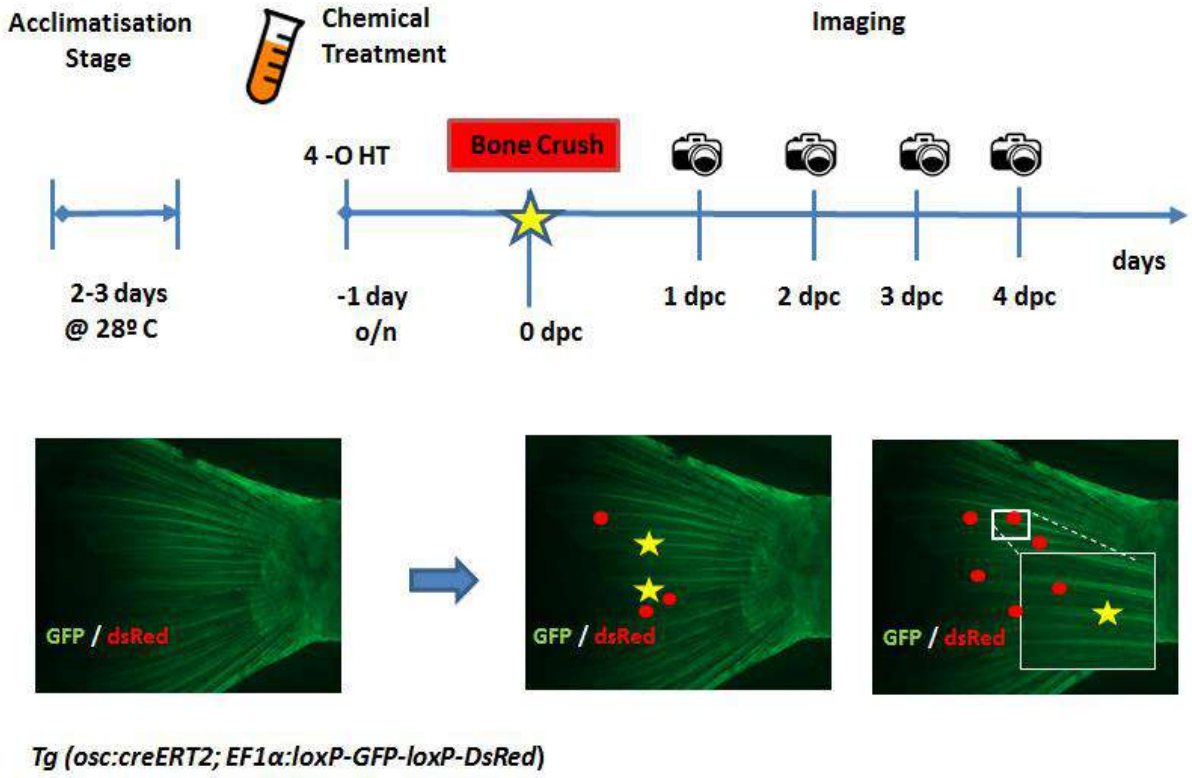

Tg (osc:creERT2; EF1α:loxP-GFP-loxP-DsRed)

Figure 2.6 Jopling`s experimental strategy for Cre^{ERt2} recombination. The *Tg (osc:creERT2; EF1a:loxP-GFP-loxP-DsRed)* transgenic line is showed to represent the expected results. A single session of fish soaked in tank water for 8 hours long with 4-OHT at a 3uM final concentration was performed to induce Cre^{ERt2} recombination. Subsequently, fish were injured and immediately photographed at different time points to detect cell recombination. The recombined tissue should express the DsRed fluorescent protein.

CHAPTER 3.

Characterisation of the different fracture healing stages in zebrafish.

3.1 Introduction

The fracture healing process involves the coordination of several cells and molecules that will repair the damaged tissue (Einhorn and Gerstenfield, 2015; Fergurson *et al.,* 1999; Einhorn 1998). In mammals, this process is divided into three stages: inflammation, repair and remodeling. In each step, specific cells and molecules are induced to form the environment of healing (Marzona and Pavolini, 2013; Schindeler *et al*., 2008); these steps overlap each other, and it is difficult to separate them. In general, the healing process is regulated by a balance between removal of damaged tissues and new tissue formation, which is regulated primarily by osteoclasts and osteoblasts. Osteoclasts are bone resorbing cells that work catabolically to remodel the bone, and osteoblasts are bone forming cells important to calcify fractured bones and repair them after damage (Marzona and Pavolini, 2013).

In this part of the project, I planned to go beyond continuing with the characterization of the novel zebrafish fracture model proposed by Sousa and colleagues (2012). Interestingly, in the last years, there were a growing number of publications focused on zebrafish caudal fin epimorphic regeneration following an amputation (Poss, 2010). But, information regarding the regeneration process that occurs after a bone fracture in zebrafish was unknown. With this intention, I took advantage of the adult zebrafish bone fracture model to find differences at the cellular and molecular level compared to what is already known in the mammalian fracture model. Thus, the different healing stages (inflammation, repair, remodeling) were tried to been characterised and compared. Moreover, I focused my attention on the first cellular events that triggers the bone healing process, such as inflammation response.

3.2 Results

3.2.1 Inflammation Stage

3.2.1.1 Rapid *IL1-β* acute inflammatory response before 24 hours post fracture.

The first cellular process to occurs during the fracture healing process is the acute inflammatory response that involves the production of several important molecules. One of these molecules is Interleukin-1 (IL-1 *β*) which is an important activator known as the 'gatekeeper' of inflammation (Dinarello *et al*., 2011) released mainly by macrophages, endothelial cells, B cells and fibroblasts (Dunne and O'Neill, 2003; Subramaniam *et al.,* 2004). In order to characterise the cellular inflammatory response that occurs during the fracture healing process in adult zebrafish, a 24-hour time course *in situ* hybridisation for IL-1 β was performed in wild-type fish. The second and fourth rays (counting them from outer to inner) were crushed using forceps, neighbors were left untouched as controls. *IL1-β in situ* showed a rapid expression at the fracture sites, whereas a high peak response was detected at 8 hours post crush (Figure 3-1). No expression was detected on the neighbour rays (controls). These results were consistent with an early role of IL1-β response after injury (fin amputation) in zebrafish larvae (Ogryzko et al., 2014), and during *in vivo* studies (bone fracture) in mice (Einhorn *et al*., 1995; Kon *et al*., 2001; Rundle *et al*., 2006; Lange *et al.,* 2010).

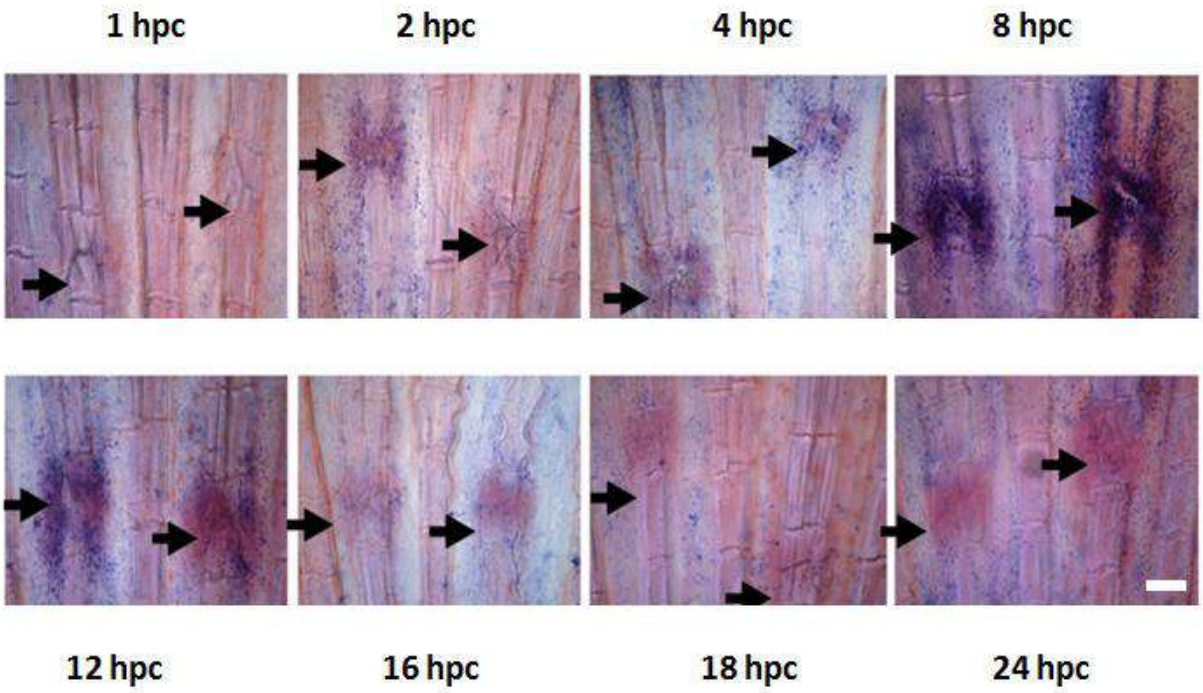

Figure 3-1. Rapid *IL1-β* acute inflammatory response before 24 hours post fracture. Time course *IL1-β in situ* hybridisation shows a high peak response at 8 hours post crush (hpc). For bone fractures in the caudal fin (black arrows), wild-type adult zebrafish were anesthetized in 0.1% tricaine and only the second and fourth rays (counting them from outer to inner) were crushed using forceps; neighbors were left untouched as controls. Experimental numbers) n = 3 fish with 12 fractured rays for each time point. 12/12 rays without signal at the fracture sites (1hpc), 7/12 rays with signal at the fracture sites (2 hpc), 8/12 with signal (4 hpc), 9/12 with strong signal (8 hpc), 10/12 with strong signal (12 hpc), 7/12 without signal (16 hpc), 10/12 without signal (18 hpc), 11/12 without signal (24 hpc). A representative picture was used per time point. Scale bar corresponds to 100 μm in all panels. Hours post crush (hpc).

3.2.1.2 Rapid neutrophil cells recruitment at the injury sites in Tg *(mpx:GFP)* line after bone crush

Due to the special interest on early events that occur after the bone fracture repair, which are essential to trigger this process, we focused on time points before 24 hours to assess how fast cells are recruited at the fractured sites. To better understand the dynamics of the inflammatory response, I have taken advantage of the transgenic line Tg *(mpx:GFP)* kindly provided by Renshaw´s lab (BMS department, Uni of Sheffield) in which neutrophils are visualized with

fluorescence. The *mpx* promoter has been used in previous studies as a neutrophil marker in zebrafish (Bennett *et al.*, 2001; Lieschke *et al.*, 2001). After inducing bone damage, data showed that neutrophil recruitment started rapidly after few hours post-crush, these cells accumulated through time at the fractured sites (Figure 3-2); this was also consistent with an early role of neutrophils in response after injury as observed in zebrafish larvae (Renshaw *et al.*, 2006) and in mice *in vivo* studies (Kubes and Mehal, 2012; Woodfin *et al.*, 2011). A peak accumulation was observed at the injury sites between 12 to 20 hpc. Moreover, neutrophils were resident in the uninjured adult fin tissue.

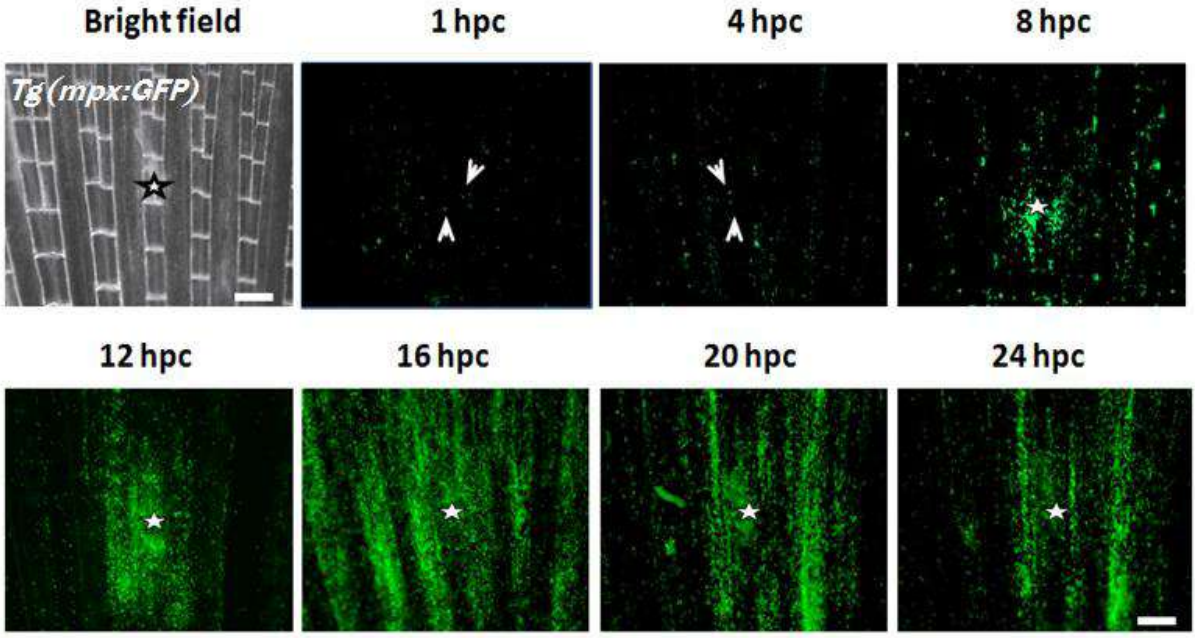

Figure 3-2. Rapid neutrophil recruitment at the injury sites in Tg *(mpx:GFP)* line after bone crush. Representative images showing a 24 hours time course of neutrophil accumulation in *Tg (mpx:GFP)* line. (Stars) indicate the bone crush sites, neighbor rays were left untouched as controls. After inducing bone damage, neutrophil recruitment started since 1 hpc; this was consistent with an early role in response after injury. A peak accumulation was observed at the injury sites between 12 to 20 hpc. Experimental numbers) n = 4 fish with 8 fractured rays for each time point. 8/8 rays with weak GFP+ signal at the fracture sites (1hpc), 7/8 rays with weak GFP+ signal at the fracture sites (4 hpc), 8/8 with GFP+ signal (8 hpc), 6/8 with strong GFP+ signal (12 hpc), 7/8 with very strong GFP+ signal (16 hpc), 8/8 with GFP+ signal (20 hpc), 8/8 with GFP+ signal (24 hpc). (hpc) hours post crush. The scale bars represent 100 μm.

3.2.1.3 ROS is induced early after damage; its production is sustained after fin amputation but not in the bone fracture model.

Reactive oxygen species (ROS) is a rapid signal originated from the wound epithelium that mediates early leukocyte recruitment in zebrafish larvae (Niethammer *et al.*, 2009). Injury-induced ROS production through the first 24 hpc was detected in live adult wild-type zebrafish by using the free permeable radical sensor (H_2DCFDA). A bone fracture was performed in anesthetized fish and fluorescence was monitored through microscopy. Fish amputations were performed as control and for comparison. Data shows that since the first hour after inducing damage, ROS was detected localised at the fracture site, and was produced uniformly at the level of the amputation plane (Figure 3-3 b, f). After 4 hours post- injury (hpi), ROS was detected in both models (Figure 3-3 c,g). At 12 hpi ROS was not detected at the fracture site or further time points (Figure 3-3 h, m-p). Surprisingly, in the amputation model, ROS was still detected at 4 hpi and its production remained until 20 hpi (Figure 3-3 d, i-k). By 24 hpi, ROS was no longer detected in the amputation plane (Fig 3-3 l). These results show that after injury, ROS is induced early and its production depends on the lesion type. Also, it suggests that regarding fin regeneration, it could be possible that ROS length production is necessary to induce mechanisms which are not required for wound repair.

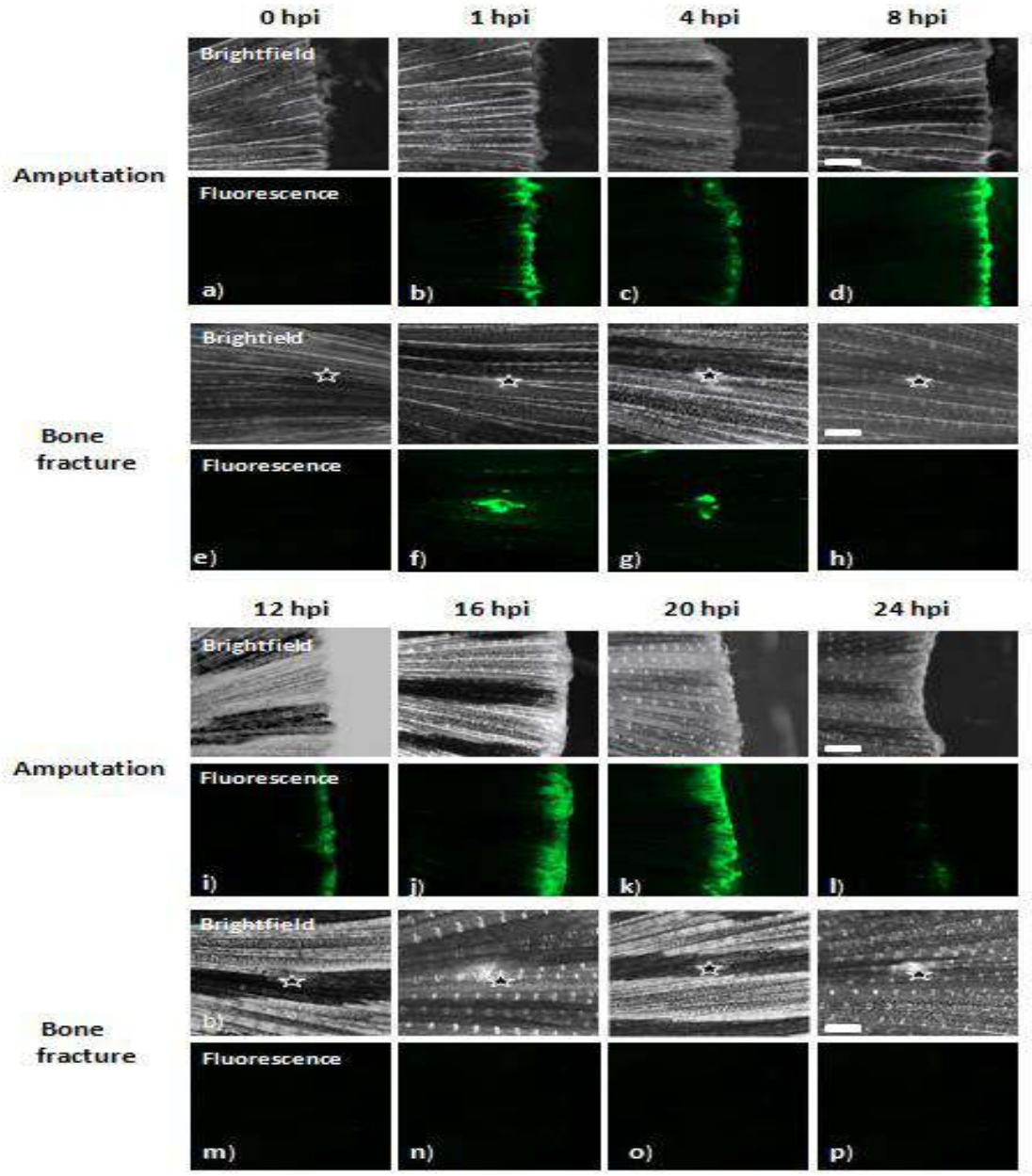

Figure 3-3. ROS production is sustained after fin amputation but not in the bone fracture model. Time course to detect ROS production with a fluorescent probe (H_2 DCFDA) in adult wt fish. A bone fracture was performed in anesthetized fish and fluorescence was monitored by microscopy; Fish amputations were performed as control and for comparison. Data shows that since the first hour after inducing damage, ROS were detected localized at the fracture site and uniformly at the level of the amputation plane after amputation (b, f). After 4 hours post- injury (hpi), ROS were detected in both models (c, g). Surprisingly, at later time points, ROS were not produced at the fracture site or elsewhere (h, m-p). In contrast, ROS were still detected and its production remained until 20 hpi (d, i-k). By 24 hpi, ROS could not be longer detected in the amputation plane (l). Experimental numbers) For each time points, n = 3 fish (Amputations) / n = 3 fish (Fractures); 8 fractured rays in total. Amputations, 3/3

fish without fluorescence (0 hpi), 3/3 fish with fluorescence at the amputation site (1 hpi), 3/3 with fluorescence (4, 8 and 12 hpi), 2/3 with strong fluorescence (16 hpi), 3/3 with fluorescence (20 hpi), 3/3 very low fluorescence (24 hpi). Fractures - 8/8 rays without fluorescence at the fracture site (0 hpi), 7/8 rays with fluorescence at the fracture site (1 hpi), 4/8 with fluorescence (4 hpi), 8/8 rays without fluorescence (8- 24 hpi). A representative picture was used per time point. hours post-injury (hpi). Scale bars represent 200 μm.

3.2.2 Repair stage

3.2.2.1 New bone was formed after 3 days post damage at the fractured sites .

After inflammation, the repair stage begins when the cartilaginous callus formation appears and bone formation occurs (Einhorn and Gerstenfield, 2015). In mammals, bone repair is characterized by high levels of osteoblast activity and represents the most active period of osteogenesis, leading to formation of mineralized bone matrix (Shapiro F, 2008). Monika Tomecka, a colleague from the laboratory performed Alizarin Red (bone) and Alcian Blue (cartilage) staining during several days after performing fractures, to follow the cartilage-bone transition mentioned previously. At day 3 and 4 post fracture, Alcian blue-positive tissue was highly stained at the fracture sites (Figure 3-4, A) but it decreased the following healing days. Whereas Alizarin red- positive calcified tissue was absent before 4 dpc and the staining increased considerably since 5 dpc which was still detected the following healing days (Figure 3-4, B). These data indicate that bone repair started by the newly Alizarin red-positive calcified bone via the Alcian blue-positive tissue.

.

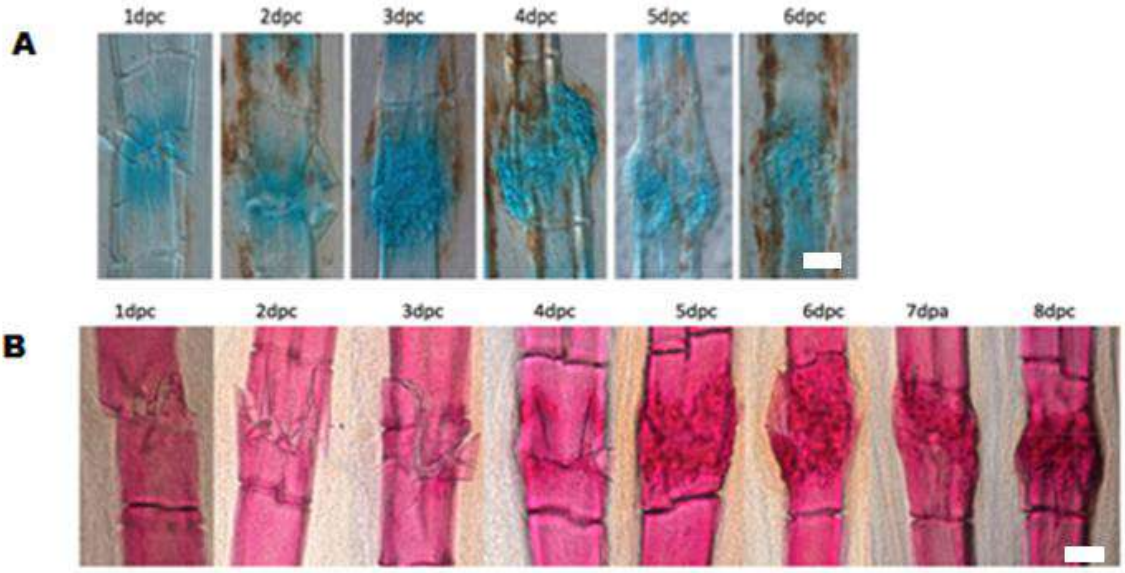

Figure 3-4. Cartilage was replaced by bone during the fracture healing process in zebrafish. Alcian Blue (cartilage) and Alizarin Red (bone) stainings were performed on fractured rays at different days to follow the cartilage-bone repair. At day 3 and 4 post fracture, (A) Alcian blue-positive tissue was highly stained at the fracture sites (3 and 4 dpc) and it decreased the following healing days. (B) Whereas Alizarin red- positive calcified tissue was absent before 4 dpc and the staining increased considerably since 5 dpc which was still detected the following healing days. Experimental numbers) n = 3 fish with 12 fractured rays for each time point. A) Alcian Blue (cartilage): 12/12 rays with weak blue staining at the fracture sites (1dpc), 10/12 rays with weak blue staining at the fracture sites (2 dpc), 9/12 with staining (3 dpc), 10/12 with strong staining (4 dpc), 12/12 with staining (5 dpc), 10/12 with staining (6 dpc). B) Alizarin Red (bone): 10/12 rays without red staining at the fracture sites (1dpc), 9/12 without red staining (2 dpc), 7/12 without red staining (3 dpc), 18/12 with weak staining (4 dpc), 9/12 with strong staining (5 dpc), 10/12 with strong staining (6 dpc), 10/12 with staining (7 dpc), 6/12 with staining (8 dpc). dpc. days post crush. The scale bars represent 100 μm

As osteocalcin is produced by mature osteoblasts, it is often used as a marker for the bone formation process (Shapiro F, 2008). To confirm osteoblast activation at the gene expression level by the bone fracture event, whole-mount *osteocalcin in situ* hybridizations were performed in wild-type adult zebrafish for this purpose; whereas fin amputation was used as a control. *Osteocalcin* was not expressed at 1 one day-post-injury (dpi) in both models (Figure 3-5. a, e). Later, at 3 dpi, *osteocalcin* induction started at the fractured sites, but not at unfractured rays used as controls (Figure 3-5, b), this was also detected at the amputation plane (Figure 3-5, f). *osteocalcin* expression was also detected in both models at 5 dpi (Fig 3-5. c, g) and at 7 dpi (Figure 3-5. d,

h). These data support results found in the previous experiment (Figure 3-4) indicating that new bone is formed at the fractured sites for repair.

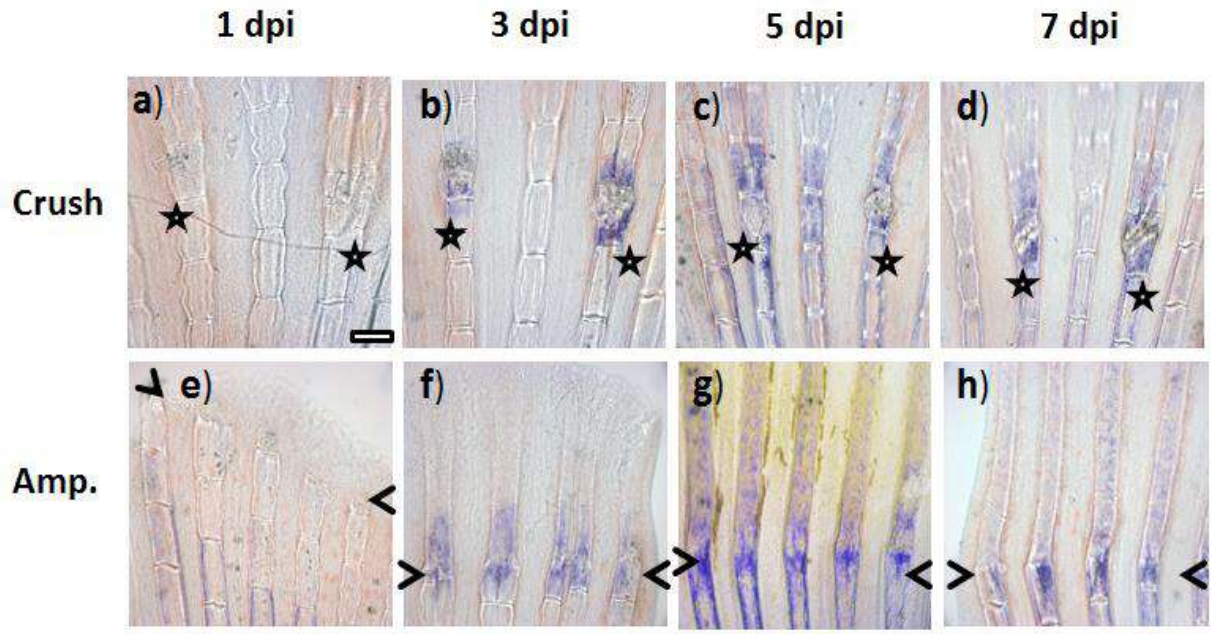

Figure 3-5. Osteocalcin is expressed at the fractured sites after 3 days post injury. Time course whole- mount osteocalcin *in situ* hybridization**.** *Osteocalcin* was induced on damaged rays after bone fracture and fin amputation since 3 dpi (b, f), expression was detected at 5 dpi (c, g) and still detected at 7 dpi (d, h) in both models. For bone fractures in the caudal fin (black stars), wild-type adult zebrafish were anesthetized in 0.1% tricaine and only the second and fourth rays (counting them from outer to inner) were crushed using forceps; neighbors were left untouched as controls. Amputations were performed with a scalpel. Arrowheads indicate the amputation plane. Experimental numbers) Crush, n = 3 fish with 12 fractured rays in total for each time point. Amputations, n = 3 fish for each time point. Crush - 12/12 rays without signal at the fracture sites (1dpi), 9/12 rays with signal at the fracture sites (3 dpi), 8/12 with signal (5 dpi), 10/12 with signal (7 dpi). Amputations - 12/12 rays without signal at the fracture sites (1dpi), 9/12 rays with signal at the fracture sites (3 dpi), 8/12 with signal (5 dpi), 10/12 with signal (7 dpi). Amputations- 3/3 fish without signal at the amputated site (1dpi), 3/3 with signal (3 dpi), 3/3 with signal (5 dpi), 3/3 with signal (7 dpi). Scale bar corresponds to 100 μm in all panels. (dpi) – days post injury.

3.2.3 Remodeling stage

Bone remodeling is essential for repairing and optimizing bone structures for mechanical function, these processes are mediated by specialized bone resorbing cells called the osteoclasts (Raggat and Patridge, 2010; Shapiro F, 2008). In mammals, osteoclasts express crucial molecules such as tartrate resistant acid phosphatase (TRAP) and cathepsin K (CTSK) that regulate bone shape (Boyle *et al.,* 2003).

Receptor activator of nuclear factor-κB ligand (RANKL), a member of the TNF (tumor necrosis factor receptor) superfamily, is expressed by osteoblasts and is the primary mediator of osteoclastogenesis (Lacey *et al.,* 1998). Through the interaction with its receptor RANK, which is expressed on osteoclasts and their precursors, RANKL promotes osteoclast differentiation, fusion and activation (Lacey *et al*., 1998).

3.2.3.1 Bone is remodeled during two stages of the fracture healing process in adult zebrafish

In mammals, during the fracture healing process, osteoclasts take part at two different moments. In the first instance, these osteoclasts initially play a role in the removal of the broken bone and a second step is necessary to remodel the new bone (Schindeler *et al*., 2008). In order to determine the role of these cells in my fracture model (6 days-post-fracture), two different methods to detect osteoclast activity were performed. First, cathepsin K *in situs* showed that cells expressing cathepsin K were detected from 1 dpc until 3 pdc at the fracture sites (Fig. 3-6 a-c) but not at later time points (d-f). Neighbor rays were left untouched as controls and did not show osteoclast recruitment. Furthermore, TRAP (+) cells were detected from 1dpc and remained through the fracture healing at the crush sites (Fig. 3-6, g-l). Interestingly, TRAP enzyme remained over the remodeling bones despite the absence of *ctsk* (+) cells.

Our results suggest that bone is remodeled at two stages during the fracture healing process in adult zebrafish, like mammalian studies (Schindeler *et al*., 2008).

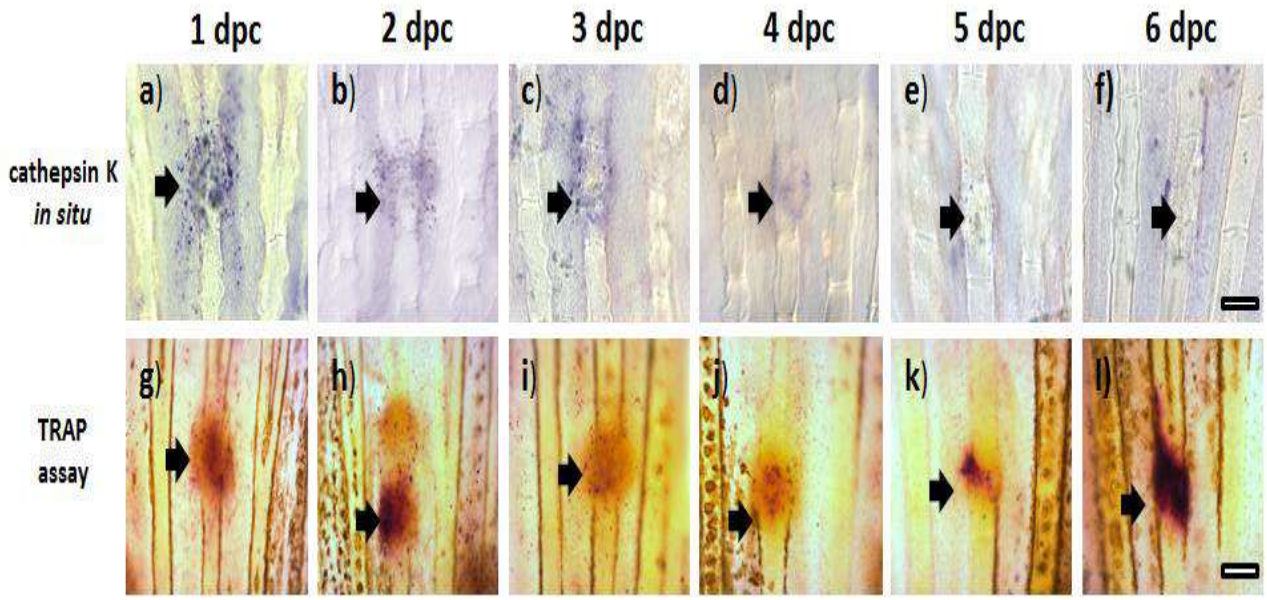

Figure 3-6. Osteoclastic activity over the course of bone healing. Time course experiment for osteoclast activity detection during the fracture healing process. TRAP (+) and cathepsin K positive cells, were detected at the bone crush sites over 6 days. TRAP assay and ctsk *in situ* experiments were performed respectively. Cells expressing cathepsin K were detected from 1dpc until 3 pdc at the fracture sites (a-c) but not at later time points. Furthermore, TRAP activity was detected from 1 dpc and remained through the fracture healing at the crush sites. For bone fractures in the caudal fin, a ray from wild-type adult zebrafish was crushed using forceps, neighbors were left untouched as controls. Experimental numbers, n = 3 fish with 12 fractured rays in total for each time point in both assays. Cathepsin K *in situ* - 11/12 rays with signal at the fracture sites (1dpc), 9/12 rays with signal (2 dpc), 7/12 with signal (3 dpc), 6/12 without signal (4 dpc), 8/12 without signal (5 dpc), 11/12 without signal (6 dpc). TRAP assay - 11/12 rays with staining at the fracture sites (1dpc), 7/12 rays with signal (2 dpc), 8/12 with signal (3 dpc), 6/12 without signal (4 dpc), 8/12 with signal (5 dpc), 9/12 with signal (6 dpc). Arrowheads indicate the bone crush sites. Scale bar corresponds to 100 μm. (dpc)- days- post -crush.

Focused on early time points, a 24 hrs time course ctsk *in situ* was performed to detect osteoclast activity during the first hours post fracture. I found that the first osteoclast cells to be recruited at the fractured site appeared at 12 hours post crush but not before this time (Figure 3-7). In the following time points, from 16 to 24 hpc, it seems that the cell number increased at the fracture sites. This result suggests that activate osteoclasts respond fast after bone damage; its role is important during the first hours post fracture.

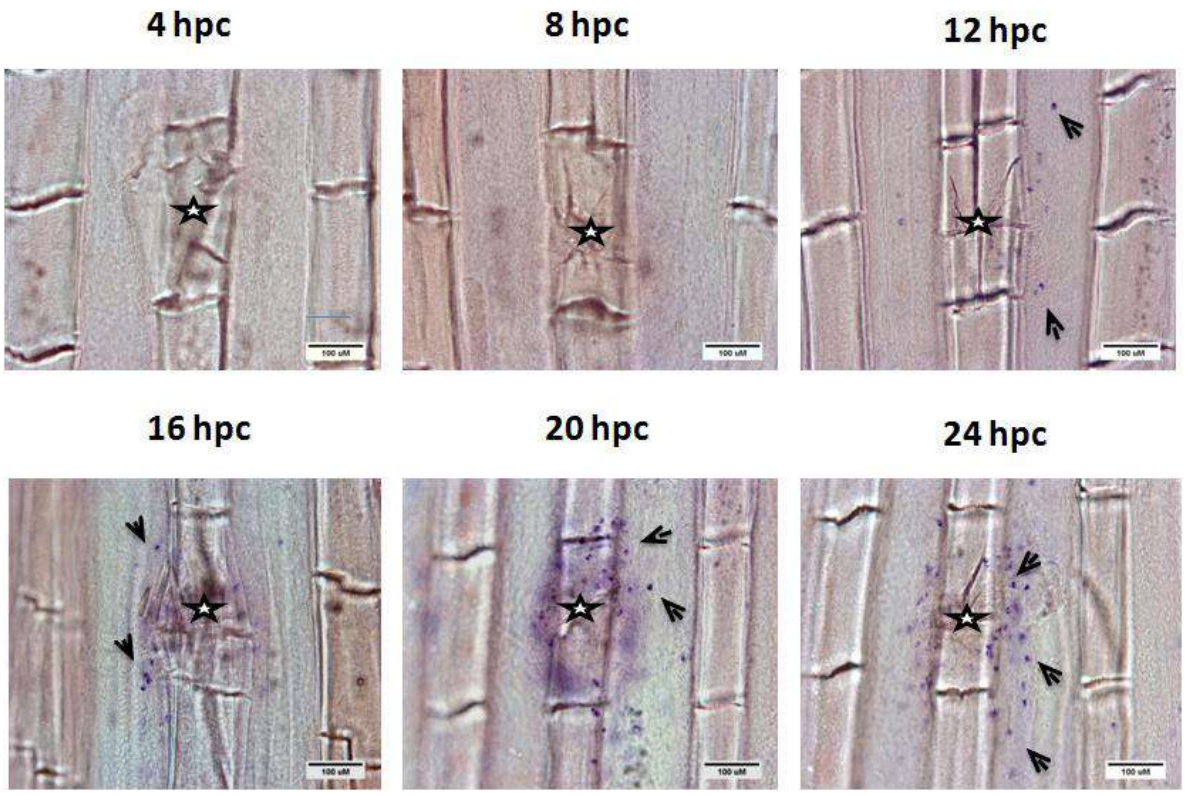

Figure 3-7. The first osteoclast cells appear after 12 hpc during the bone fracture healing process. Time course (24 hrs) ctsk *in situ* for early osteoclast activity detection. At 12 hpc, cathepsin K positive cells (black arrows) were detected first at the bone crush sites (white stars) but not before this time point. In the following time points from 16 to 24 hpc, the number of these cells increased at the fracture sites. Wild-type adult zebrafish were anesthetized in 0.1% tricaine and a ray was crushed using forceps, neighbors were left untouched as controls. Experimental numbers, n = 3 fish with 12 fractured rays in total for each time point. 12/12 rays without signal at the fracture sites (4 hpc), 11/12 rays without signal (8 hpc), 7/12 with signal (12 hpc), 9/12 with signal (16 hpc), 11/12 with signal (20 hpc), 9/12 with signal (24 hpc). hpc- hours post crush. The scale bars represent 100 μm.

3.3 Discussion

3.3.1 Inflammation

Regarding the inflammation response after injury, an IL1-β *in situ* was performed after bone fracture in adult zebrafish. Results showed that IL1-β presents an early enhancement suggesting an important role in initiating the inflammatory response in the bone fracture healing context (Figure 3-1). This IL1-β response has been observed also in zebrafish larvae after fin amputation (Ogryzko *et al.*, 2014); and during fracture healing in mice (Einhorn *et al.*, 1995; Kon, T *et al* 2001; Lange *et al.*, 2010).

Furthermore, neutrophils are cells that migrate and accumulate to sites of injury by responding to stimulation by IL1-β cytokines (de Oliveira *et al.*, 2016). Several studies in zebrafish larvae had shown that this occurs after tail fin amputation (Renshaw *et al.*, 2006; Yoo *et al.*, 2011; Colucci-Guyon *et al.*, 2011). This evidence suggests that neutrophils are like mammalian cells. Whether these cells are functionally important for wound healing in adult zebrafish was unknown when this project started. To better understand the dynamics of the inflammatory response during the fracture healing context, the *Tg(mpx:GFP)* line was used to visualize neutrophils. After inducing bone damage, data showed that neutrophil recruitment started early after at bone fracture sites compared to controls (unfractured rays). Also, a peak accumulation was observed at the injury sites between 12 to 20 hpc. Recently, Petrie and colleagues, showed similar results regarding neutrophil response after injury by inducing tail fin amputation in adult zebrafish (Petrie *et al.*, 2014). However, it is important to mention that in this study Tg(*mpo*:GFP) line was used; mpo promoter is another marker to label neutrophils in zebrafish (Mathias *et al.*, 2006; Renshaw *et al.*, 2006).

Interestingly, Yan and colleagues investigated if a difference existed regarding neutrophil recruitment in wounding versus an infection model in zebrafish larvae. They demonstrated that the Myd88-dependent IL-1 receptor signaling pathway is essential for neutrophil recruitment in response to an injury (tail amputation) but not for a bacterial infection. Moreover, this pathway functions independently to ROS signaling which is also necessary for neutrophil recruitment (Yan B *et al.*, 2014).

Furthermore, reactive oxygen species (ROS) signaling, specifically H_20_2, is one of the main early signals known to be directly sensed by neutrophils in a tissue gradient manner after wounding in zebrafish larvae (Niethammer *et al.*, 2009). H_20_2 it has been shown that this molecule promotes chemotaxis of human and mouse neutrophils *in vitro (*Yoo *et al.*, 2006; Klyubin *et al.*, 1996). Having this in mind I analyzed the injury-induced ROS production during the first 24 hours-post-injury (hpi) in the fracture healing model versus fin amputation as control, by using a fluorescent probe (H_2DCFDA) (Figure 3-3). Interestingly, the results showed that a brief injury-induced ROS production happens in the fracture model. In contrast, ROS production after tail amputation was sustained several hours, detected until 20 hpi. However, in zebrafish larvae this does not occur as it was shown that H_20_2 is produced at a short time window with levels peaking at 20 minutes post amputation (Niethammer *et al.*, 2009). My data suggests that after injury, ROS production depends on the lesion type. Regarding fin regeneration, it could be possible that ROS production is sustained thorough longer times to induce cellular mechanisms which are not required for wound repair. Recently, these questions were address by Gauron and colleagues in adult zebrafish. They compared fin amputation versus a wounding model; in this case, they caused an injury by cutting slits in the fin between rays. My results are similar, ROS injury-production was brief (2 hours) during wounding, but remained until 20 hpi during regeneration. They showed that a sustained production of ROS is an essential signal for blastema formation (Gauron *et al.,* 2013).

3.3.2 Repair stage

Osteocalcin *in situs* and cartilage-bone staining experiments (Figure 3-4, 3-5) revealed that new bone starts to form after 3 days post injury at the fracture sites; this process lasts several days. Recently, another group developed a similar fracture healing model in medaka fish (*Oryzias latipes*) (Takeyama *et al.*, 2014), the difference between models consists on the way caudal fin rays are fractured. Authors performed this by using a glass capillary without injuring the other surrounding tissues including blood vessels. By using the same cartilage-bone staining approach, they showed that bone formation started at a similar time point compared to my fracture model (Takeyama *et al.*, 2014). Important to mention is the fact that several zebrafish larvae studies have shown that mature osteoblasts dedifferentiate after tail fin amputation (osteoblasts get a progenitor phenotype that will provide an important source of newly forming bone) (Knopf *et*

al., 2011; Sousa *et al.*, 2011). Interestingly, mature osteoblasts do not contribute to bone repair in mammals; it has been shown that new osteoblasts are formed by mesenchymal stem cells differentiation (Park *et al.*, 2012). The tools used in this section to characterize the repair stage cannot answer the question regarding whether osteoblasts dedifferentiate during bone repair in the fracture healing process, as it occurs in a regeneration context. Therefore, new tools are needed to demonstrate this hypothesis, which is going to be described in Chapter 5.

3.3.3 Remodeling stage

I have found that activated osteoclasts are recruited early at the fracture sites (since 12 hpc) in the fracture model (Figure 3-7) and remained during several days -post- fracture. Interestingly, at 6 dpc *ctsk* (+) cells were not detected while TRAP staining remained. It has been demonstrated that this enzyme still active degrading bone, even without an osteoclast presence (Ballanti *et al.,* 1997). As I mentioned previously, another group developed a similar fracture healing model in medaka fish. By using a transgenic line that label osteoclasts Tg (TRAP:GFP) they found that two different types of functional osteoclasts were induced before and after osteoblast (bone-forming cells) callus formation (Takeyama *et al.*, 2014). Similarly, their results and mine show comparable results to what it is known in mammals; whereas early osteoclast recruitment is important to the removal of the broken bone and a second wave is necessarily after bone formation to remodel it (Schindeler *et al.*, 2008).

Moreover, it is now well established that cells associated to bone (osteoblasts, osteoclasts) and immune cells (neutrophils, macrophages etc.) are functionally interconnected. Diverse interactions between these cells occur during normal bone development and the bone fracture healing process (Zupan *et al.,* 2012; Bastian *et al.*, 2011). To illustrate this, it has been demonstrated that IL1-β which is expressed mainly by macrophages, endothelial cells, B cells, fibroblasts and by neutrophils to a lesser extent (Dunne and O'Neill, 2003; Subramaniam *et al.,* 2004); participate in various steps of osteoclast development (activation, survival) (Lee *et al.*, 2010; Yao et al., 2008). Specifically, this cytokine up regulates RANKL (the osteoclast master regulator) (Jimi *et al.,* 1999; Chakravarti *et al.*, 2009).

My data suggests that in the zebrafish fracture model, osteoclast recruitment is also coordinated

with the inflammatory response. Further support for this claim comes from observations that IL1-β cytokine has a response peak between 8 and 12 hours post fracture (Fig 3-1). This, correlates in time with the appearance of the first activated osteoclast cells that arrive at the fracture site (Figure 3-7). In addition, neutrophils started to accumulate at similar time points, according to literature, these cells are stimulated by IL1-β cytokine from several sources and produce it as well to induce osteoclast activation (Jimi *et al.,* 1999; Chakravarti *et al.*, 2009).

Further experiments using transgenic lines labeling each cell type with different fluorescent proteins could be useful to perform experiments *in vivo* to understand the interactions between immune and bone-related cells.

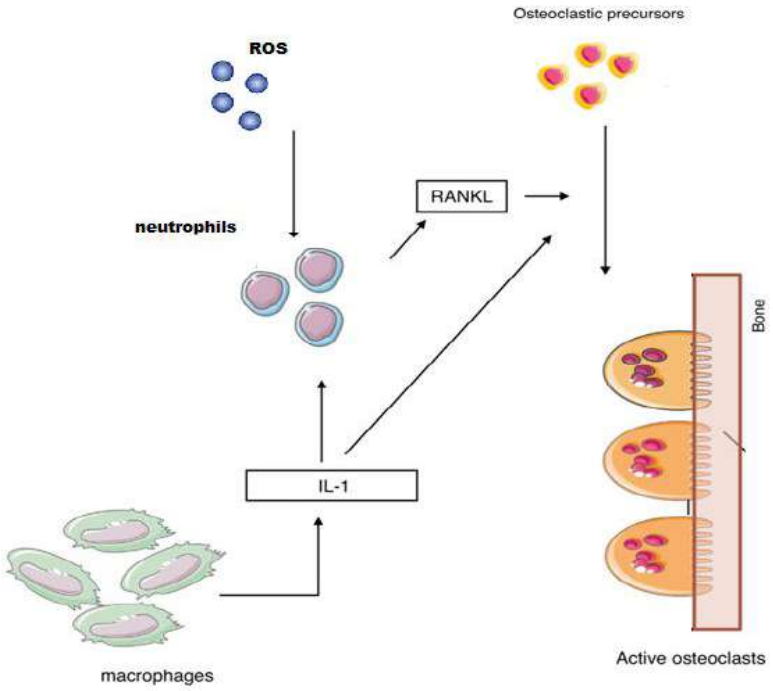

Figure 3-8. Possible cellular scenario occurring within the first 24 hours post fracture. H_20_2 is released by damaged cells inducing neutrophil recruitment to the injury site. These cells and macrophages release IL1-β cytokines which induce osteoclastic activation.

3.4 Conclusions

The objective of this first part of the research was to characterize the three different stages (inflammation, repair and remodeling) that occur during the bone fracture healing process in adult zebrafish, to find potential differences in respect to the mammalian model.

The experiments described here suggest that the three different stages (inflammation, repair and remodeling), also occur during the bone fracture healing process in adult zebrafish, like mammalian fracture repair. This confirms a high degree of conservation regarding healing mechanisms in fish and mammals.

My analysis shows that within the first 24 hours-post-fracture, different cell types and molecules take part in a coordinated manner. IL1 cytokine is induced early after bone damage, which has a peak response. Also, neutrophils are recruited after few hours to the fracture sites. Both seem to induce directly or indirectly the recruitment of activated osteoclasts towards the damage zone in the first hours. These bone remodeling cells, participate early but also remained active after several days.

Moreover, reactive oxygen species (ROS) production and maintenance, seems to depend on the lesion type in adult zebrafish. Lastly, the data suggests that bone repair starts due to activated osteoblasts at the fracture sites.

Considering the following aspects: the relative low costs of animal maintenance compared to other classic models, the speed of bone repair, the availability of novel genetic tools, and a high degree of mechanisms conservation, I propose that the fracture model is very useful to investigate various aspects of vertebrate bone biology, making it a good complement to mice studies. Thus, the zebrafish fracture model characterized in this first part of the project will aid in understanding the key mechanisms of bone repair. Furthermore, this could lead to clinical applications to understand fracture healing disorders in humans, for example.

After characterizing the zebrafish fracture model, the importance to develop transgenic lines to perform experiments *in vivo* for lineage tracing and fate mapping studies arose. In the next chapters, these topics are going to be developed.

CHAPTER 4.

Construction of a zebrafish transgenic line to enable tracking of osteoclasts *in vivo*

4.1 Introduction

As I mentioned previously, the fracture healing process involves different stages. Remodeling (removal of bone), is a necessary event that occurs due to the activity of specialized cell types called the osteoclasts. These cells possess several nuclei and are formed by the differentiation and fusion of haematopoietic precursors (Teitelbaum, 2000). Important to mention is that recently, in mice it has been demonstrated that these precursors of osteoclast formation are provided through the capillary blood supply (Kristensen *et al.*, 2013). Also, different chemokines stimulate this action including Sphingosine-1-phosphate (S1P) (Ishii *et al.*, 2010).

Moreover, osteoclast precursors require close interaction with osteoblasts (bone forming cells) for their activation. Development and differentiation of osteoclasts is controlled by growth factors and cytokines, two different molecules are essential to promote the process known as osteoclastogenesis: macrophage colony-stimulating factor (M-CSF) and receptor for activation of nuclear factor kappa B (NF-kB) (RANK) ligand (RANKL). The first, binds to its receptor c-Fms, on early osteoclasts precursors, which provides essential signals for its survival and proliferation (Udawaga *et al.*, 1990). The second, is a member of the TNF superfamily, which is expressed by osteoblasts. (Lacey, 1998)

Furthermore, because hematopoietic and osteoclast cells share the same origin, it is not surprising that different cytokines and colony-stimulating factors that are involved in hematopoiesis also affect the development of these cells. Among a variety of molecules, we can mention IL-1**,** IL-3, IL-6, IL-11, tumor necrosis factor (TNF), granulocyte macrophage-colony stimulating factor (GM-CSF) and M-CSF (Manolagas *et al.*, 2006).

As osteoclasts develop and become active, these cells attach to bone, creating a tight seal. The micro- environment formed between the cell and the bone surface becomes acidic due to the activation of H^+ATPase proton pumps (Blair, 1989). Cathespin K, one of the major bone-resorbing proteases, is essential for bone remodeling and degradation of the skeletal matrix (Goto, 2003). This molecule is considered a marker of mature osteoclasts and was used to create

a zebrafish transgenic line to enable tracking of osteoclasts *in vivo* to determine whether two osteoclast waves participate during the fracture healing process as described by (Takeyama *et al.*, 2014) in medaka fish.

4.2 Background

In Roehl´s lab the study of osteoclasts has been of great interest since some years ago, the generation of a transgenic line that could label osteoclasts with fluorescence in adult zebrafish has the potential to perform different studies *in vivo* that could answer several questions regarding my project. These questions include how osteoclasts interact *in vivo* with osteoblasts or with different immune cells (macrophages, neutrophils) during the fracture healing process, as examples. A fluorescent labeled osteoclast line would make studies more feasible than doing *in situ* analysis. Therefore, a previous fellow PhD student, tried to generate a stable *cathepsin K* fluorescent transgenic line using BAC recombination (Lee *et al.*, 2001) to mark developing and mature osteoclasts. Unfortunately, no founder fish was identified with visible fluorescent protein expression (Elks, P. M. 2008).

Moreover, in this part of my project the goal was to generate a *cathepsin k*: kaede transgenic line which could give us a powerful tool to track several cells or even at a single cell level. This was made possible thanks to a special sub-set of fluorescent proteins: photoactivatable fluorescent proteins (PAFPs). Included in this family is the PAFP found naturally in coral, Kaede; which is able to convert from green to red when exposed to ultraviolet light (Stark and Kulesa, 2007). To illustrate this, Phil Jankun a lab fellow; generated a transgenic fish line that expressed Kaede protein in the whole body (ubiquitous promoter). He showed that converted kaede was visible 48 hours post conversion in larval tails (Jankun P. J. 2015) (Figure 4.1)

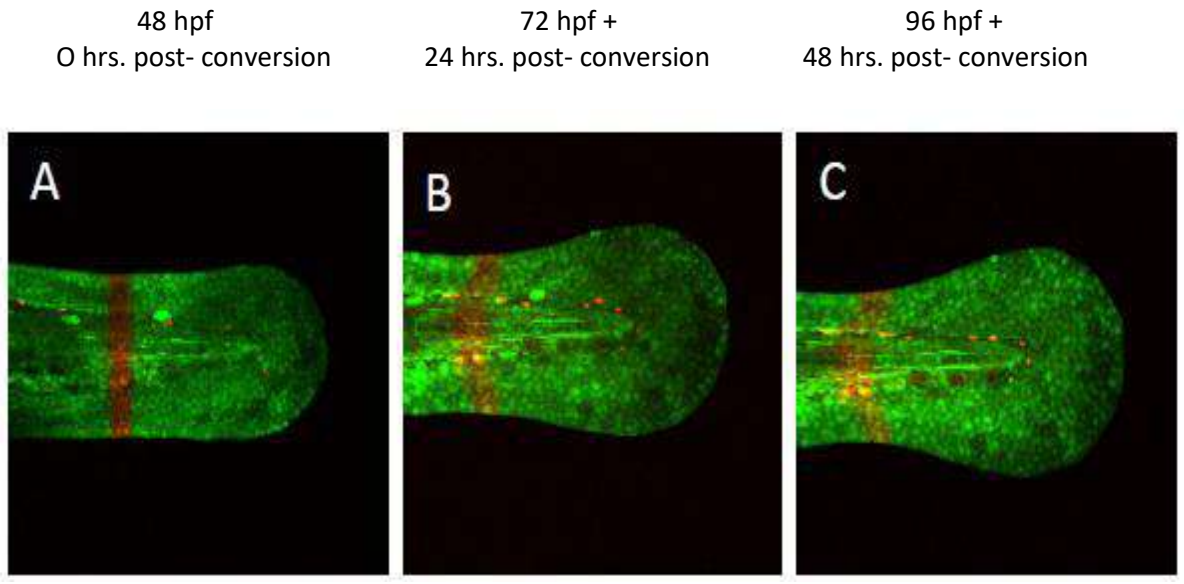

Figure 4.1. Converted kaede is visible 48 hours post conversion in larval tail.
(A-C) Uncut caudal fins of wild-type ubi-kaedesh343 (48 hpf) were manipulated with laser to induce a UV-converted strip of kaede (red). Samples were analyzed and photographed at (A) 48 hpf + 0 hrs. post-conversion (B) 72 hpf + 24 hrs post- conversion (C) 96 hpf + 48 hrs post-conversion, respectively. Red dots are auto fluorescence, not converted cells. Images taken on an Olympus confocal microscope with a 20X objective. All images represent one sample. (Jankun P.J 2015)

4.3 Results

4.3.1 Generation of the Tg (*cathepsin K*: Kaede) transgenic line

4.3.2 Gateway clonase to produce a *cathepsin K: kaede* expression vector.

The Tol2kit, which is a multisite gateway-based construction kit for *Tol2* transposon transgenesis constructs, was used to create the construct needed to generate the transgenic line (Kwan *et al.*, 2007). To illustrate, a vector was obtained from Dr. Cristoph Winkler (University of Singapour) whereas a 3.18 kb upstream sequence of the *cathepsin K* gene (ENSORLT00000019682), including 80 nucleotides of exon 1 from medaka fish (*Oryzias latipes)* was cloned. Winkler´s lab previously generated a stable osteoclast reporter medaka line expressing membrane bound EGFP (mEGFP) under control of this promoter fragment (To TT *et al.*, 2012) (Figure 4.2)

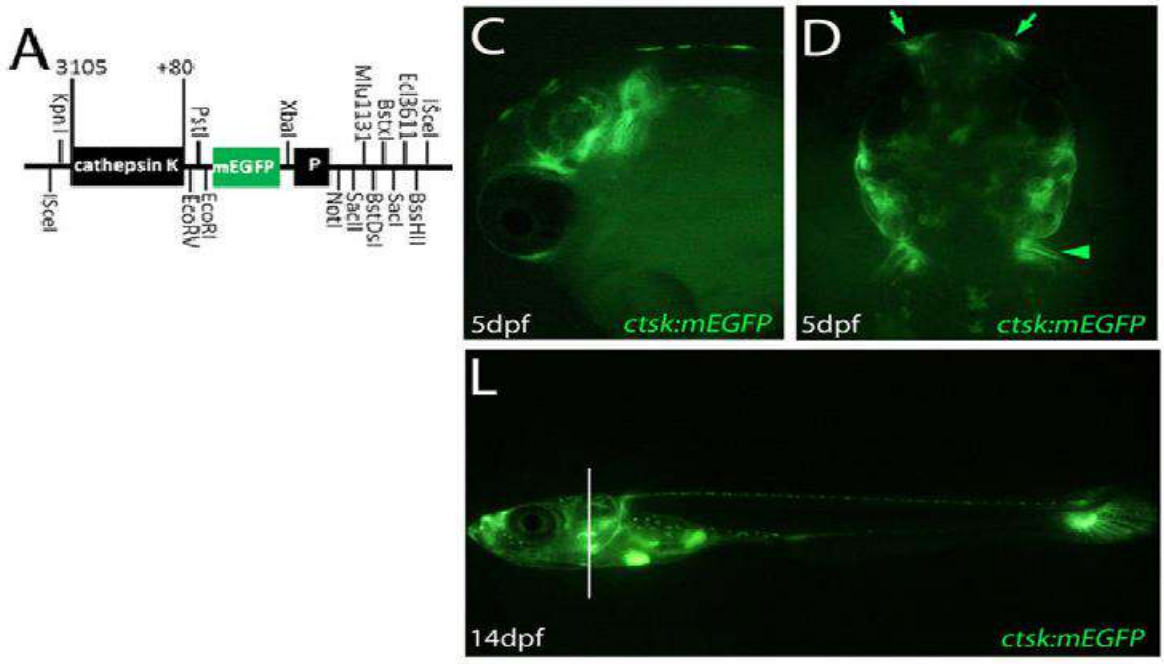

Fig 4.2. Medaka Tg (*ctsk: m EGFP*) generated in Winkler`s lab to label osteoclasts. (**A**) *ctsk:mEGFP* construct (medaka) obtained from Winkler's lab and used to generate a zebrafish transgenic line. P, polyadenylation signal. (**C-D**) Higher magnification views of head regions of embryo. C, lateral; D, dorsal. Arrows in D indicate olfactory pits. (**L**) *ctsk*:mEGFP expression at larvae stage (12 dpf). Modified from (To TT *et al.*, 2012).

In order to generate a *ctsk: kaede* zebrafish line, 3.18 kb of *cathepsin K* promoter were subcloned in the entry vector p5e-MSC (p473) with the use of KpnI – XmaI and KpnI – AgeI restriction enzymes, respectively. The generated entry vector was annotated as p5e (p702) (Figure 4.3). Both digested plasmids were observed in an electrophoresis gel and the correct DNA fragments were selected, purified and ligated (Chapter 2. Material and Methods).

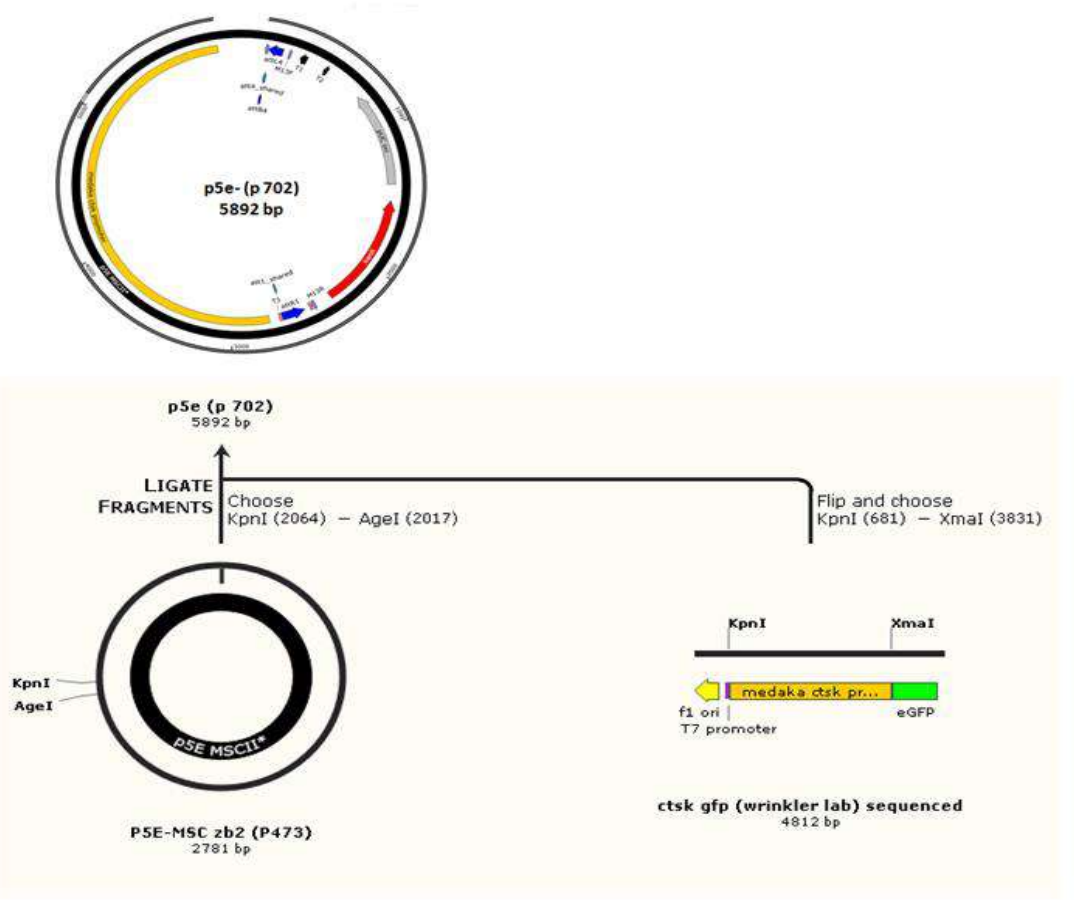

Figure 4.3 A schematic showing the strategy for creating the entry vector p5e (p702). 3.18 kb of *cathepsin K* medaka promoter (Winkler´s lab) were subcloned in the entry vector p5e-MSC (p473) with the use of KpnI – XmaI and KpnI – AgeI restriction enzymes, respectively.

Using the gateway clonase technology (Kwan *et al*., 2007) (see Materials and Methods for a description), three components of the construct- p5e- *ctsk* promoter (p702), pMe- Kaede (kindly supplied by Rob Wilkinson, Van Eeden lab), and p3e-PolyA (p302) – were inserted into the destination vector (p480) to generate the final construct p *ctsk: Kaede* (p765).

In order to calculate the correct amount of each vector the following formula was used:

10* N * 0.000330
N= number of base pairs

- p 5e - *ctsk* promoter (p702)
- p Me- Kaede (Wilkinson´s lab)
- p 3e- PolyA (p302)
- p Dest *Tol2* – (480)

p *ctsk : Kaede* (p765)

The final concentration units were in nanograms (ng) /µl. Each concentration was multiplied x2. Then, 5 µl of each component (p5e- pMe – p3e-) were taken and mixed with another 5 µl of TE (Tris, EDTA) buffer giving a 20 µl final volume. From this, just 2 µl were used and mixed with 1 µl of the clonase enzyme; 1 µl of the destination vector and 1 µl TE Buffer. Finally, the clonase enzyme (Invitrogen) was added to the reaction mix and incubated for 16 hours at 25°C to synthesize the final construct. To end the reaction 1 µl ProK was added to the mix for 10 min at 37°C. The final map of *ctsk: Kaede* construct (p765) is shown in figure (4.4)

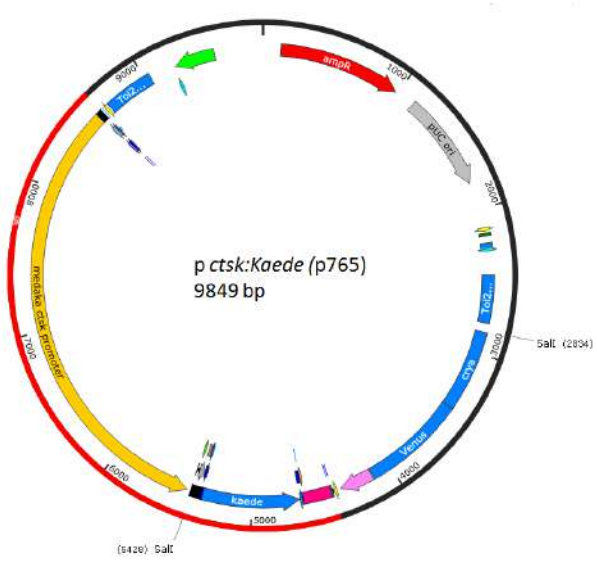

Figure 4.4. A schematic showing *the ctsk- kaede* construct (p765) after the gateway clonase reaction. The *medaka ctsk* promotor (yellow) drives the photo-convertible kaede expression, which includes a polyA tail for efficient translation of RNA to protein. The final plasmid size has 9849 bp.

To confirm that the DNA construct was correct, it was sequenced and also diagnostic digestions were performed with Sal I-HF (NEB) restriction enzyme; the expected fragments size after DNA digestion were of 7.2 and 2.5 kbs. (Figure 4.5)

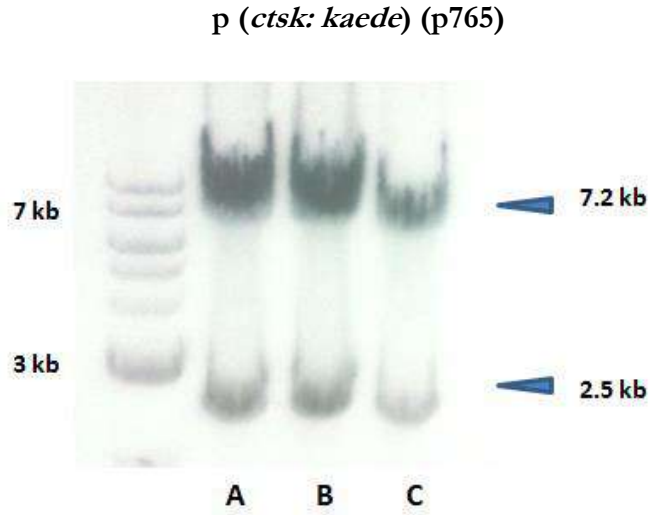

Figure 4.5 Diagnostic digest of p (*ctsk: kaede*) (p765) with Sal I-HF restriction enzyme in different clones (A, B and C). The gel electrophoresis showed correct expected band sizes (7.2 and 2.5 kb).

This process was followed by bacterial transformation and plasmid preparation for micro injections (for description Chapter 2. Material and Methods).

4.3.3 Identification of transgenic founder fish by reporter gene expression

The *ctsk: kaede* construct (p765) was microinjected into one –cell zebrafish embryos (for details Materials and Methods section). At 3 days post-fertlization (dpf), zebrafish larvae were screened for transient expression, positive fish were selected by expressing GFP in the eyes (transgenesis marker). Detection of the marker suggested the success of injection. These selected larvae (80 positive fish) were raised to produce F0 adults to establish the transgenic fish line. When F0 fish became sexually mature (3 months old), fish were separated and screened for germline transgenesis by outcrossing each to wild-type zebrafish independently to obtain FI generation. The obtained eggs from an outcross of an F0, were examined the same way as mentioned previously; after this procedure, only 5 potential F0 parents were found. From those, the

percentage of siblings expressing the dominant marker was low (1 %) from a total of approximately 100 samples each. These larvae were kept and analyzed by microscopy for expression of the *ctsk* promoter at different development stages (5 dpf and 2 months old). Two medaka *ctsk:* GFP transgenic lines generated by different groups were used as a reference (To TT *et al.*, 2012; Chatani *et al.*, 2011) and also different ctsk *in situ* studies done in zebrafish to detect osteoclast activity (Chatani *et al.*, 2011; Elks, P. M. 2008. Doctoral dissertation). Unfortunately, no fish was identified with visible fluorescent protein expression driven by the *ctsk* promoter at different developmental stages (Figure 4.6); this result suggested that the heterologous promoter cloned from medaka cannot drive the *ctsk* gene expression in zebrafish (Figure 4.6)

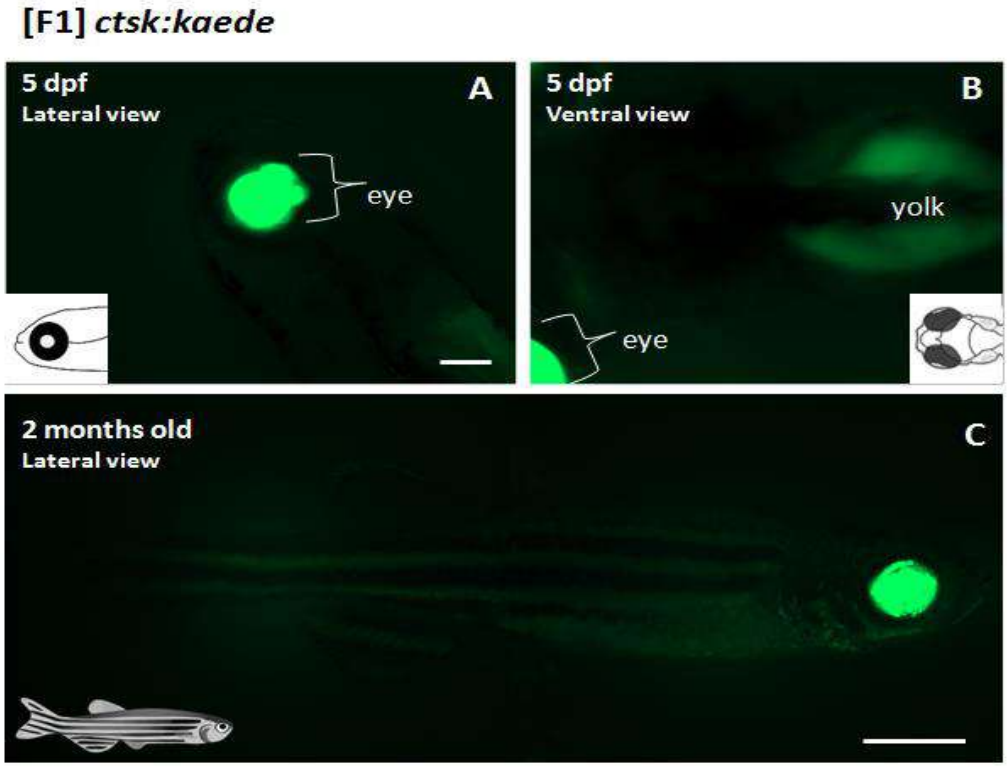

Figure 4.6 [F1] fish didn´t show visible fluorescent protein expression driven by the *ctsk* promoter at different developmental stages. Representative images of *ctsk: kaede* [F1] fish analyzed by microscopy. At 5 dpf, lateral and ventral views of larvae head showed only expression of the transgenesis marker (eye lenses), but no signal was seen on facial bones, whereas osteoclasts are expected to appear at first instance (A.B). In (B) the yolk auto-fluorescence was also seen. (C) [F1] fish expressing the transgenesis marker were also analyzed after two months, but no

expression driven by *ctsk* promoter was detected in different reported areas whereas osteoclasts participate (head, fins, vertebral column).

4.4 Discussion

Although some (F1) fish were found by expressing the transgenesis marker (γ-crystalin promoter) in the eye lenses, no possible founder fish was identified; this due to the lack of Cathepsin K fluorescent protein detection in those fish after its microscopy analysis at different developmental stages.

First thing to remember is that when a transgenic line is generated, the initial quality control step comes from the expression of the transgenesis marker incorporated in the construct. This reporter provided a relative easy method of subsequent genotyping. Previous efforts using PCR to detect positive fish from Phil Elks to create a stable *ctsk* transgenic line in the lab gave some positive-negative results (Elks, P. M. 2008). The raise of several injected positive embryos increased the chances to find fish with germline integration. However, an aspect to consider is the fact that F0 animals with visible transgene marker expression indicates successful injection, but does not predict successful transgene transmission (Clark *et al.*, 2012)

In general, germline transgenesis in F1 generation is mosaic, this means that the expression will not be Mendelian at this generation. If F0s are transmitting the construct to the germline, it is common to see about 10 to 15% of the embryos expressing the dominant marker (Clark *et al.*, 2012). In contrast, I just found 5 potential F0 parents after performing FI screenings, but only 1% of its siblings (approximately 100 fish) expressed the transgenesis marker. Those positive fish were kept for *cathepsin K* fluorescent protein expression. Surprisingly, no fish was identified with visible fluorescent protein expression driven by the *ctsk* promoter (Figure 4.6). One first possibility exist that bone remodeling was not occurring; thus, the lack of fluorescence signal. In this case, pictures taken at different developmental stages were compared with published data from two different labs that previously generated a stable *ctsk* line in medaka fish (To TT *et al.*, 2012; Chatani *et al.*, 2011). At 5 dpf, they detected *ctsk:GFP* expression on bones associated to the head which started to suffer bone remodeling, after two months, no visible signal was detected as well, according to literature *ctsk*:GFP signal can detected at that stage in several

regions, such as: the fins and vertebral column (Figure 4.2). Moreover, ctsk *in situ* studies in zebrafish have showed osteoclast activity at the same analyzed developmental stages (Chatani *et al.*, 2011; Elks, P. M. 2008. Doctoral dissertation).

Moreover, another possibility that could explain the lack of *ctsk:kaede* signal in the analyzed fish is the fact the cloned heterologous promoter from medaka cannot drive the *ctsk:kaede* gene expression in zebrafish. Certainly, several zebrafish transgene expressing lines have been created using heterologous promoters from different animals, including those from *Xenopus*, carp, medaka, goldfish, mouse, and rat, for example. In fact, studies have been performed to test heterologous promoters in zebrafish to discover conserved regulatory elements (Barton *et al.,* 2001; Motoike *et al.,* 2000; Reinhard *et al.*, 1994; Udvadia *et al.*, 2001; Westerfield *et al.*, 1992).

The possibility exists that the *ctsk* promoter sequence cloned from medaka lacks important regulatory sequences for its expression in zebrafish. Moreover, it is important to consider that the strength and fidelity of the transgene expression from heterologous promoters will depend on how well the regulatory sequences, and the factors that bind them, are conserved between the two species for a specific gene (Udvadia and Linney, 2003).

Also, it has been suggested that the use of promoter sequences from other species could lead to transgene silencing, that means, reduced or no expression of one or more copies of a transgene introduced into an organism (Higashijima *et al.*, 1997). This possibility cannot be discarded, but the finding that some (F1) fish expressing the transgene marker in the eye lens suggests that at least the complete construct inserted into zebrafish genome is not susceptible to gene silencing.

.

4.5 Conclusion

A zebrafish transgenic line that fluorescently identify osteoclasts has the potential to be a useful tool to answer several questions involving osteoclast participation during the fracture healing model. This coupled with the fact that the use of photoactivatable fluorescent proteins (PAFPs) such as Kaede protein, can permit cell tracking studies. The aim was therefore to construct a stable *cathepsin K: kaede* fluorescent transgenic line using the Tol2kit (Kwan *et al*., 2007) to mark osteoclasts within the living zebrafish.

Unfortunately, no founder fish have been identified to date with visible ctsk:Kaede fluorescent protein expression. Moreover, the transgenesis marker expression in F0s suggested successful injections but F1 larvae screening, showed a low germline transmission. Also, positive F1 larvae expressing the transgenesis marker didn´t show the *cathepsin k: kaede* signal when analyzed by microscopy at different developmental stage.

Future experiments are needed to assess the cause of not Kaede protein expression in the *cathepsin k: kaede* transgenic line. A bioinformatic analysis that check and compare zebrafish and medaka ctsk promoters is a first attempt to understand the issue.

If this transgenic line can work afterwards, it could be crossed with different transgenic lines from Renshaw`s lab to study osteo-immunology questions during fracture healing process, for example.

CHAPTER 5

Construction of zebrafish transgenic lines with bone- associated promoters to induce controlled site-specific recombination.

5.1 Introduction

Spatiotemporal transgene regulation by using transgenic DNA recombinases is a powerful tool used nowadays for reverse genetics. To be specific, Cre recombinase enzyme (from bacteriophage P1-derived cyclic), since its discovery in the early 1980´s and its subsequent use in the mouse in the early 1990´s, it has become useful for genome manipulation (Sternberg and Hamilton, 1981; Lakso *et al*., 1992; Orban *et al*., 1992).

The system known as Cre-lox consists of the Cre enzyme that promotes strand exchanges between *lox* (from locus of X-ing over) target sites without any additional cofactors (Dymecki and Kim, 2007). To give a better illustration, this system needs the generation of two different transgenic lines; the first contains the effector gene flanked by loxP sites in such a way that prevents its expression (also known as *lox* Switch lines). Secondly, another transgenic line which contains the coding sequences for the expression of Cre recombinase under the control of tissue-specific regulatory elements. Due to this feature, scientists have had the chance to carry out different types of DNA manipulation, such as, gene activation and repression, or even exchange for other genes, as well (Detrich *et al*., 2011).

Important to mention is that chimeric Cre recombinases are available to allow temporal control of Cre-mediated recombination. This is due to a Cre fused to the mutated human ligand-binding domain of the estrogen receptor ($CreER^{T2}$) which was shown to possess ligand sensitivity and inducible recombination efficiency in mice (Metzger *et al*., 1995; Feil *et al*., 1997). $CreER^{T2}$ enzyme allowed that Cre enzyme can be expressed in a cell type or triggered by a chemical signal or a heat shock.

Moreover, this ligand-inducible $CreER^{T2}$ version was used for zebrafish studies with successful results as well (Hans *et al.,* 2009). Therefore, different tissue-specific Cre ERT2 driver lines are now available and have shown its importance to perform several studies (Detrich *et al*., 2011).

The same has occurred with the *lox* switch lines whereas better versions have been generated to drive ubiquitous transgene expression at different developmental stages including adulthood (Mosimann *et al.*, 2011).

5.2 Background

At the time when I started to work on this project, different lab members joined their efforts to implement the Cre-lox system to study different topics in larvae such as, epimorphic regeneration. Montserrat García a lab fellow, during her PhD generated and characterized a set of 6 different tissue specific CreER^{T2} -driver lines, in order to perform lineage tracing analysis after fin amputation. She showed that most of the generated lines could undergo tissue recombination and that this event was tightly dependent of 4OHT administration (García Romero. 2016. PhD dissertation). Her results suggested that Cre-lox system success was working in larvae and its success was promoter dependent.

The aim of this part of the project was to use this novel tool available in the lab in order to generate different CreER^{T2} -driver lines that could allow us to temporally control Cre-mediated recombination in adult zebrafish for the following purposes:

It was unknown whether osteoblast dedifferentiation is restricted to appendage regeneration, or a more general process found in fish bone, such as repair after a fracture. Also, whether osteoblast cells at the fracture site participate in the repair process or not. In order to answer this question, I generated two different Cre driver transgenic lines, Tg *(osc:creER^{T2}-ins)* and Tg *(twist2:creER^{T2})* to enable tracking of bone cells *in vivo*. The rationale was because osteocalcin is specifically expressed in differentiated osteoblasts and I could use that line to label few mature osteoblasts to perform my studies, for example. Likewise, previous studies showed that a *osteocalcin*:GFP transgenic fish labeled osteoblasts specifically (Knopf *et al.*, 2011; Gavaia *et al.*, 2006).

Moreover, it has been shown that *twist2* expression transiently inhibits *Runx2* which is a master regulator for osteoblast differentiation. *Twist2* expressing cells are considered to show a pre-osteoblast phenotype (Bialek *et al.*, 2004)

The generation of a Tg (*cathepsin K*: ER^{T2}*Cre*-ins) transgenic line to enable tracking of osteoclast cells *in vivo* was a project thought to be done in parallel to the Tg (*ctsk K*: Kaede) line as a complement. The goal was to assess with the Cre lox system whether the same osteoclast cells participate at different time points during the fracture process or not. Also, the system could allow us to determine whether osteoclast cell division occur after its arrival at the fracture site; the Kaede approach couldn`t help us to answer this question, for example.

5.3 Results

5.3.1 Generation of the $CreER^{T2}$ - driver lines.

In contrast to the ones created by the fellow Montserrat García, my $CreER^{T2}$ - driver lines were designed with additional features for its optimization, based on previous experience from lab members working with this technology.

To illustrate, the expressed Cre recombinase was fused to only one mutated human ligand-binding domain of the estrogen receptor (ER^{T2}), instead of two domains (ER^{T2}*Cre*ER^{T2}) to induce recombination after 4-Hydroxytamoxifen (4OHT) administration. The reason of this change, was because lab members had difficulties by inducing Cre-mediated recombination in the generated lines expressing (ER^{T2}*Cre*ER^{T2}). Experiments suggested that 4OHT was not able to reach two ER^{T2} sites at the same time. Additionally, a pair of insulator sequences (*SINE CD* insulator sequence was kindly provided by Dr. Kelsh, Bath University) were inserted flanking the promoter and Cre sequences within the transgene constructs. The reason was to use insulators as DNA barriers that could prevent the effect of external sequences in *cis* during recombination. Specifically, to avoid Cre leakiness (Cre recombination without 4OHT administration). The following table shows important information regarding the generated Cre-driver lines:

Table 5-1: Cre-driver lines generated, general information.

Transgenic line	Tissue specific promoter	Expected tissue/cells recombination	Source
Tg (*osc:* ER^{T2}*Cre*-ins)	*osteocalcin*	Mature osteoblasts	Inohaya *et al*., 2007
Tg (*twist2*: ER^{T2}*Cre*-ins)	*twist2*	Chondrocytes and sclerotomal cells	Inohaya *et al*., 2007
Tg (*cathepsin K*: ER^{T2}*Cre*-ins)	*cathepsin K*	Osteoclasts	(To TT *et al.,* 2012) medaka

5.3.2 Gateway clonase system to produce the expression vectors

The Tol2kit (Kwan *et al*., 2007), which is a multi-site gateway-based construction kit for *Tol2* transposon transgenesis constructs, was also used to generate a set of different transgenic lines. The shared technical information regarding the creation of the construct and generation of the lines has been described in detail. Material and methods section (Chapter 2). All the gateway components were the same, except the 5' entry clone which was specific for each construct.

5.3.3 Tg (*osc:* ER^{T2}*Cre*-ins) transgenic line

The following components of the construct (5', middle, and 3' entry clones) were inserted into the destination vector p Tol2*cryaa*: venus (p518) generated in the lab by Montserrat García which possess the transgenesis marker that is expressed in the eye lenses (See Material and Methods). The following plasmids were used to generate the final construct:

- p 5e - *osc* promoter (p397)
- p Me- ER^{T2}*Cre* (p512)
- p 3e- PolyA (p302)
- p Dest- *CryA* – (p518)

} p *osc:* ER^{T2}*Cre*-ins (p578)

The final plasmid map is shown:

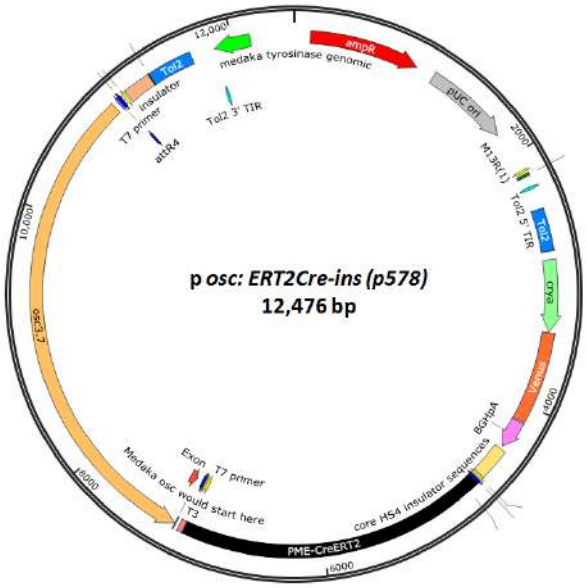

- **Figure 5.1** Plamid map (*osc:* ER^{T2}*Cre*-ins) construct (p578).

To confirm that the DNA construct was correct, it was sequenced and diagnostic digestions were performed with Not I (NEB) restriction enzyme; the expected fragments size after DNA digestion were of 2.7 and 9.6 kbs. (Figure 5.2)

p (*osc:* ER^{T2}*Cre*-ins) (p578)

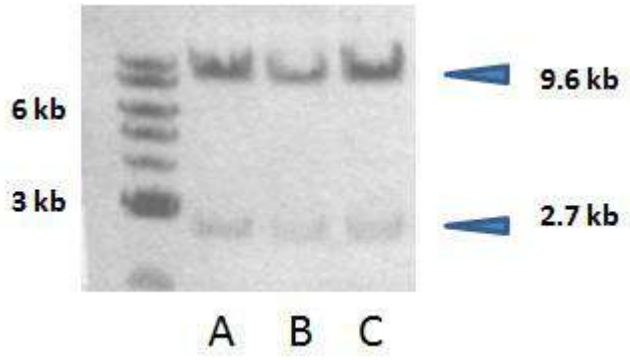

Figure 5.2 Diagnostic digest of p *osc:* ER^{T2}*Cre*-ins (p578) with NotI restriction enzyme in different clones (A, B and C). The gel electrophoresis showed correct expected band sizes (9.6 and 2.7 kb).

5.3.4 Tg (*twist2*: ER^{T2}*Cre*-ins) transgenic line

In this case, the following plasmids were used to generate the final construct:

- p 5e - *twist2* promoter
- p Me- ER^{T2}*Cre* (p512)
- p 3e- PolyA (p302)
- p Dest- *CryA* – (p518)

} p *twist2*: ER^{T2}*Cre*-ins (p579)

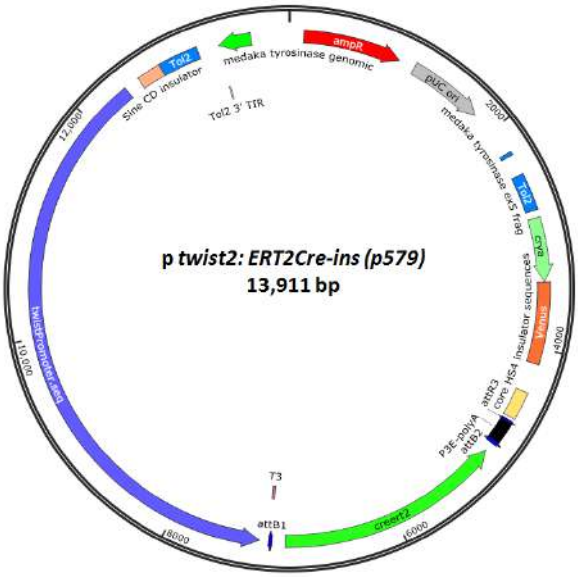

Figure 5.3. **Plasmid map (*twist2:* ER^{T2}*Cre*-ins) construct (p579).**

The DNA construct was sequenced and diagnostic digestions were performed with Spe I (NEB) restriction enzyme; the expected fragments size after DNA digestion were of 6.2, 4.9 and 2.7 kbs. (Figure 5.4)

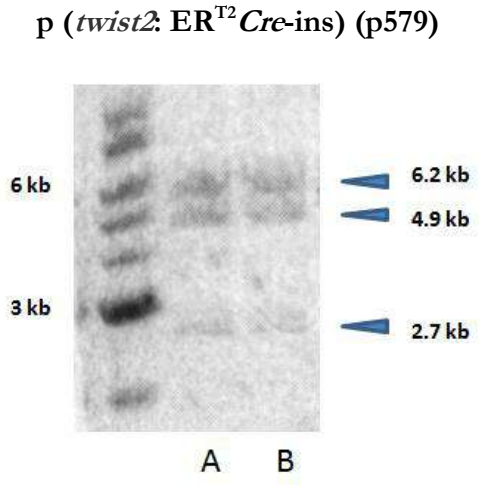

Figure 5.4 Diagnostic digest of p (*twist2*: ER^{T2}*Cre*-ins) (p579) with SpeI restriction enzyme in different clones. The gel electrophoresis showed correct expected band sizes (6.2,4.9 and 2.7 kb).

5.3.5 Tg (*cathepsin K*: ER^{T2}*Cre*-ins) transgenic line

For this transgenic line, almost all the components that were used to generate the Tg (*cathepsin K*: kaede) (Chapter # 4) were used as well, only the destination vector was the difference, (p518) was included for this case.

The following plasmids were used to generate the final construct:

- p 5e - *ctsk* promoter (p473)
- p Me- ER^{T2}*Cre* (p512)
- p 3e- PolyA (p302)
- p Dest- *CryA* – (p518)

p *cathepsin K*: ER^{T2}*Cre*-ins (p764)

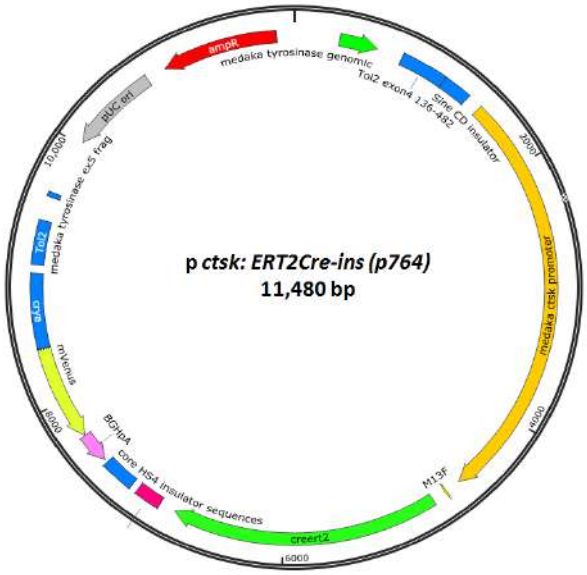

Figure 5.5 Plasmid map (*ctsk:* ER^{T2}*Cre*-ins) construct (p764).

The DNA construct was sequenced and also diagnostic digestions were performed independently with KpnI and StuI (NEB) restriction enzymes; the expected fragments size after DNA digestion were of (6.1, 3.2, 2.4 kbs) and (7, 3.4, 1.4 kbs) respectively (Figure 5.6)

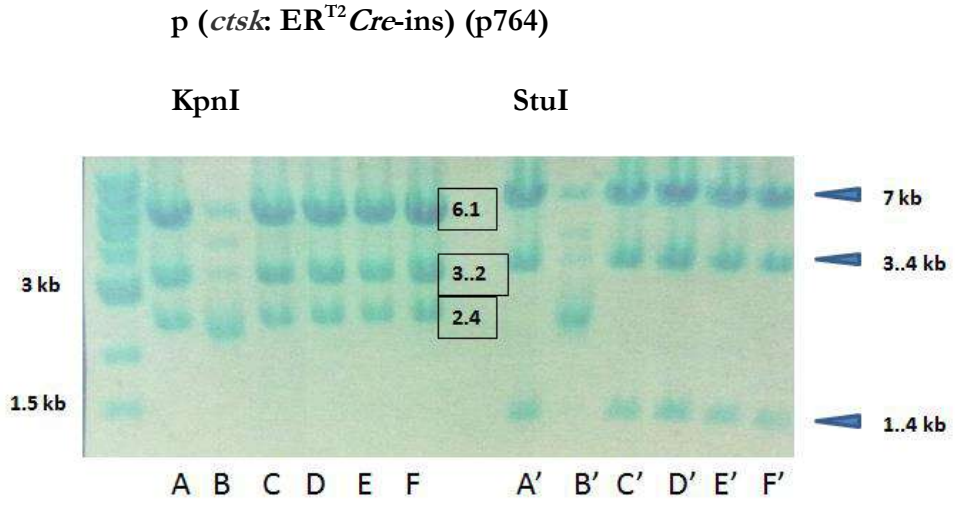

Figure 5.6 Diagnostic digestions of p (*ctsk:* ER^{T2}*Cre*-ins) (p764)with KpnI and StuI restriction enzymes in different clones . The gel electrophoresis showed correct expected band sizes (6.1, 3.2, 2.4 kbs) and (7, 3.4, 1.4 kbs) respectively

After the constructs generation, the process was followed by bacterial transformation and plasmid preparation for micro injections (for description Chapter 2. Material and Methods).

5.3.6 Identification of transgenic founder fish by reporter gene expression

The three different Cre-driver constructs were microinjected into one –cell zebrafish embryos (for details Materials and Methods section). At 3 days-post-fertilization (dpf), zebrafish larvae were screened for transient expression, positive fish were selected by expressing GFP in the eyes (transgenesis marker). Approximately 100 positive fish were raised to produce F0 adults to establish each transgenic fish line. When F0 fish became sexually mature (3 months old), fish were separated and screened for germline transgenesis by outcrossing to wild-type zebrafish independently to obtain the FI generation. Founders (n= 80 fish) were isolated and the screening procedure was repeated to get the F2 generation of each transgenic line.

5.3.7 Generation of double transgenic lines (*Cre*ER^{T2} driver x *lox* Switch lines)

F2 generation fish are considered to be stable, thus; to investigate whether the three generated tissue-specific *Cre*ER^{T2} driver lines Tg (*ctsk*:ER^{T2}*Cre*-ins), Tg (*osc*:ER^{T2}*Cre*-ins) and Tg(*twist2*:ER^{T2}*Cre*-ins) can chemically induce recombination, each generated *Cre*ER^{T2} driver line were crossed independently with two different *lox* switch reporter lines which were available in the lab to generate double transgenic animals (dTg) (Figure 5.7). The Tg (*EF1*α:*lox*PGFP*lox*P-*DsRed*) (Hans *et al.*, 2009) and Tg (*ubiquitin*:*lox*P*GFPlox*P-*mCherry*) (Mosimann *et al.*, 2011) are green-to-red reporter lines for easy detection of Cre activity; its ubiquitous expression at all stages of development and functionality to perform Cre/*loxP*-based lineage tracing experiments were ideal lines to work with. Moreover, important to mention is the fact that this type of studies were performed in larvae by Monterrat García in the lab, which showed its functionality, as well (García Romero. 2016. PhD dissertation).

To illustrate, each double transgenic line (dTg) expresses DsRed2 or mCherry constitutively, under the control of the *Xenopus Elongation Factor 1 alpha* (*EF1*α) or the zebrafish *ubiquitin* (*ubi*) promoter. After tamoxifen addition or its active metabolite 4-hydroxytamoxifen (4-OHT), we expected that the chemical triggers dose-dependent Cre^{ERt2}-mediated *loxP* excision events. Thus, after a period the change of color from Green to Red fluorescence in specific tissue would suggest a successful recombination event.

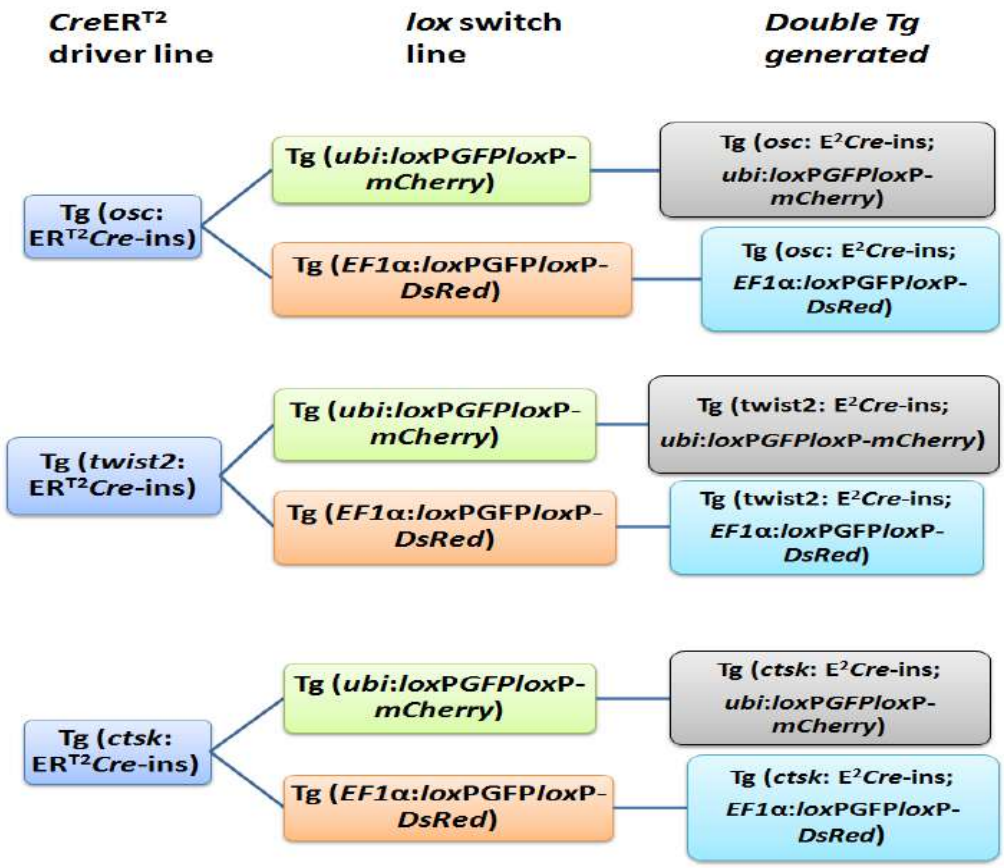

Figure 5.7. Schematics of the Cre-lox double transgenics generated. Tissue-specific CreER^{T2} drivers were crossed independently with l*ox* switch Tg (*EF1*α:*lox*PGFP*lox*P-*DsRed*) (Hans *et al.*, 2009) and Tg (*ubiquitin*:*lox*P*GFPlox*P-*mCherry*) (Mosimann *et al.*, 2011), to generate double transgenic lines.

Also, the following CreER^{T2} driver lines: Tg (*fli1*α:ERT2*Cre*ERT2, Tg (*osc*:ERT2*Cre*ERT2-ins) and Tg (*nestin*:ERT2*Cre*ERT2) generated by Montserrat García and Dr. Carlos Cruz (Roehl lab), were crossed independently with the two *lox* reporter lines previously mentioned as controls (Table 5-2, Figure 5.8).

Table 5-2: Cre-driver lines used as controls, general information.

Transgenic line	Tissue specific promoter	Expected tissue/cells recombination	Source	Synthesis
Tg (*osc*:ERT2*Cre*ERT2-ins)	*osteocalcin*	Mature osteoblasts	Inohaya *et al.*, 2007	M. García
Tg (*fli1*α:ERT2*Cre*ERT2	*fli1*α	Blood vessels	Lawson *et al.*, 2002	M. García
Tg (*nestin*:ERT2*Cre*ERT2)	*nestin*	Neural stem cells	Chen *et al.*, 2009	Carlos Cruz

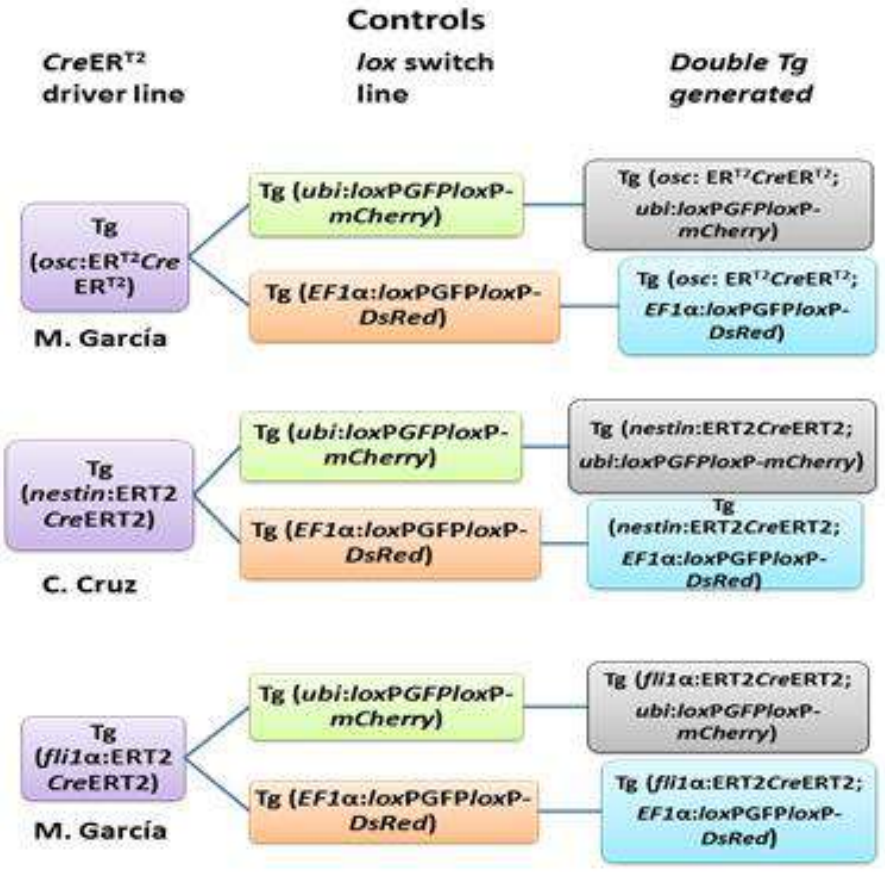

Figure 5.8. Schematic of the Cre-lox double transgenics generated as controls. Tissue-specific CreER^{T2} drivers generated by different lab members, were crossed independently with two l*ox* switch transgenic lines Tg (*EF1*α:*lox*PGFP*lox*P-*DsRed*) (Hans *et al.*, 2009) and Tg (*ubiquitin*:*lox*P*GFPlox*P-*mCherry*) (Mosimann *et al.*, 2011).

For each double transgenic lines, positive siblings expressing strong GFP in all visible external organs, such as the skin, eyes, and fins were screened and selected. Positive fish were also analyzed for Cre leakiness (Cre recombination without 4OHT administration), DsRed or mCherry signals were not detected in any fish expressing strong GPF; this indicating tight regulation of CreER^{T2} in the respective CreER^{T2} driver lines. To illustrate this, representative images of the generated double transgenic line, dTg (*osc*:ER^{T2}*Cre*-ins;*EF1a*:l*ox*PGFP*lox*P-*dsRed*) and dTg (*osc*:ER^{T2}*Cre*-ins; *ubiquitin*:*lox*P*GFPlox*P-*mCherry*) are shown as examples of the generated set lines (Figure 5.9, 5.10). Positive siblings (5dpf) expressing strong GFP signal in all visible external organs, such as the skin, eyes, and fins were screened and collected. Selected fish were also analyzed for Cre leakiness (Cre recombination without 4OHT administration), dsRed or mCherry signals were not detected in fish expressing strong GPF. These animals were sent to raise (2 tanks of 40 fish each); after 3 months, fish were examined again by fluorescence microscopy to detect ubiquitous and strong GFP expression in adulthood; also, dsRed or mCherry signals were still absent indicating a lack of Cre leakiness. The data suggested that the generated double transgenic lines were suitable to perform drug-inducible experiments in adults, however, it has been previously shown that recombination depends on the expression strength of CreER^{T2} (Hans *et al.,* 2009) for example. Furthermore, TAM or 4- OHT conditions needed to be tested and optimized for each CreER^{T2} driver line. These experiments are going to be described in the next Chapter.

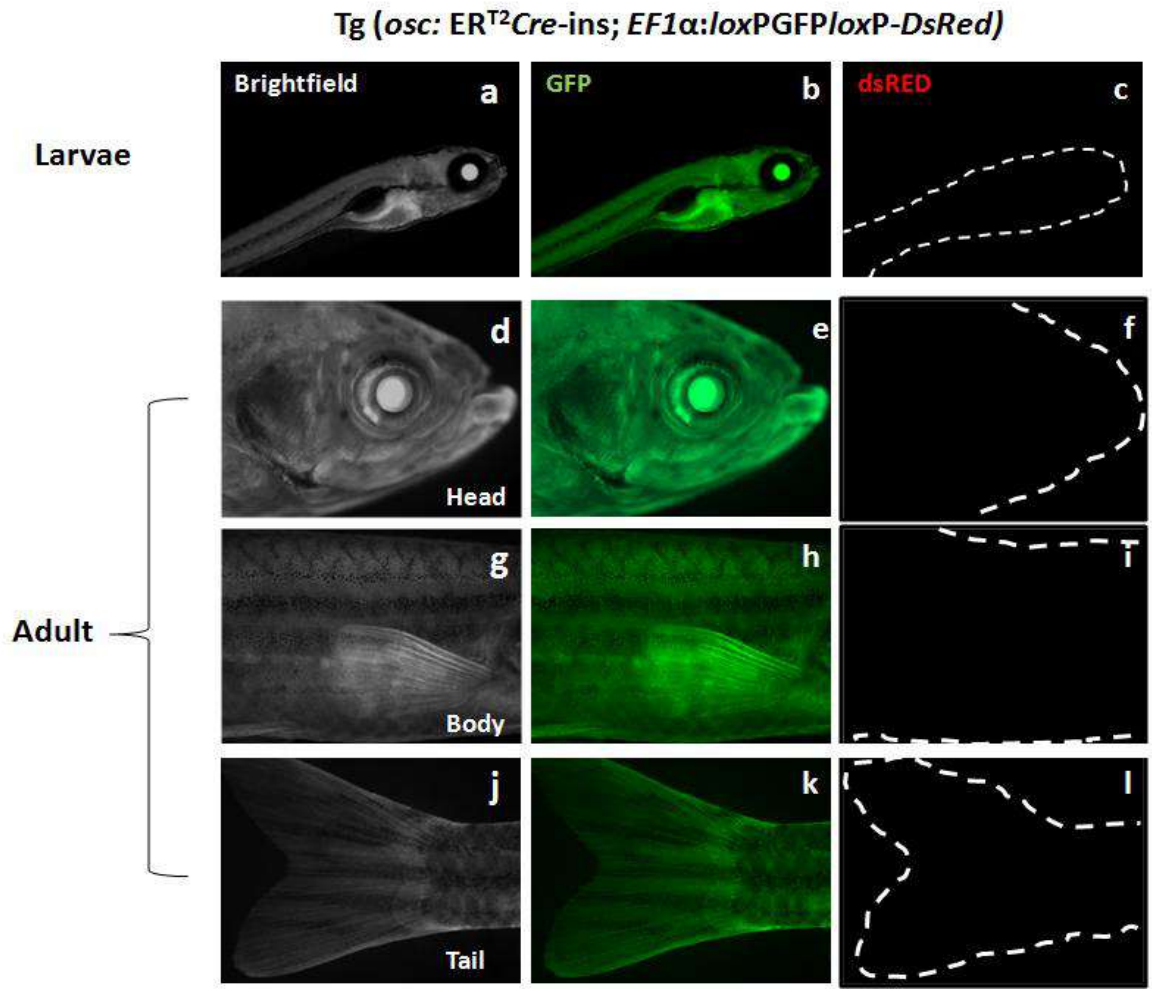

Figure 5.9. **The dTg *(osc*:ER^{T2}*Cre*-ins;*EF1α*:l*ox*PGFP*lox*P-*dsRed*) showed high ubiquitous GFP expression at different developmental stages.** No Cre leakiness (Cre recombination without 4OHT administration) was detected as well. Representative images of this dTg is shown as an example of the CreER^{T2} drivers crossed with the *lox* Switch line tg (*EF1α*:*lox*PGFP*lox*P-*DsRed*). Positive siblings (5dpf) expressing strong GFP signal in all visible external organs, such as the skin, eyes, and fins were screened and selected (a-b). Selected fish were also analyzed for Cre leakiness (Cre recombination without 4OHT administration), dsRed signal was not detected in fish expressing strong GPF (c). These animals were sent to raise (2 tanks of 40 fish each); after 3 months, fish were examined again by fluorescence microscopy to detect ubiquitous and strong GFP expression (d,e,g,h,j,k) in adulthood; Cre leakiness was still absent (f,i,l).

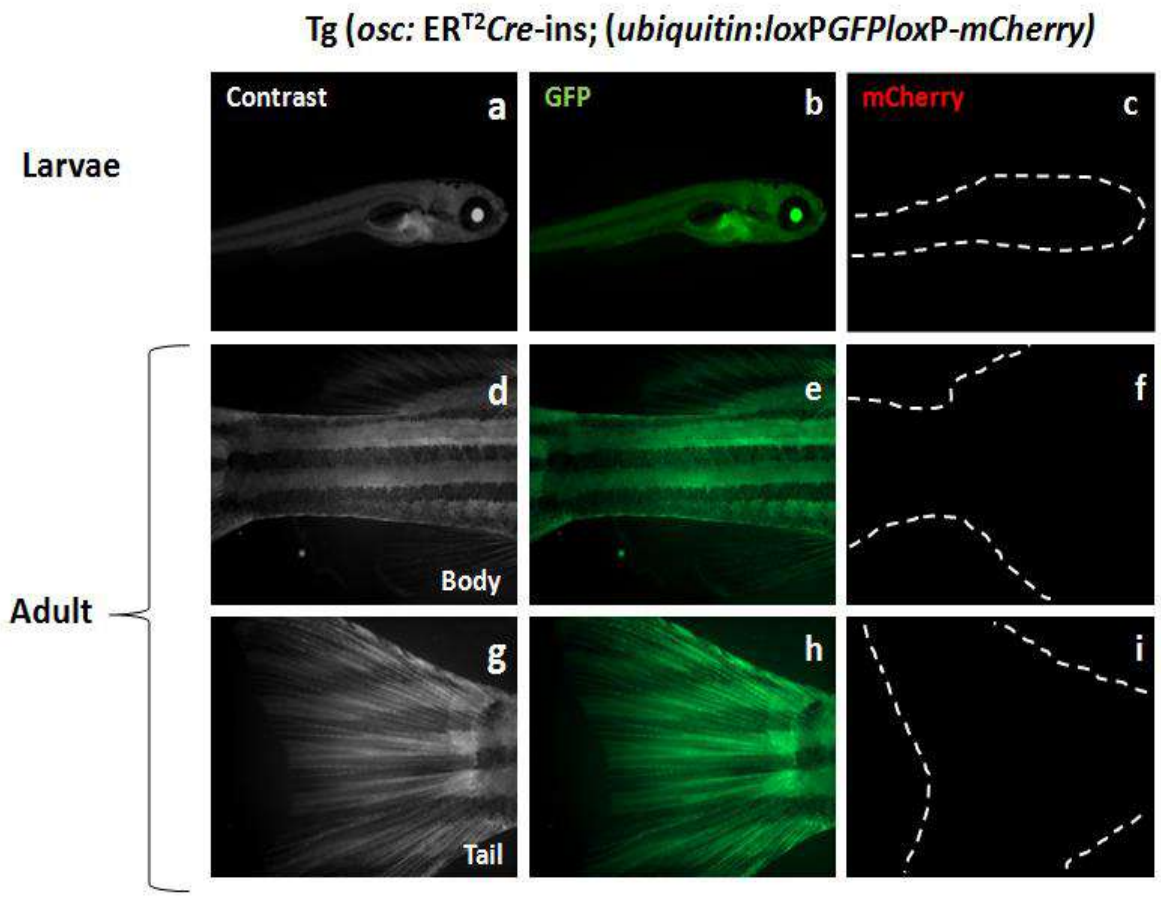

Figure 5.10. The dTg (*osc*:ER^{T2}*Cre*-ins; *ubiquitin*:*lox*P*GFPlox*P-*mCherry*) showed high ubiquitous GFP expression at different developmental stages. No Cre leakiness (Cre recombination without 4OHT administration) was detected as well. Representative images of this dTg is shown as an example of the CreER^{T2} drivers crossed with the *lox* Switch line tg (*ubiquitin*:*lox*P*GFPlox*P-*mCherry*). Positive siblings (5dpf) expressing strong GFP signal in all visible external organs, such as the skin, eyes, and fins were screened and selected (a-b). Selected fish were also analyzed for Cre leakiness (Cre recombination without 4OHT administration), mCherry signal was not detected in fish expressing strong GPF c). These animals were sent to raise (2 tanks of 40 fish each); after 3 months, fish were examined again by fluorescence microscopy to detect ubiquitous and strong GFP expression (d,e,g,h) in adulthood; Cre leakiness was still absent (f,i).

5.4 Discussion

5.4.1 Generation of double transgenic lines dTg to perform Cre/*loxP* - based lineage tracing experiments

In general, the Cre-lox system has been used with successful results in zebrafish at different developmental stages, since Langenau and colleagues demonstrated that this system could be applied in this animal model (Langenau *et al*., 2005).

Therefore, taking advantage of this system a set of different double transgenic lines were generated to assess different questions in a fracture healing context in adult zebrafish.

Knopf and colleagues (Knopf *et a*l. 2011) showed that osteoblast dedifferentiation is restricted to appendage regeneration but it is interesting to determine whether this is a more general process found in fish bone, such as repair after a fracture.

Moreover, in what regards osteoclast participation during a fracture process, I wanted to determine whether the same osteoclast cells participate at different time points during the fracture process or not. In addition, whether osteoclast cell division occurs after its arrival at the fracture site, are questions I want to tackle.

Thus, three different tissue-specific drivers were generated for this purpose: Tg (*osc:* ER^{T2}*Cre*-ins), Tg (*twist2:* ER^{T2}*Cre*-ins) and Tg (*ctsk:* ER^{T2}*Cre*-ins). Certainly, one aspect to consider is to know that the endogenous gene transcript of each Cre-driver is expressed during the fracture healing process. This was confirmed by *in situ* experiments, Figures 3.5 (*osc)* and 3.7 (*cathepsin k*) in Chapter 3 showed that these genes are induced during the fracture healing process in zebrafish. Also, *twist2* expression was detected post-fracture (data not shown). It has been shown that *twist2* is expressed after an injury in zebrafish. In the regeneration context, the gene is induced in the first 24 hours -post-amputation in preosteoblasts near the amputation site to maintain them in a mesenchymal state that later will form the new bone.

Furthermore, complementary analyses, such as mRNA *in situ* to detect *creERT2* transgene in the double lines can help to ensure faithful transgene expression. Unfortunately, these experiments couldn´t be performed in the generated lines to assess the levels of Cre expression due to the

unsuccessful production of a Cre probe. Attempts to detect the Cre RNA by ISH in transgenic lines paired with one ERT2 were done without success. The generation of an antisense Cre probe that can detect only the ER section could solve this issue. Also, RT-PCR could be done to determine Cre expression in the constructed transgenic lines.

5.4.2 Double transgenic lines showed ubiquitous and strong GFP expression until adulthood.

Lox Switch lines that has efficient promoters that drive ubiquitous transgene expression in larvae and adult tissues in zebrafish was challenging for the community. Some attempts by using *Xef1a* or *B-actin* promoter –controlled *lox* cassettes containing fluorescent protein genes were reported by different groups (Langenau *et al*., 2005; Yoshikawa *et al*., 2008; Hans *et al*., 2010), but these were inefficient. Moreover, lines with *EF1a* and *ubiquitin* promoters showed ubiquitous expression in adulthood, which is important to get successful Cre-lox experiments in my case. Thus, double transgenic lines were generated either with *lox* Switch transgenic lines: Tg (*EF1a*:l*ox*PGFP*lox*P-*dsRed*) or Tg (*ubiquitin*:*lox*P*GFPlox*P-*mCherry*). Representative images of dTg (*osc*:ER^{T2}*Cre*-ins;*EF1a*:l*ox*PGFP*lox*P-*dsRed)* (Figure 5.9) *and (osc*:ER^{T2}*Cre*-ins; *ubiquitin*:*lox*P*GFPlox*P-*mCherry)* (Figure 5.10) were used to illustrate that ubiquitous strong GFP expression was detected at larvae and adulthood stages. However, not all the animals analyzed had the same result; transgene silencing (non- expression of the transgene at particular tissues or body parts due to different effects) was observed in different fish as well. This effect is commonly observed in adult transgenic lines (Detrich *et al*., 2011). The use of insulators that flank the DNA cassette can prevent gene silencing due to the intrusion of chromatin condensations (Burgess-Beusse *et al*., 2002), but it seems that these DNA elements couldn´t avoid the effect at all.

5.4.3 No Cre mediated leakiness was detected in double transgenic lines (dTg)

The first Cre-drivers generated in zebrafish contained hsp70-controlled Cre (*hsp70:cre* and *hsp70:EGFP-cre*) offering temporal control through heat shock-inducible activity of the

promoter. But they lacked efficiency due to "leakiness" of the promoter and its low expression (Le *et al.*, 2007; Thummel *et al.*, 2005). The integration of DNA insulators (DNA sequences that act as barriers) that flank the DNA cassette probably helped to increase the recombination efficiency of Cre enzyme. The analyzed samples didn´t show Cre-recombination in the tail fin or other body parts either at larvae or adulthood stages. Figures (5.9 b,e,h,k) and (5.10 b,e,h). Moreover, these observations were also seen in different transgenic lines that also incorporated DNA insulators that flank the DNA cassette. The observations were seen in larvae by 6Monsterrat García in the laboratory (García Romero. 2016. PhD dissertation). This information suggested that Tamoxifen-induced- Cre-lox recombination experiments could be performed in adult zebrafish.

5.5 Conclusions

Three different Cre-driver bone-associated transgenic lines were generated as a first step to induce controlled site-specific recombination in zebrafish tail fins. To do this, the Cre-drivers were crossed with two available *lox* Switch reporter lines that contain different ubiquitous promoters. Thus, different double transgenic lines were generated to find the most suitable to perform Cre-lox lineage tracing experiments in a bone fracture healing context. Moreover, fish adulthood is the stage of interest to perform experiments; thus, double transgenic lines were analyzed by microscopy and those fish showing strong and ubiquitous GFP expression were selected for cell tracking experiments. Also, the analysis showed that no Cre mediated leakiness was detected in the generated double transgenic lines (dTg).

CHAPTER 6

Usage of different strategies to induce Cre-recombination in adult double transgenic lines.

6.1 Introduction

The appearance of a modified Cre recombinase version fused to the human ligand-binding domain of the estrogen receptor (ER) allowed for recombination events to be performed with a tight temporal and spatial control. Therefore, the main feature of this Cre version is its insensitivity to natural estrogen but not to the chemicals Tamoxifen or its derivate 4-hydroxitamoxifen (4-OHT) (Feil *et al*., 1997; Metzger *et al*., 1995). Therefore, the sensitivity and recombination efficiency increased considerably compared to the original Cre enzyme.

In general, the system works as the following, in the default state the CreERT2 version is sequestered in the cytoplasm and can only be translocated into the nucleus when Tamoxifen or (4-OHT) are added. After this action, the modified enzyme mediates *lox* excision; resulting in a tight temporal control over recombination. Moreover, depending on the *lox* sites orientation the recombination event not only can cause excisions, also invertions of the DNA cassette flanked by these sites can be done. In addition, these *lox* sites have been modified by mutagenesis (such as *lox*2272 and *lox*N) to increase its efficiency (Livet *et al.,* 2007)

Important to realize is the fact that in mice the administration of Tamoxifen or 4-OHT induces an effect that can be problematic due to the body size, ways of administration, etc. In contrast, zebrafish drug administration is easier; drugs can be added directly into the water which causes effective $CreER^{T2}$ responses (Hans *et al* 2009; Mosimann *et al*., 2011). Moreover, according to Hans and colleagues, in zebrafish the optimal Tamoxifen/4-OHT dose for a specific $CreER^{T2}$ driver paired with a *lox* switch requires individual tests to get the best results (Hans *et al*., 2009).

6.2 Background

As mentioned in the previous Chapter, at the time I started to work on this project, different lab members joined their efforts to implement the Cre-lox system in the laboratory in order to perform studies related to epimorphic regeneration in zebrafish larvae. Related to this, Montserrat García a lab fellow, during her PhD generated and characterized a set of 6 different tissue specific $CreER^{T2}$-driver lines to perform lineage tracing analysis after fin amputation. She showed that most of the generated lines could undergo tissue recombination and that this event was tightly dependent of 4OHT administration (García Romero. 2016. PhD dissertation). Thus, her results showed that Cre-lox system was working in the laboratory and that at least for experiments performed in larvae, the conditions to induce recombination were established.

Therefore, the objective of the project was to perform Cre-lox based experiments in adult zebrafish, which compared to larvae, a considerable smaller number of publications were available. Also, working with adult zebrafish represented additional challenges such as, the amount of chemical needed to perform experiments and the appearance of transgene silencing, a phenomenon commonly observed in transgenic lines during adulthood (Detrich *et al*., 2011).

6.3 Results

6.3.1 Tamoxifen couldn´t induce recombination in the tested transgenic lines

$CreER^{T2}$ - mediated *lox* recombination can be induced at concentrations as low as 0.5 μM Tamoxfen (TAM) or 4-OHT in zebrafish larvae (Hans *et al*., 2009; Mosimann *et al*., 2011).

Moreover, at the moment when the different set of double transgenic lines were ready to perform Cre lox experiments, different lab members had technical difficulties to obtain satisfactory results with 4-OHT administration; thus, Tamoxifen was planned to be tested first. Few references were found which used Tamoxifen and not 4-OHT to induce Cre-based recombination experiments in adult zebrafish. For instance, Tamoxifen was administrated at a final concentration of 1 μM added to fish water for 1 hour during a regimen of 3 consecutive

days prior imaging to obtain results. But importantly to consider, authors used the Gal4-ERT system which is a different way to induce temporal Cre-recombination (Akerberg *et al.*, 2014). Also, CreERT2-mediated recombination in adult zebrafish was showed to be induced by four or five soakings (10 hours each) in 5 μM Tamoxifen in a DMSO/fishwater (1:1000) solution (Kroehne *et al.*, 2011).

First, groups of 3 wild-type adult fish (6-8 months old) were soaked independently in fish water with a specific final Tamoxifen concentration [0.5, 1, 2, 5 or 10 μM] to determine chemical toxicity. In addition, vehicle DMSO was added in water with the same experimental drug concentration in controls. After 30 minutes fish were checked and the experiment showed that 5 and 10 μM were lethal for fish. The rest of the groups didn´t show adverse effect and completed the first 8 hours session. Then, when the second (8 hr) session finished only 1/3 fish of the 2 μM group was alive; in contrast, fish of 0.5 and 1 μM groups survived and completed four hour sessions soaked in Tamoxifen without showing evident signals of chemical toxicity. Importantly, control fish didn´t show toxicity effects suggesting that this was due to the chemical concentration. Thus, these experiments showed that in my hands addition of Tamoxifen at a final 5 and 10 μM are lethal to fish, 2 μM showed to be less toxic but was not suitable for Cre-Lox experiments. Moreover, 0.5 and 1 μM were not toxic to finish with potential to use them in experiments. The summary is shown in the following Table 6.1:

Table 6.1 Tamoxifen toxicity experiment (adult zebrafish)					
Concentration []	0.5 μM	1 μM	2 μM	5 μM	10 μM
Effect	Not toxic	Not toxic	Toxic	Lethal	Lethal
Observation	4 sessions 8 hrs long, no effect	4 sessions 8 hrs long, no effect	Toxic after 2nd session	Immediate toxicity	Immediate toxicity
# wt	3/3 fish	3/3 fish	2/3 fish	3/3 fish	3/3 fish

Therefore, after Tamoxfen toxicity experiments I decided to test [0.5 and 1 μM] to induce Cre recombination in double transgenic lines that have the *lox* reporter (*EF1α:loxPGFPloxP-DsRed).* The reason was due to observations from different lab members who got better results with the switch from GFP to DsRed (tissue recombination) in the target tissues in zebrafish larvae.
To perform experiments, 3 fish of each double transgenic lines: dTg (*ctsk*:ER^{T2}*Cre*-ins; *EF1α:loxPGFPloxP-DsRed*), dTg (*osc* ER^{T2}*Cre*-ins; *EF1α:loxPGFPloxP-DsRed*) and dTg (*twist2*: ER^{T2}*Cre*-ins; *EF1α:loxPGFPloxP-DsRed*) were soaked in fish water with a specific final Tamoxifen concentration [0.5 and 1 μM]. Drug treatments were repeated 4 times (8 hours long). Also, the dTg (osc:CreERT2;*EF1α:loxPGFPloxP-DsRed*) was also tested. This line was generated by Montserrat García in the lab to label mature ostebolasts as well, it is similar to the line generated by me dTg (*osc* ER^{T2}*Cre*-ins; *EF1α:loxPGFPloxP-DsRed*) because it shares the same *osteocalcin* promoter but differs in some specific features (section 5.3.1). In addition, the positive control dTg (*fli1a:ERT2CreERT2;EF1a:loxPGFPloxP-DsRed*) which label blood vessels was also included in experiments (García Romero. 2016. PhD dissertation). Furthermore, vehicle DMSO was added in the water with the same experimental drug concentration as controls.

Subsequently, two ray fractures were induced in the tail fin and immediately photographed after the insult (O hpc) and at different time points (once every 24 hours post- injury during 5 consecutive days) in order to detect tissue recombination. The recombined tissue should express the DsRed fluorescent protein.

Thus, I searched for DsRed signal detection in the tail fin of all the tested transgenic lines but couldn´t find Cre-recombination induced by Tamoxifen addition; the rest of the body of each fish was also analyzed but results were negative as well. DsRed protein was not detected during the drug treatments or after inducing two bone fractures on each side of the tail fin. Also, due to the fact that recombination effect could take several hours, fish were monitored during 5 days post fracture to detect DsRed signal but it was unsuccessful. Moreover, fish treated with vehicle (EtOH) didn´t show DsRed protein in any transgenic line, suggesting that Cre leakiness (recombination without Tamoxifen addition) was not present. In addition, the positive control dTg (*fli1a:ERT2CreERT2;EF1a:loxPGFPloxP-DsRed*) didn´t express DsRed protein in the blood vessels as expected. Thus, the available evidence suggested that tested Tamoxifen conditions and/or treatment are not able to induce Cre recombination in the analyzed transgenic lines, but other reasons could exist which are mentioned in the discussion section.

In the following figure (6.1) I show representative images of dTg (*osc* ER^{T2}*Cre*-ins; *EF1α:lox*PGFP*lox*P-*DsRed*) and positive control dTg (*fli1a:ERT2CreERT2;EF1a:loxPGFPloxP-DsRed*) as examples.

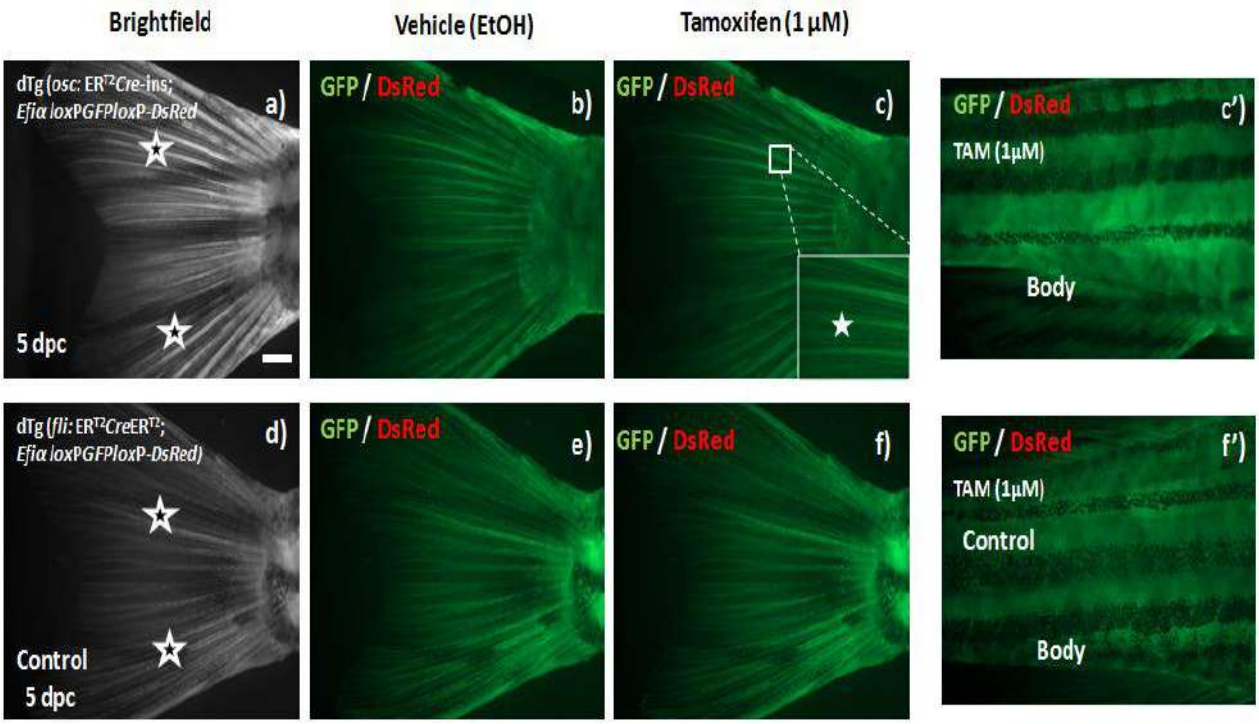

Figure 6.1. No tissue recombination was detected in the double transgenic lines after Tamoxifen treatments. Representative images of dTg (*osc* ER^{T2}*Cre*-ins; *EF1α:lox*PGFP*lox*P-*DsRed*) (a-c, c´) and positive control (*fli1a:ERT2CreERT2;EF1a:loxPGFPloxP-DsRed*) (d-f, f´) are shown as examples.
Transgenic lines were soaked in fish water with a final [1 μM] Tamoxifen concentration during 8 hours (x4) times. Furthermore, vehicle EtOH was added in fish water with the same experimental drug concentration as controls. Subsequently, two bone fractures were induced on both sides of the tail fin (stars) and imaged once every 24 hours post- fracture during 5 consecutive days in order to detect tissue recombination (change from GFP to DsRed). Experiments showed that DsRed signal detection was absent on tail fins and wasn´t detected after several days post fracture (c), suggesting the lack of recombination event. DsRed signal was also absent from the positive control (f). Other body parts were also analyzed with negative results as well (c´, f´). Moreover, fish treated with vehicle (EtOH) didn´t show DsRed protein in any transgenic line, suggesting that Cre leakiness (recombination without Tamoxifen addition) was not present in tested transgenic lines (b, e). Stars indicate the bone crush sites. (dpc)- days post

6.3.2 4-hydroxitamoxifen (4-OHT) couldn´t induce recombination in the tested transgenic lines

Tamoxifen requires to be transformed chemically in order to produce 4-hydroxitamoxifen (4-OHT). Thus, it introduces a potential lag in CreERT2 response. Due to this, nowadays most of Cre-lox experiments are performed using (4-OHT) which provides a direct activity and is less toxic to the animal (Detrich *et al.*, 2011). Moreover, to illustrate, the Cre recombinase-based genetic cell-labeling approach has been used in adult zebrafish to study bone regeneration after fin amputation by tracking osteoblast cells (Knopf *et al.*, 2011). In order to perform these studies, authors used 4-OHT at a 0.5 uM final concentration during 3 consecutive sessions (8 hours long each one). By the time I planned to perform experiments, members from Jopling´s lab (Uni. of Montpellier. France) recommended a treatment with 4-OHT at a 3 uM final concentration with a single session of fish soaked in tank water for 8 hours long. Therefore, due to the fact that Jopling´s lab members use regularly a similar *lox* Switch reporter line, Tg (*EF1a:loxP DsRed loxP-EGFP)* with successful results, I decided to perform experiments with the same protocol on double transgenic lines that have, either (*EF1a:loxP DsRed loxP- EGFP)* or (*ubiquitin*:*lox*P*GFPlox*P-*mCherry)* lox Switch reporters to detect the best for experiments.

Details of both protocols are annotated in the following Table 6.2:

Tamoxifen (4-OHT) Concentration used	Drug treatment	Reference
0.5 uM	3 consecutive sessions (8 hours long each)	Knopf *et al.*, 2011
3 uM	1 session (8 hours long)	Jopling´s lab protocol. Uni. of Montpellier. France

To perform experiments, the following double transgenic lines were analyzed:

Table 6.3

Tansgenic line	**Recombination**	**Target tissue (after recombination event)**
dTg (*osc* ER^{T2}*Cre*-ins; *EF1*α:*lox*PGFP*lox*P-*DsRed*)	From GFP to DsRed	Mature osteoblasts
dTg (*twist2*: ER^{T2}*Cre*-ins; *EF1*α:*lox*PGFP*lox*P-*DsRed)*	From GFP to DsRed	Chondrocytes and sclerotomal cells
dTg *(osc* ER^{T2}*Cre*-ins; *ubiquitin*:*lox*P*GFPlox*P-*mCherry)*	From GFP to mCherry	Mature osteoblasts
	From GFP to mCherry	Chondrocytes and sclerotomal cells

dTg *(twist2* ER^{T2}*Cre*-ins; *ubiquitin*:*lox*P*GFPlox*P-*mCherry)*		
Positive Controls		
dTg (*fli1a:ERT2CreERT2*; *EF1*α:*lox*PGFP*lox*P-*DsRed)* Montserrat García	From GFP to DsRed	Blood vessels
dTg (*fli1a:ERT2CreERT2*; *ubiquitin*:*lox*P*GFPlox*P-*mCherry* Montserrat García	From GFP to mCherry	Blood vessels

To perform experiments, 3 fish of each double transgenic lines (Table 6.3) were soaked independently in fish water with a specific final Tamoxifen (4-OHT) concentration [3 μM] and kept during 8 hours. Furthermore, vehicle EtOH was added in the water with the same experimental drug concentration in controls.

Subsequently, fish were injured and immediately photographed after the insult (O hpc) and at different time points (once every 24 hours post- injury during 5 consecutive days) in order to detect tissue recombination. The recombined tissue should express DsRed or mCherry fluorescent proteins respectively.

As a result, I searched for DsRed or mCherry signal detection in the tail fin of all the tested transgenic lines but couldn´t find Cre-recombination induced by Tamoxifen addition. Representative images of dTg *(osc* ER^{T2}*Cre*-ins; *ubiquitin*:*lox*P*GFPlox*P-*mCherry)* (Fig 6.2 a-c, c´)*;* (*osc* ER^{T2}*Cre*-ins; *EF1*α:*lox*PGFP*lox*P-*DsRed*) (Fig 6.2. g-i, i´) and positive controls dTg (*fli1a:ERT2CreERT2*; *ubiquitin*:*lox*P*GFPlox*P-*mCherry)* (Fig 6.2 . d-f, f´)*;* and (*fli1a:ERT2CreERT2*; *EF1*α:*lox*PGFP*lox*P-*DsRed)* (Fig 6.2. j-l, l´)*,* are shown as examples.

Transgenic lines were soaked in fish water with a final [3 μM] Tamoxifen concentration during 8 hours (x1) time. Furthermore, vehicle EtOH was added in fish water with the same experimental drug concentration as controls. Subsequently, two bone fractures were induced on both sides of the tail fin (stars) and imaged once every 24 hours- post- fracture during 5 consecutive days in order to detect tissue recombination (change from GFP to DsRed or mCherry respectively). Experiments showed that DsRed or mCherry signal detection was absent on tail fins and couldn´t be detected after several days post fracture (Fig 6.2 g, i), indicating the lack of Cre- recombination event. DsRed or mCherry signal was also absent from the positive controls (Fig 6.2 f, l). Other body parts were also analyzed and no Cre-recombination was detected (Fig 6.2 c´, i´), either in positive controls (Fig 6.2 f´, l´). Moreover, , fish treated with vehicle (EtOH) didn´t show DsRed/mCherry protein in any transgenic line, suggesting that Cre leakiness (recombination without Tamoxifen addition) was not present in tested transgenic lines (Fig 6.2 b, e, h, k).

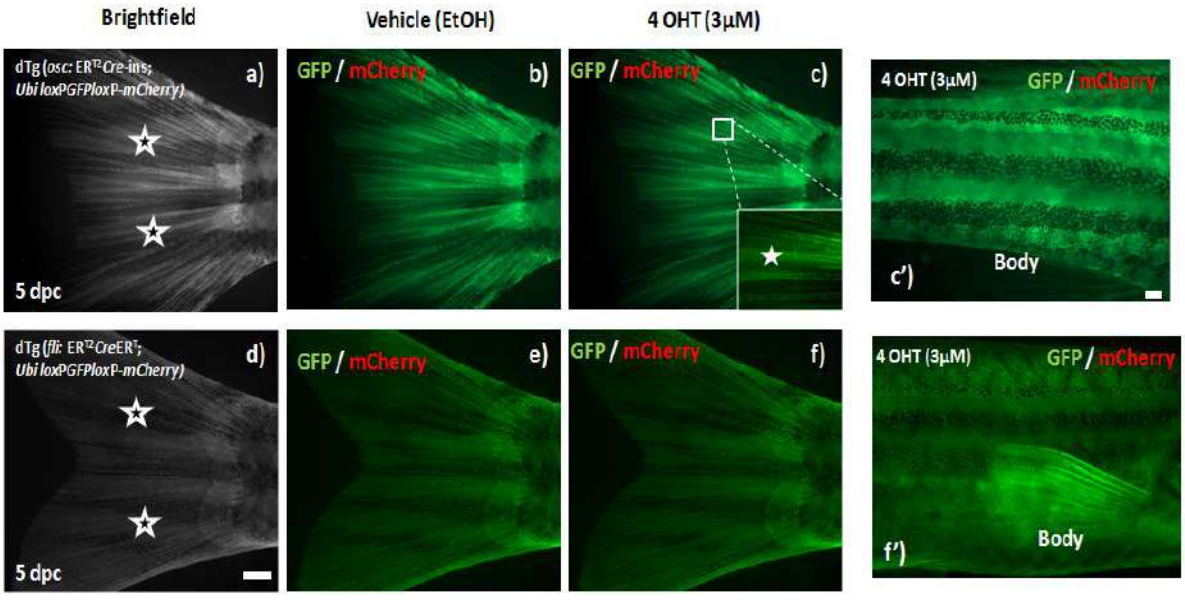

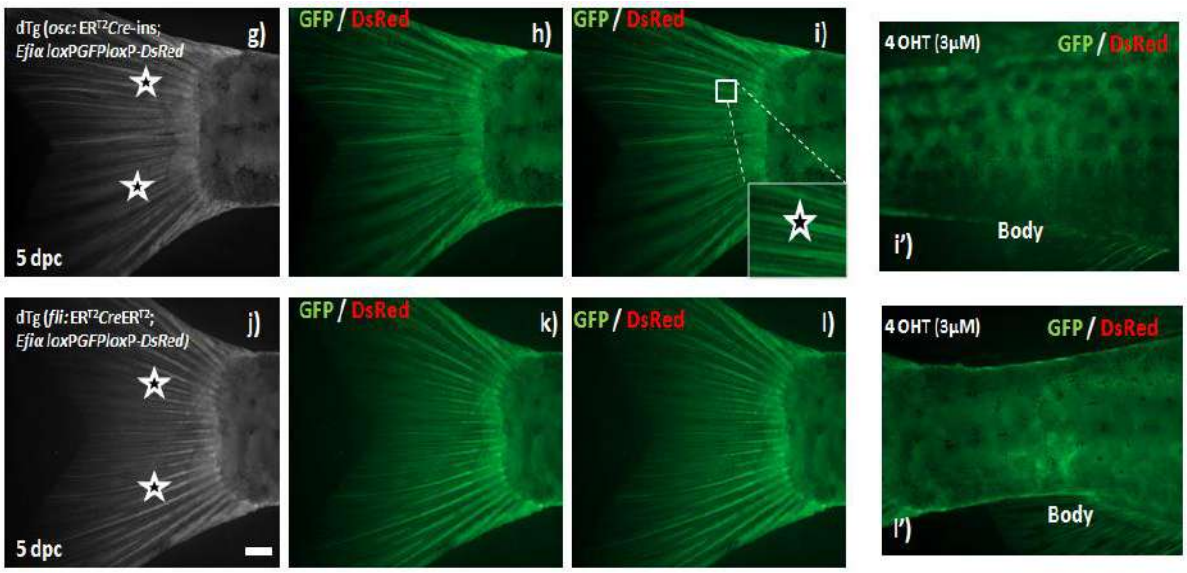

Figure 6.2. No tissue recombination was detected in the double transgenic lines after 4-OHT treatment.
Representative images of dTg *(osc* ER^{T2}*Cre*-ins; *ubiquitin*:*lox*P*GFPlox*P-*mCherry)* (a-c, c´)*;* (*osc* ER^{T2}*Cre*-ins; *EF1α*:*lox*PGFP*lox*P-*DsRed*) (g-i, i´) and positive controls dTg (*fli1a:ERT2CreERT2*; *ubiquitin*:*lox*P*GFPlox*P-*mCherry)* (d-f, f´)*;* and (*fli1a:ERT2CreERT2*; *EF1α*:*lox*PGFP*lox*P-*DsRed)* (j-l, l´)*,* are shown as examples.
Transgenic lines were soaked in fish water with a final [3 μM] Tamoxifen concentration during 8 hours (x1) time. Furthermore, vehicle EtOH was added in fish water with the same experimental drug concentration as controls. Subsequently, two bone fractures were induced on both sides of the tail fin (stars) and imaged once every 24 hours-post- fracture during 5 consecutive days in order to detect tissue recombination (change from GFP to DsRed or mCherry respectively). Experiments showed that DsRed or mCherry signal detection was absent on tail fins and couldn´t be detected after several days post fracture (g, i), indicating the lack of Cre- recombination event. DsRed or mCherry signal was also absent from the positive controls (f, l). Other body parts were also analyzed and no Cre-recombination was detected (c´, i´), either in positive controls (f´, l´). Moreover, , fish treated with vehicle (EtOH) didn´t show DsRed/mCherry protein in any transgenic line, suggesting that Cre leakiness (recombination without Tamoxifen addition) was not present in tested transgenic lines (b, e, h, k). Stars indicate the bone crush sites. (dpc)-days post

6.4 Discussion

A set of Cre-driver transgenic lines were generated to perform Cre-lox lineage tracing experiments in adult zebrafish. To assess this, different strategies were performed to induce Cre recombination in the transgenic lines by adding Tamoxifen or 4-OHT; unfortunately, I couldn`t get positive results.

6.4.1 Tamoxifen /4-OHT- did not mediate CreERT2 induction

One of the first aspects to consider when issues exist regarding the lack of Cre-lox recombination is to consider the chemical handling.

The relative efficacies of TAM and 4-OHT for CreERT2 induction are difficult to assess due to their instability, both are light- and temperature- sensitive chemicals. Therefore, it is advised to keep them in the dark and to use fresh or recently dissolved chemical stocks because it was found that prolonged storage decreases recombination efficiency over time (Mosimann *et al.*, 2011). This phenomenon was also observed by laboratory fellows in larvae studies as well. Tamoxifen and 4-OHT experiments were performed with fresh stocks most of the times. In few occasions, 1 month old (4-OHT) stocks were used because laboratory fellows still got good recombination efficiency in larvae

6.4.2 The optimal induction time point still needs to be determined for each transgenic line.

CreERT2-mediated *lox* recombination can be triggered in zebrafish at concentrations as low as 0.5 μM Tamoxifen or 4-OHT in larvae (Hans *et al.*, 2009; Mosimann *et al.*, 2011). The same Tamoxifen concentration can also produce efficient recombination in adult zebrafish (Knopf *et al.*, 2011). Interestingly, zebrafish larvae can tolerate 10 – 20 μM 4-OHT treatments without adverse effects, which are high concentrations. In contrast, adult zebrafish seems to be more sensitive than larvae, Tamoxifen or 4-OHT treatments are not exceptions. After performing a Tamoxifen chemical test, in my hands only fish treated with 0.5 and 1 μM Tamoxifen survived

(Table 6.1). It is possible that higher Tamoxifen concentrations are ideal to induce recombination in the different transgenic lines but fish couldn´t tolerate treatments higher than 1 μM. (Figure 6.1)

Moreover, it is known that 4-OHT is less toxic than Tamoxifen; this prodrug requires metabolic transformations to produce 4-OHT. Thus, it introduces a potential lag in CreERT2 response. This is one of the reasons why most of Cre-lox recombination experiments use 4-OHT rather than Tamoxifen, also due to its less toxicity as mentioned before. The treatment I used (I session, 3 μM 4-OHT) suggested by Jopling´s lab (Univ. of Montpellier), didn´t induce Cre recombination in the tested transgenic lines, either in the positive controls dTg (*fli1a:ERT2CreERT2*;*ubiquitin*:*lox*P*GFPlox*P-*mCherry)* or (*fli1a:ERT2CreERT2*; *EF1α*:*lox*PGFP*lox*P-*DsRed)* that label blood vessels after a recombination event (Figure 6.2). Given these points, further experiments need to be done to determine the suitable conditions (chemical concentration and treatment) to induce recombination in the generated transgenic lines. I would suggest the use of intraperitoneal injections as it has been performed to induce Cre-recombination for adult cardiomyocyte studies, for example (Jopling *et al*., 2010; Kikuchi *et al*., 2010)

6.5 Conclusion

A set of different Cre- driver lines were crossed with two different *lox* Switch lines to perform Cre-Lox lineage tracing experiments in the fracture healing context. Furthermore, to induce Cre recombination in adult fish, different strategies that involved Taxmoxifen or 4-OHT chemicals were tested. Unfortunately, no recombination was detected after several days- post-treatment. Positive controls didn´t show recombination either suggesting that optimal conditions were still needed to get positive results. I suggest the screening of more fish to find adult fish that when crossed with a lox Switch reporter line, express high level of Cre recombinase. Also, it is necessarily to test fish during larvae stages.

CHAPTER 7

7.1 General Discussion

In recent years, zebrafish has become an attractive model in the Biomedical Science field, due to the constant development and availability of molecular tools that enable studies which cannot be performed in other classical models so far. The use of zebrafish to study skeletogenesis is one of those fields where the model can be very useful. Thus, in my project I continued with the characterization of the bone fracture model that was proposed originally by Sousa and colleagues (Sousa et al., 2012). In this publication, authors focused their analysis on the expression of different regeneration markers during fracture healing compared with fin regeneration after amputation.

Moreover, the analysis made in this PhD thesis of the different fracture healing stages (inflammation, bone formation, remodeling) suggest that molecular and cellular events are similar between zebrafish and mammals, as suggested by different studies (Flores *et al.*, 2004; Yan *et al.*, 2005; Li *et al.*, 2009); probably, the main difference is the time frame needed in each animal model for healing.

Notably, during the process of this PhD project, two groups proposed different bone fracture models in medaka and zebrafish, which differ in the way bone fracture is performed. First, Takeyama and colleagues, performed bone fractures on fin hemirays with special needles to avoid blood vessels and surrounding tissue damage (Takeyama et al., 2014). From my point of view, the way those fractures are performed, do not mimic the fracture healing context at all. When this process takes place, tissues at the site and surroundings are seriously damaged (including blood vessels). Therefore, this effect triggers different restoration mechanisms (Schindeler et al., 2008). Also, in zebrafish with a similar method to induce damage like in medaka study, Geurtzen and colleagues with the use of photoconvertible Kaede protein and Cre-driven genetic fate mapping, showed that osteoblasts migrate to the site of injury to replace damaged tissue. Their finding suggests that adult fish osteoblasts display elevated cellular plasticity compared with mammalian bone-forming cells (Geurtzen et al., 2014).

Moreover, as suggested in the previous chapter, further strategies are needed to determine the suitable conditions to induce Cre-recombination in the target tissue of the different created transgenic lines. For example, to explore whether the generated transgenic lines offspring have the capacity to be stimulated by Tamoxifen (4-OHT) addition, I crossed the tg (osc ERT2Cre-ins; EF1:loxPGFPloxP-DsRed) and tg (twist2 ERT2Cre-ins; EF1:loxPGFPloxP-DsRed) lines with wildtype fish. In collaboration with my lab fellow Monsterrat García, I performed Cre-lox based experiments in larvae (5 dpf), to confirm the hypothesis. Interestingly, after adding 10 μM 4OHT to tg (twist2 ERT2Cre-ins; EF1:loxPGFPloxP-DsRed) line, experiments showed tissue recombination after some days in the jaw area. The cells that expressed the DsRed protein seemed to have chondrocyte identity, which are cells that creates cartilage matrix (Perka et al., 2000). Data suggested that possibly, the specific optimal conditions to induce recombination in adult still need to be found.

However, when the same experiments were performed in tg (osc ERT2Cre-ins; EF1:loxPGFPloxPDsRed), recombination was not observed in larvae. It has been reported that osteocalcin is expressed at 7 dpf on the fifth ceratobranchial (Gavaia et al., 2006). To consider, another publication reported the expression of GFP until 22 dpf in a tg (osteocalcin:GFP) line. Thus, fish were kept for several days until almost 30 dpf for analysis but recombination was still absent. For these experiments, no Cre mRNA could be tested due to the lack of a suitable Cre probe. Also, I confirmed by DNA sequencing that osteocalcin promoter sequence doesn´t have any abnormality. Moreover, Monika Tomecka, a lab fellow, generated the tg (osc:Kaede) line to track cells. She reported the expression of Kaede protein (photoconvertible) (Ando *et al.*, 2002) in adult fin rays, where osteocalcin is normally expressed. Further experiments need to be done to discard the idea that the integrated transgene suffers a silencing effect that doesn´t allow gene expression in the transgenic line.

7.2 Future Directions

The characterization of the fracture healing model in adult zebrafish, proposed originally by Sousa and colleagues (2012) suggests that this process is similar to mammalian fracture repair.

Advances in imaging, genetic tools and chemical genetics have positioned zebrafish as a powerful tool to dissect the temporal and spatial relationship between inflammation and injury repair, such as a bone fracture. The identification of reverse neutrophil migration as a mechanism that can resolve local inflammation is an example on how zebrafish studies had uncover new mechanisms related to wound healing (Mathias et al., 2006). Therefore, I propose to test this mechanism in adults in the fracture healing context. To do this, a collaboration with Renshaw´s lab (University of Sheffield) to use the available Tg (mpx:Kaede) line and see if it is functional in adult fish. Thus, this could permit the tracking of neutrophil cells after performing bone fracture.

Also, taken advantage of the Nitroreductase-mediated cell/tissue ablation technology in zebrafish, it could be possible to ablate specifically neutrophils for example, to analyze their influence on bone formation through the fracture healing process. Same experiments could be performed on osteoclasts or macrophages as well by using *ctsk* and *mpeg1* promoters respectively.

Moreover, the participation of macrophages in the same fracture healing context needs to be addressed as well. One first attempt was done to study these cells *in vivo* with the use of the Tg (mpeg1: GFP) line, but this promoter seemed to label resident macrophages and Langerhans cells (dendritic cells similar in shape and function as macrophages) (data not shown). Thus, it was difficult to differentiate them; a transgenic line that possess a different promoter that label macrophages could be helpful. In 2015, Walton and colleagues described *mfap4* as a new macrophage-specific promoter in zebrafish with better features than *mpeg1* because it remained stable during more time and a Cre transgenic line under the control of this promoter showed promising results (Walton *et al.*, 2015).

Furthermore, understanding the interactions between immune (neutrophils, macrophages, cytokines) and skeletal cells (osteoblasts, osteoclasts) during the fracture healing process in zebrafish is an interesting field to explore. To be precise, Osteo-immunology is the field that studies interactions between these cells. The possibility to generate double transgenic lines that label two different cells with fluorescent proteins could be useful to perform in vivo studies after

a bone fracture. For example: the generation of a dTg (IL1:GPF; osc; DsRed) line (to label IL1 cytokines an osteoblasts) or dTg (IL1: GFP; ctsk: dsRed) (to label IL1 cytokines and osteoclasts) could help us on exploring the way how bone and immune cells interact *in vivo* during the fracture healing process, something which has just started to be explored.

In addition, regarding the Cre-lox experiments, further studies are needed to identify the optimal conditions necessary to induce Cre recombination in the generated double transgenic lines. Intraperitoneal injections which consist in injections into the abdominal cavity of adult zebrafish could promote successful Cre-recombination. Also, the usage of specific zebrafish codons could enhance Cre expression within cells to get positive recombination results. Moreover, it is needed further screenings to detect more founders for each transgenic line to perform Cre recombination experiments.

7.3 General Conclusions

Firstly, the analysis of the fracture healing steps (inflammation, repair, remodeling) by different approaches in adult zebrafish, showed no remarkable differences at the cellular or molecular level in comparison to mammalian fracture repair. These results suggested an important level of conservancy regarding bone repair mechanisms between fish and mammals.

Notably, reactive oxygen species (ROS) production, which are one of the first signals to be induced after damage, depend on the lesion type in adult zebrafish. Amputation lesions released and maintained ROS for longer time compared to bone fracture which was brief. Also, my analysis shows that within the first 24 hours-post-fracture, different cell types and molecules take part in a coordinated manner. IL1β cytokine is induced early after bone damage and neutrophils are recruited at the fracture site after few hours as well. Both seem to induce directly or indirectly osteoclast recruitment. These bone remodeling cells, participate early but also remained active after several days.

Moreover, the second objective of this project was to determine whether osteoblasts dedifferentiation is restricted to appendage regeneration, or a more general process found in zebrafish, such as repair after a fracture. To solve this, efforts were done during the project to stablish in the laboratory the Cre-Lox system in adult zebrafish. As a first step, a set of double transgenic lines were created to enable tracking of bone cells *in vivo*. Afterwards, different tamoxifen-induced Cre-recombination strategies were performed in adult zebrafish but unfortunately, no successful results were obtained in any tested organism with different drug treatments. Further research is needed to get positive results.

The knowledge generated in this research can contribute to set the basis for the development of further studies of bone repair in zebrafish that can complement the ones performed in classical models.

CHAPTER 8

8.1 References

Akerberg, A. A., Stewart, S., & Stankunas, K. (2014). Spatial and temporal control of transgene expression in zebrafish. *PloS one*, *9*(3), e92217.

Akimenko, M. A., Marí-Beffa, M., Becerra, J., & Géraudie, J. (2003). Old questions, new tools, and some answers to the mystery of fin regeneration. *Developmental dynamics*, *226*(2), 190-201.

Al-Aql ZS, Alagl AS, Graves DT, Gerstenfeld LC, Einhorn TA. (2008). Molecular mechanisms controlling bone formation during fracture healing and distraction. *Osteogenesis. J Dent Res* 87: 107-18.

Ando, R., Hama, H., Yamamoto-Hino, M., Mizuno, H., & Miyawaki, A. (2002). An optical marker based on the UV-induced green-to-red photoconversion of a fluorescent protein. *Proceedings of the National Academy of Sciences*, *99*(20), 12651-12656.

Ballanti, P., Minisola, S., Pacitti, M. T., Scarnecchia, L., Rosso, R., Mazzuoli, G. F., & Bonucci, E. (1997). Tartrate-resistant acid phosphate activity as osteoclastic marker: sensitivity of cytochemical assessment and serum assay in comparison with standardized osteoclast histomorphometry. *Osteoporosis international*, *7*(1), 39-43.

Barnes GL, Kostenuik PJ, Gerstenfeld LC, Einhorn TA. (1999). Growth factor regulation of fracture repair. *J Bone Miner Res* 14: 1805-15.

Barton LM, Göttgens B, Gering M, Gilbert JG, Grafham D, Rogers J, Bentley D, Patient R, Green AR (1998) Regulation of the stem cell leukemia (SCL) gene: a tale of two fishes. *Proc Natl Acad Sci USA* 2001: 6747–6752.

Bastian O, Pillay J, Alblas J, Leenen L, Koenderman L, et al. (2011) Systemic inflammation and fracture healing. J Leukoc Biol. 89: 669–673.

Becker T, Wullimann MF, Becker CG, Bernhardt RR, Schachner M (1997) Axonal regrowth after spinal cord transection in adult zebrafish. J Comp Neurol, 377:577-595.

Bely, A. E., & Nyberg, K. G. (2010). Evolution of animal regeneration: re-emergence of a field. *Trends in Ecology & Evolution*, *25*(3), 161-170.

Bennett, C. M., Kanki, J. P., Rhodes, J., Liu, T. X., Paw, B. H., Kieran, M. W., ... & Look, A. T. (2001). Myelopoiesis in the zebrafish, Danio rerio. *Blood*, *98*(3), 643-651.

Bialek P, Kern B, Yang X, Schrock M, Sosic D, Hong N, Wu H, Yu K, Ornitz DM, Olson EN, Justice MJ, Karsenty G. (2004). A twist code determines the onset of osteoblast differentiation. *Dev Cell* 6: 423–435.

Blair HC, Teitelbaum SL, Ghiselli R, Gluck S (1989). Osteoclastic bone-resorption by a polarized vacuolar proton pump. Science 245(4920): 855-857.

Blum, N. and Begemann, G. (2012) Retinoic acid signaling controls the formation, proliferation and survival of the blastema during adult zebrafish fin regeneration. Development 139, 107–116

Blum N, Begemann G (2015) Retinoic acid signaling spatially restricts osteoblasts and controls ray-interray organization during zebrafish fin regeneration. Development, 142:2888-2893.

Blum N, Begemann G (2015) Osteoblast de- and redifferentiation are controlled by a dynamic response to retinoic acid during zebrafish fin regeneration. Development, 142:2894-2903.

Boyle, W.J., Simonet, W.S., Lacey, D.L. (2003). Osteoclast differentiation and activation. Nature 423, 337–342.

Brockes, J. P., & Kumar, A. (2005). Appendage regeneration in adult vertebrates and implications for regenerative medicine. *Science*, *310*(5756), 1919-1923.

Burgess-Beusse, B., Farrell, C., Gaszner, M., Litt, M., Mutskov, V., Recillas-Targa, F., ... & Felsenfeld, G. (2002). The insulation of genes from external enhancers and silencing chromatin. *Proceedings of the National Academy of Sciences*, *99*(suppl 4), 16433-16437.

Chablais, F. and Jazwinska, A. (2010) IGF signaling between blastema and wound epidermis is required for fin regeneration. Development 137, 871–879.

Chakravarti, A., Raquil, M. A., Tessier, P., & Poubelle, P. E. (2009). Surface RANKL of Toll-like receptor 4–stimulated human neutrophils activates osteoclastic bone resorption. *Blood*, *114*(8), 1633-1644.

Chatani, M., Takano, Y., & Kudo, A. (2011). Osteoclasts in bone modeling, as revealed by in vivo imaging, are essential for organogenesis in fish. *Developmental biology*, *360*(1), 96-109.

Cho TJ, Gerstenfeld LC, Einhorn TA. (2002). Differential temporal expression of members of the transforming growth factor beta superfamily during murine fracture healing. *J Bone Miner Res* 17: 513-520.

Claes, L., Recknagel, S., & Ignatius, A. (2012). Fracture healing under healthy and inflammatory conditions. *Nature Reviews Rheumatology*, *8*(3), 133-143.

Colnot C. (2005). Cellular and molecular interactions regulating skeletogenesis. *J Cell Biochem* 95:688–697.

Colucci-Guyon, E., Tinevez, J. Y., Renshaw, S. A., & Herbomel, P. (2011). Strategies of professional phagocytes in vivo: unlike macrophages, neutrophils engulf only surface-associated microbes. *J Cell Sci*, *124*(18), 3053-3059.

Detrich, H. W., Westerfield, M., & Zon, L. I. (2011). The zebrafish: genetics, genomics and in informatics (Vol. 2). Academic Press.

Dinarello, C.A. (2009) Immunological and inflammatory functions of the interleukin- 1 family. Annu Rev Immunol 27, 519-550.

Dunne A, O'Neill LA. (2013). The interleukin-1 receptor/Toll-like receptor superfamily: signal transduction during inflammation and host defense. Science's STKE: signal transduction knowledge environment. (171):re3

Dymecki SM, Kim JC (2007) Molecular neuroanatomy's "Three Gs": a primer. Neuron 54: 17–34.

Einhorn TA, Majeska RJ, Rush EB, Levine PM, Horowitz MC (1995). The expression of cytokine activity by fracture callus. J Bone Miner Res. 10:1272–81

Einhorn TA. (1998). The cell and molecular biology of fracture healing. *Clin Orthop Relat Res* 355: S7-21

Elks, P. M. (2008). Genetic analysis of the regulation of bone development by Wnt signalling in zebrafish. (Doctoral dissertation). University of Sheffield.

Feil, R., Wagner, J., Metzger, D., & Chambon, P. (1997). Regulation of Cre recombinase activity by mutated estrogen receptor ligand-binding domains. *Biochemical and biophysical research communications*, *237*(3), 752-757.

Ferguson, C., Alpern, E., Miclau, T., & Helms, J. A. (1999). Does adult fracture repair recapitulate embryonic skeletal formation? *Mechanisms of development*, *87*(1), 57-66.

Flores, M. V.; Tsang, V. W.; Hu, W.; Kalev-Zylinska, M.; Postlethwait, J.; Crosier, P.; Crosier, K.; Fisher, S., (2004): Duplicate zebrafish runx2 orthologues are expressed in developing skeletal elements. Gene Expr. Patterns 4, 573–581.

García R. M. (2016) Molecular and Cellular Dissection of Zebrafish Larvae Tail Regeneration. PhD dissertation. University of Sheffield.

Gauron, C. et al. (2013) Sustained production of ROS triggers compensatory proliferation and is required for regeneration to proceed. Sci. Rep. 3, 2084

Gavaia P. J., Simes D. C., Ortiz-Delgado J. B., Viegas C. S. B., Pinto J. P., Kelsh R. N., Sarasquete M. C., Cancela M. L. (2006). Osteocalcin and matrix Gla protein in zebrafish (Danio rerio) and Senegal sole (Solea senegalensis): comparative gene and protein expression during larval development through adulthood.Gene Expr. Patterns 6, 637-652.

Gerstenfeld LC, Barnes GL, Shea CM, Einhorn TA. (2003b). Osteogenic differentiation is selectively promoted by morphogenetic signals from chondrocytes and synergized by a nutrient rich growth environment. *Connect Tissue Res* 44(Suppl 1): 85-91.

Gerstenfeld LC, Cullinane DM, Barnes GL, Graves DT, Einhorn TA. (2003). Fracture healing as a post-natal developmental process: molecular, spatial, and temporal aspects of its regulation. J Cell Biochem 88(5): 873-884.

Geurtzen et al., (2014). Mature osteoblasts dedifferentiate in response to traumatic bone injury in the zebrafish fin and skull. Development 141, 2225-2234.

Glynne Andrew, J., Andrew, S. M., Freemont, A. J., & Marsh, D. R. (1994). Inflammatory cells in normal human fracture healing. *Acta Orthopaedica Scandinavica*, *65*(4), 462-466.

Goto T, Yamaza T, Tanaka T (2003). Cathepsins in the osteoclast. J Electron Micros 52(6): 551-558.

Grotek, B. et al. (2013) Notch signaling coordinates cellular proliferation with differentiation during zebrafish fin regeneration. Development 140, 1412–1423 41

Hall, B. K.; Witten, P. E., (2007): Plasticity of and transitions between skeletal tissues in vertebrate evolution and development. In: Major transitions in vertebrate evolution. J. S. Anderson, H. Sues (Eds), Indiana University Press, Bloomington, pp. 13–56.

Han P, Zhou X-H, Chang N et al (2014) Hydrogen peroxide primes heart regeneration with a derepression mechanism. Cell Res 24:1091–1107

Hans, S., Kaslin, J., Freudenreich, D. and Brand, M. (2009). Temporally controlled site-specific recombination in zebrafish. PLoS ONE 4, e4640.

Hans S, Freudenreich D, Geffarth M, Kaslin J, Machate A, Brand M (2011) Generation of a non-leaky heat shock-inducible Cre line for conditional Cre/lox strategies in zebrafish. Dev Dyn 240(1):108–115

Higashijima S, Okamoto H, Ueno N, Hotta Y, Eguchi G (1997) High-frequency generation of transgenic zebrafish which reliably express GFP in whole muscles or the whole body by using promoters of zebrafish origin. Dev Biol ;192(2):289–299.

Hirose, K. et al. (2014) Mechanistic target of rapamycin complex 1 signaling regulates cell proliferation, cell survival, and differentiation in regenerating zebrafish fins. BMC Dev. Biol. 14, 42

Histing T, Garcia P, Holstein JH, Klein M, Matthys R, et al. (2011) Small animal bone healing models: Standards, tips, and pitfalls results of a consensus meeting. Bone 49: 591–599. doi: 10.1016/j.bone.2011.07.007

Inohaya K, Takano Y, Kudo A (2007). The teleost intervertebral region acts as a growth center of the centrum: *in vivo* visualization of osteoblasts and their progenitors in transgenic fish. *Dev Dyn* 236: 3031–3046.

Ishii M, Kikuta J, Shimazu Y, Meier-Schellersheim M, Germain RN. (2010) Chemorepulsion by blood S1P regulates osteoclast precursor mobilization and bone remodeling in vivo. *J Exp Med* . 207:2793–2798.

Jankun P. J (2015) The Study of Molecular Interactions during Zebrafish Tail Regeneration for use in Glycotherapeutics (Doctoral dissertation). University of Sheffield.

J. Itou, I. Oishi, H. Kawakami, T.J. Glass, J. Richter, A. Johnson, T.C. Lund, Y. Kawakami (2012) Migration of cardiomyocytes is essential for heart regeneration in zebrafish. Development, 139, pp. 4133–4142

Jimi E, Nakamura I, Duong LT, Ikebe T, Takahashi N, Rodan GA, Suda T (1998) Interleukin 1 induces multinucleation and bone-resorbing activity of osteoclasts in the absence of osteoblasts/stromal cells. *Exp Cell Res* 247:84–93

Johnson SL, Weston JA (1995) Temperature-sensitive mutations that cause stage-specific defects in Zebrafish fin regeneration. Genetics, 141:1583-1595.

Jopling, C., Sleep, E., Raya, M., Martí, M., Raya, A., & Belmonte, J. C. I. (2010). Zebrafish heart regeneration occurs by cardiomyocyte dedifferentiation and proliferation. *Nature*, *464*(7288), 606-609.

Kawakami, A. (2010). Stem cell system in tissue regeneration in fish. *Development, growth & differentiation*, *52*(1), 77-87.

Kikuchi, K., Holdway, J. E., Werdich, A. A., Anderson, R. M., Fang, Y., Egnaczyk, G. F., ... & Poss, K. D. (2010). Primary contribution to zebrafish heart regeneration by gata4+ cardiomyocytes. *Nature*, *464*(7288), 601-605.

Klyubin, I. V., Kirpichnikova, K. M. & Gamaley, I. A. (1996). Hydrogen peroxide-induced chemotaxis of mouse peritoneal neutrophils. Eur. J. Cell Biol. 70, 347–351.

Knopf, F. et al. (2010) Dually inducible TetON systems for tissue-specific conditional gene expression in zebrafish. Proc. Natl. Acad. Sci. U.S.A. 107, 19933–19938

Kragl, M. et al. (2009) Cells keep a memory of their tissue origin during axolotl limb regeneration. Nature 460, 60–65

Kristensen HB, Andersen TL, Marcussen N, Rolighed L, Delaisse JM. (2013) Increased presence of capillaries next to remodeling sites in adult human cancellous bone. *J Bone Miner Res* ;28:574–585.

Kroehne, V., Freudenreich, D., Hans, S., Kaslin, J., & Brand, M. (2011). Regeneration of the adult zebrafish brain from neurogenic radial glia-type progenitors. *Development*, *138*(22), 4831-4841.

Kubes, P., Mehal, W. Z. (2012) Sterile inflammation in the liver. Gastroenterology 143, 1158 – 1172.

Kujawski, S. et al. (2014) Calcineurin regulates coordinated outgrowth of zebrafish regenerating fins. Dev. Cell 28, 573–587.

Kwan, K. M., Fujimoto, E., Grabher, C., Mangum, B. D., Hardy, M. E., Campbell, D. S., ... & Chien, C. B. (2007). The Tol2kit: a multisite gateway-based construction kit for Tol2 transposon transgenesis constructs. *Developmental dynamics*, *236*(11), 3088-3099.

Lacey, D. L., Timms, E., Tan, H. L., Kelley, M. J., Dunstan, C. R., Burgess, T., ... & Hsu, H. (1998). Osteoprotegerin ligand is a cytokine that regulates osteoclast differentiation and activation. *cell*, *93*(2), 165-176.

Lakso M, Sauer B, Mosinger B, Lee EJ, Manning RW, Yu SH, Mulder KL, Westphal H (Jul 1992). "Targeted oncogene activation by site-specific recombination in transgenic mice". Proceedings of the National Academy of Sciences of the United States of America. 89 (14): 6232–6236.

Lange, J., Sapozhnikova, A., Lu, C., Hu, D., Li, X., Miclau, T., & Marcucio, R. S. (2010). Action of IL-1β during fracture healing. *Journal of Orthopaedic Research*, *28*(6), 778-784.

Langenau, D. M., Feng, H., Berghmans, S., Kanki, J. P., Kutok, J. L., & Look, A. T. (2005). Cre/lox-regulated transgenic zebrafish model with conditional myc-induced T cell acute lymphoblastic leukemia. Proceedings of the National Academy of Sciences, *102*(17), 6068-6073.

Le, X., Langenau, D. M., Keefe, M. D., Kutok, J. L., Neuberg, D. S., & Zon, L. I. (2007). Heat shock-inducible Cre/Lox approaches to induce diverse types of tumors and hyperplasia in transgenic zebrafish. Proceedings of the National Academy of Sciences, 104(22), 9410-9415.

Lee, Y. M., Fujikado, N., Manaka, H., Yasuda, H., & Iwakura, Y. (2010). IL-1 plays an important role in the bone metabolism under physiological conditions. *International immunology*, *22*(10), 805-816.

Lehoczky, J.A. et al. (2011) Mouse digit tip regeneration is mediated by fate-restricted progenitor cells. Proc. Natl. Acad. Sci. U.S.A. 108, 20609–20614

Li, X., Quigg, R. J., Zhou, J., Ryaby, J. T., & Wang, H. (2005). Early signals for fracture healing. *Journal of cellular biochemistry*, *95*(1), 189-205.

Lieschke, G. J., Oates, A. C., Crowhurst, M. O., Ward, A. C., & Layton, J. E. (2001). Morphologic and functional characterization of granulocytes and macrophages in embryonic and adult zebrafish. *Blood*, *98*(10), 3087-3096.

Lieschke, G. J., & Currie, P. D. (2007). Animal models of human disease: zebrafish swim into view. *Nature Reviews Genetics*, *8*(5), 353-367.

Livet, J., Weissman, T. A., Kang, H., Draft, R. W., Lu, J., Bennis, R. A., ... & Lichtman, J. W. (2007). Transgenic strategies for combinatorial expression of fluorescent proteins in the nervous system. *Nature*, *450*(7166), 56-62.

Maes, C., Kobayashi, T., Selig, M. K., Torrekens, S., Roth, S. I., Mackem, S., ... & Kronenberg, H. M. (2010). Osteoblast precursors, but not mature osteoblasts, move into developing and fractured bones along with invading blood vessels. *Developmental cell*, *19*(2), 329-344.

Marí-Beffa M, Santamaría JA, Murciano C, Santos-Ruiz L, Andrades JA, Guerado E, Becerra J. 2007. Zebrafish fins as a model system for skeletal human studies. *Sci World J* 7: 1114–1127.

Martin, P., & Parkhurst, S. M. (2004). Parallels between tissue repair and embryo morphogenesis. *Development*, *131*(13), 3021-3034.

Marsell R, Einhorn TA. (2009). The role of endogenous bone morphogenetic proteins in normal skeletal repair. *Injury* 40(3): S4-7.

Marzona, L., & Pavolini, B. (2009). Play and players in bone fracture healing match. *Clinical cases in mineral and bone metabolism*, *6*(2), 159-162.

Mateus R., Lourenço R., Fang Y., Brito G., Farinho A., Valério F., et al. . (2015). Control of tissue growth by Yap relies on cell density and F-actin in zebrafish fin regeneration. Development 142, 2752–276

Mathias, J. R., Dodd, M. E., Walters, K. B., Yoo, S. K., Ranheim, E. A., & Huttenlocher, A. (2009). Characterization of zebrafish larval inflammatory macrophages. Dev Comp Immunol, 33(11), 1212-1217.

Mathias, J. R., Perrin, B. J., Liu, T. X., Kanki, J., Look, A. T., & Huttenlocher, A. (2006). Resolution of inflammation by retrograde chemotaxis of neutrophils in transgenic zebrafish. *Journal of leukocyte biology*, *80*(6), 1281-1288.

Metzger, D., Clifford, J., Chiba, H., & Chambon, P. (1995). Conditional site-specific recombination in mammalian cells using a ligand-dependent chimeric Cre recombinase. *Proceedings of the National Academy of Sciences*, *92*(15), 6991-6995.

Motoike T, Loughna S, Perens E, Roman BL, Liao W, Chau TC, Richardson CD, Kawate T, Kuno J, Weinstein BM, Stainier DY, Sato TN. (2000). Universal GFP reporter for the study of vascular development. *Genesis* 28: 75–81.

Mosimann, C., & Zon, L. I. (2011). Advanced zebrafish transgenesis with Tol2 and application for Cre/lox recombination experiments. *The zebrafish: genetics, genomics and informatics, 104*.

Mountziaris PM, Mikos AG. (2008). Modulation of the inflammatory response for enhanced bone tissue regeneration. *Tissue Eng B Rev* 14(2): 179-186.

Munch, J. et al. (2013) Notch regulates blastema proliferation and prevents differentiation during adult zebrafish fin regeneration. Development 140, 1402–1411

H. Nakamura H,Sato G, Hirata A, Yamamoto T. (2004). Immunolocalization of matrix metalloproteinase-13 on bone surface under osteoclasts in rat tibia. Bone, 34, pp. 48–56.

Nakatani, Y., Takeda, H., Kohara, Y., & Morishita, S. (2007). Reconstruction of the vertebrate ancestral genome reveals dynamic genome reorganization in early vertebrates. *Genome research*, *17*(9), 1254-1265.

Niethammer, P., Grabher, C., Look, A. T. & Mitchison, T. J. (2009) A tissue-scale gradient of hydrogen peroxide mediates rapid wound detection in zebrafish. Nature 459, 996–999.

Nechiporuk, A., & Keating, M. T. (2002). A proliferation gradient between proximal and msxb-expressing distal blastema directs zebrafish fin regeneration. *Development*, *129*(11), 2607-2617.

Oberpriller, J. O., & Oberpriller, J. C. (1974). Response of the adult newt ventricle to injury. *Journal of Experimental Zoology*, *187*(2), 249-259.

Ogryzko, N. V., Hoggett, E. E., Solaymani-Kohal, S., Tazzyman, S., Chico, T. J., Renshaw, S. A., & Wilson, H. L. (2014). Zebrafish tissue injury causes upregulation of interleukin-1 and caspase-dependent amplification of the inflammatory response. *Disease models & mechanisms*, *7*(2), 259-264.

Orban PC, Chui D, Marth JD (Aug 1992). "Tissue- and site-specific DNA recombination in transgenic mice". Proceedings of the National Academy of Sciences of the United States of America. 89 (15): 6861–6865.

O'Steen, W. K., & Walker, B. E. (1962). Radioautographic studies of regeneration in the common newt III. Regeneration and repair of the intestine. *The Anatomical Record*, *142*(2), 179-187.

Poss, K. D., Shen, J., & Keating, M. T. (2000). Induction of lef1 during zebrafish fin regeneration. *Developmental dynamics*, *219*(2), 282-286.

Poss KD, Wilson LG, Keating MT (2002) Heart regeneration in zebrafish. Science, 298:2188-2190.

Poss, K. D., Keating, M. T., & Nechiporuk, A. (2003). Tales of regeneration in zebrafish. *Developmental Dynamics*, *226*(2), 202-210.

Pivonka, P., & Dunstan, C. R. (2012). Role of mathematical modeling in bone fracture healing. *BoneKEy reports*, *1*.

Quint, E., Smith, A., Avaron, F., Laforest, L., Miles, J., Gaffield, W., & Akimenko, M. A. (2002). Bone patterning is altered in the regenerating zebrafish caudal fin after ectopic expression of sonic hedgehog and bmp2b or exposure to cyclopamine. *Proceedings of the National Academy of Sciences*, *99*(13), 8713-8718.

Raggatt LJ, Partridge NC. (2010) Cellular and molecular mechanisms of bone remodeling. J Biol Chem. 285(33):25103–25108.

Reddien, P. W., & Alvarado, A. S. (2004). Fundamentals of planarian regeneration. *Annu. Rev. Cell Dev. Biol.*, *20*, 725-757.

Renshaw, S. A., Loynes, C. A., Trushell, D. M., Elworthy, S., Ingham, P. W., & Whyte, M. K. (2006). A transgenic zebrafish model of neutrophilic inflammation. Blood, 108(13), 3976-3978.

Rivadeneira F, Styrkarsdottir U, Estrada K, Halldorsson BV, Hsu YH, et al. (2009) Twenty bone-mineral-density loci identified by large-scale meta-analysis of genome-wide association studies. Nat Genet 41: 1199–1206.

Rinkevich, Y. et al. (2011) Germ-layer and lineage-restricted stem/ progenitors regenerate the mouse digit tip. Nature 476, 409–413

Rundle C.H. Wang H. Yu H. Chadwick R.B. Davis E.I. Wegedal J.E. Lau K.-H.W. Mohan S. Ryaby J.T. Baylink D.J. (2006) Microarray analysis of gene expression during the inflammation and endochondral bone formation stages of rat femur fracture repair. Bone. 38:521.

Schindeler A, McDonald MM, Bokko P, Little DG. (2008). Bone remodelling during fracture repair: The cellular picture. *Semin Cell Dev Biol* 19:459-466.

Shalhoub V, Senaldi G, Guo J, Delaney J, Boyle WJ. (1998). Osteoprotegerin (OPG) ligand is a cytokine that regulates osteoclasts differentiation and activation. Cell 93(2): 165-17

Shapiro, F. (2008). Bone development and its relation to fracture repair. The role of mesenchymal osteoblasts and surface osteoblasts. *Eur Cell Mater*, *15*(53), e76.

Singh, S. P., Holdway, J. E., & Poss, K. D. (2012). Regeneration of amputated zebrafish fin rays from de novo osteoblasts. *Developmental cell*, *22*(4), 879-886.

Sousa, S., Afonso, N., Bensimon-Brito, A., Fonseca, M., Simões, M., Leon, J., ... & Jacinto, A. (2011). Differentiated skeletal cells contribute to blastema formation during zebrafish fin regeneration. *Development*, *138*(18), 3897-3905.

Sousa, S., Valerio, F., & Jacinto, A. (2012). A new zebrafish bone crush injury model. *Biology open*, *1*(9), 915-921.

Spoorendonk, K. M., Peterson-Maduro, J., Renn, J., Trowe, T., Kranenbarg, S., Winkler, C., & Schulte-Merker, S. (2008). Retinoic acid and Cyp26b1 are critical regulators of osteogenesis in the axial skeleton. *Development*, *135*(22), 3765-3774.

Stark, D. and Kulesa, P. (2007). An *in vivo* comparison of photoactivatable fluorescent proteins in an avian embryo model. Dev. Dyn., 236(6), pp.1583-1594.

Sternberg N, Hamilton D (1981). "Bacteriophage P1 site-specific recombination. I. Recombination between loxP sites". Journal of Molecular Biology. 150 (4): 467–486

Stewart, S., & Stankunas, K. (2012). Limited dedifferentiation provides replacement tissue during zebrafish fin regeneration. *Developmental biology*, *365*(2), 339-349.

Stewart, S., Gomez, A. W., Armstrong, B. E., Henner, A., & Stankunas, K. (2014). Sequential and opposing activities of Wnt and BMP coordinate zebrafish bone regeneration. Cell reports, 6(3), 482-498.

Stoick-Cooper, C. L., Moon, R. T., & Weidinger, G. (2007). Advances in signaling in vertebrate regeneration as a prelude to regenerative medicine. *Genes & development*, *21*(11), 1292-1315.

Subramaniam S, Stansberg C, Cunningham C. (2004). The interleukin 1 receptor family. Developmental and comparative immunology. 28(5):415-28

Takeyama, K., Chatani, M., Takano, Y., & Kudo, A. (2014). In-vivo imaging of the fracture healing in medaka revealed two types of osteoclasts before and after the callus formation by osteoblasts. *Developmental biology*, *394*(2), 292-304.

Tal, T. L., Graves, L. M., Silbajoris, R., Bromberg, P. A., Wu, W., & Samet, J. M. (2006). Inhibition of protein tyrosine phosphatase activity mediates epidermal growth factor receptor signaling in human airway epithelial cells exposed to Zn 2+. *Toxicology and applied pharmacology*, *214*(1), 16-23.

Tanaka, E. M., & Reddien, P. W. (2011). The cellular basis for animal regeneration. *Developmental cell*, *21*(1), 172-185.

Teitelbaum SL (2000) Bone resorption by osteoclasts. Science; 289:1504–8.

Thisse, C., & Thisse, B. (2008). High-resolution in situ hybridization to whole-mount zebrafish embryos. *Nature protocols*, *3*(1), 59-69.

Thummel, R., Burket, C. T., Brewer, J. L., Sarras, M. P., Li, L., Perry, M., ... & Godwin, A. R. (2005). Cre-mediated site-specific recombination in zebrafish embryos. *Developmental dynamics*, *233*(4), 1366-1377.

To TT, Witten PE, Renn J, Bhattacharya D, Huysseune A, Winkler C (2012). Rankl induced osteoclastogenesis leads to loss of mineralization in a medaka osteoporosis model. Development 139: 141–150.

Tu, S., & Johnson, S. L. (2011). Fate restriction in the growing and regenerating zebrafish fin. *Developmental cell*, *20*(5), 725-732.

Udagawa, N., Takahashi, N., Akatsu, T., Tanaka, H., Sasaki, T., Nishihara, T., ... & Suda, T. (1990). Origin of osteoclasts: mature monocytes and macrophages are capable of differentiating into osteoclasts under a suitable microenvironment prepared by bone marrow-derived stromal cells. *Proceedings of the national academy of sciences*, *87*(18), 7260-7264.

Udvadia, A. J., Koster, R. W., & Skene, J. P. (2001). GAP-43 promoter elements in transgenic zebrafish reveal a difference in signals for axon growth during CNS development and regeneration. *Development Cambridge-*, *128*(7), 1175-1182.

Udvadia, A. J., & Linney, E. (2003). Windows into development: historic, current, and future perspectives on transgenic zebrafish. *Developmental biology*, *256*(1), 1-17.

Walton EM, Cronan MR, Beerman RW, Tobin DM. The macrophage-specific promoter mfap4 allows live, long-term analysis of macrophage behavior during mycobacterial infection in zebrafish. PLoS One. 2015

Wehner, D., & Weidinger, G. (2015). Signaling networks organizing regenerative growth of the zebrafish fin. *Trends in Genetics*, *31*(6), 336-343.

Westerfield, M., Wegner, J., Jegalian, B. G., DeRobertis, E. M., & Püschel, A. W. (1992). Specific activation of mammalian Hox promoters in mosaic transgenic zebrafish. *Genes & Development*, *6*(4), 591-598.

Witten, P. E.; Huysseune, A., (2009): A comparative view on mechanisms and functions of skeletal remodelling in teleost fish, with special emphasis on osteoclasts and their function. Biol. Rev. Camb. Philos. Soc. 84, 315–346.

Whitehead, G. G., Makino, S., Lien, C. L., & Keating, M. T. (2005). fgf20 is essential for initiating zebrafish fin regeneration. *Science*, *310*(5756), 1957-1960.

Woodfin, A., Voisin, M. B., Beyrau, M., Colom, B., Caille, D., Diapouli, F. M., Nash, G. B., Chavakis, T., Albelda, S. M., Rainger, G. E., Meda, P., Imhof, B. A., Nourshargh, S. (2011) The junctional adhesion molecule JAM-C regulates polarized transendothelial migration of neutrophils in vivo. Nat. Immunol. 12, 761–769.

Yan, Y. L.; Willoughby, J.; Liu, D.; Crump, J. G.; Wilson, C.; Miller, C. T.; Singer, A.; Kimmel, C.; Westerfield, M.; Postlethwait, J. H., 2005: A pair of Sox: distinct and overlapping functions of zebrafish sox9 co-orthologs in craniofacial and pectoral fin development. Development 132, 1069–1083.

Vihtelic TS, Hyde DR (2000) Light-induced rod and cone cell death and regeneration in the adult albino zebrafish (Danio rerio) retina. J Neurobiol, 44:289-307.

Yao Z, Xing L, Qin C, Schwarz E, Boyce B. (2008). Osteoclast precursor interaction with bone matrix induces osteoclast formation directly by an interleukin-1-mediated autocrine mechanism. J Biol Chem; 283: 9917-24

Yoo, S. K., Starnes, T. W., Deng, Q. & Huttenlocher, A. (2011) Lyn is a redox sensor that mediates leukocyte wound attraction in vivo. Nature 480, 109–112.

Yoshikawa, S., Kawakami, K., & Zhao, X. C. (2008). G2R Cre reporter transgenic zebrafish. *Developmental Dynamics*, *237*(9), 2460-2465.

Zupan, J., Komadina, R., & Marc, J. (2012). The relationship between osteoclastogenic and anti-osteoclastogenic pro-inflammatory cytokines differs in human osteoporotic and osteoarthritic bone tissues. *Journal of biomedical science*, *19*(1), 28.

Abbreviations

4 OHT	4-Hydroxytamoxifen
BSA	Bovine Serum Albumin
ºC	Centigrade
DIG	Digoxigenin
DMSO	Dimethyl Sulfoxide
Dpa	Days post- Amputation
Hpc	Hours post-Crush
DsRed	Discosoma RED
EF1alpha	Elongation Factor 1 Alpha
ER	Estrogen Receptor
F1	First Generation
F2	Second Generation
FGF	Fibroblast Growth Factor
GFP	Green Fluorescent Protein
Hh	Hedgehog
Hpa	Hours post Amputation
Hpc	Hours post Crush
Hpf	Hours post Fertilization
IGF	Insulin-like Growth Factor
ISH	*In situ*-Hybridization
ISP	Study Plan
LB	Lysogeny Broth
Mg	Milligrams

ml	Milliliter
mM	Milimolar
mq	Mili-q
NBCS	New Born Calf Serum
NEB	New England Biolabs inc
NEBinc	New England Biolabs
Ng	Nanograms
Nm	Nanometers
PBST	Phosphate buffered saline plus 0.1% tween 20
PCR	Polymerase Chain Reaction
PFA	Paraformaldehyde
PK	Proteinase K
RA	Retinoic Acid
raldh2	Retinaldehyde Dehydrogenase 2
RNA	Ribonucleic Acid
Rpm	Revolution per minute
rSAP	Shrimp Alkaline Phosphatase
RT	Room Temperature
SOC	Super Optimal Broth
TBE	Tris,Borate, EDTA
tcf7	Transcritption Factor 7
TE	Tris, EDTA
μM	Micromolar
UV	Ultra Violet
X	Times

µl	Microliter
ng	Nanogram